iNTERWAVE ANALYZER

User Manual

Version 2

Interwave Analyzer

User Manual

developer	Rafael de Carvalho Bueno
co-developers	Tobias Bleninger
	Andreas Lorke
Version	**2.00.0**

Contents

1 Introduction

The **Interwave Analyzer** is an open-source software developed to investigate the occurrence and dynamics of physical processes in lakes and reservoirs, with particular emphasis on large-scale circulation phenomena such as basin-scale internal waves. In addition, it provides a wide range of stratification indices and state-of-the-art metrics to characterize mixing and thermal structure based on high-frequency underwater temperature measurements. The software offers a comprehensive suite of analytical tools to quantify key physical parameters that describe the likelihood of internal wave activity, stratification stability, and vertical mixing in aquatic systems. By combining theoretical formulations with data-driven approaches, the Interwave Analyzer supports advanced research in lake hydrodynamics, limnology, and environmental modeling.

Designed for both experts and non-experts in baroclinic motion, the Interwave Analyzer offers a powerful, accessible, and versatile platform for analyzing internal waves using high-frequency temperature data from instrumented buoys and meteorological forcing data. Its modular framework combines a robust computational engine with an intuitive **Graphical User Interface (GUI)**, allowing users to perform advanced analyses without the need for programming experience.

Beyond its usability, the Interwave Analyzer stands out for its adherence to well-established physical theories of stratified lake dynamics, including formulations for modal decomposition, wave energetics, and mixing efficiency. The software enables classification of lake mixing regimes, detection and characterization of internal wave patterns, and assessment of conditions leading to the degeneration of basin-scale internal oscillations.

This **User Manual** provides comprehensive guidance on installing, configuring, and operating the Interwave Analyzer. It includes a complete reference for all software functions, input and output structures, and methodological underpinnings of the implemented analyses. The manual is organized as follows:

Section 2:
> Explains how to download, install, and run the Interwave Analyzer—either through the precompiled executable version or by executing the source code within a Python environment.

Section 3:
> Provides a detailed overview of the program's menu system and Graphical User Interface (GUI), explaining how each module and option operates.

Section 4:
> Provides a comprehensive description of all available additional parameters, including their physical meaning, mathematical formulation, underlying assumptions, and step-by-step calculation procedures.

Section 5:
> Summarizes all graphical and text-based results generated by the software, including file naming conventions, formats, and interpretation guidelines.

Section 6:
> Describes how the software computes key physical variables and explains the mathematical formulations and numerical methods behind the analyses.

Section 7:
> Offers a step-by-step tutorial for first-time users, providing a hands-on introduction and verification of a successful software setup.

If this is your first experience with the Interwave Analyzer, we strongly recommend reading Section 3 carefully to become familiar with the interface and analysis options, followed by Section 7, which guides you through your first analysis.

The Interwave Analyzer is a research-based project under continuous development. Its evolution is driven by community feedback, scientific advancements, and practical needs observed in lake and reservoir studies. We

encourage users to report bugs, share suggestions, and propose new features that could enhance the software's capabilities. Suggestions and communication can be directed to: decarvalhobueno@gmail.com.

This manual applies to **Interwave Analyzer version 2.0**. Additional information, updates, and examples are available at our official website: https://sites.google.com/view/interwaveanalyzer/interwave-analyzer and the open-source repository: https://github.com/buenorc/interwaveanalyzer.

Change history

Version	Description
1.00.0	Reference version for these change notes.
1.00.1	Added new functionalities, including the Thorpe scale and multi-layer power spectral density analysis. Users can define reference level z_0, window size for spectral analysis, and a fixed surface elevation. Export of selected results as text files was implemented.
1.00.2	Bug fixes and graphical improvements, including a clearer visualization of consecutive wind events and enhancements to the final report.
1.00.3	Introduced statistical significance testing for spectral densities and a numerical mode decomposition module. Solar radiation became optional input. Windrose dependency removed.
1.01.0	Implemented full-period modal decomposition, allowing analysis of the temporal variability of internal wave periods and associated velocity structures. Added pre- and post-processing options for temporal resolution control and expanded output file generation.
1.01.2	Updated thermistor indexing (from 1 to N instead of 0 to N–1). Fixed modal decomposition issues, added more output text files, and included improved warning messages and documentation updates.
2.0.0	**Major release.** The computational core of Interwave Analyzer has been extensively refactored to enhance numerical stability, modularity, and overall flexibility. Version 2 introduces the *Additional Parameters Framework*, which provides a flexible interface for future extensions, user-defined indices, and customized analyses. A major enhancement in this version is that bathymetry is now treated as an input variable, enabling the use of a second-axis representation of the basin. This improvement allows for more accurate calculations of the Lake Number, Schmidt stability, and the slope criticality parameter by accounting for variations in effective basin length and layer geometry. The previously generated static PDF report has been replaced by an interactive HTML dashboard with dynamic visualizations, while the data processing pipeline has been optimized for speed and memory efficiency. The GUI has been redesigned for better usability, and several new diagnostic checks and validation routines have been implemented. Due to the refactoring and improvements in numerical treatment, some computed values may differ slightly from those obtained in previous versions. These differences reflect corrections and refinements in the algorithms rather than inconsistencies. Detailed notes describing the methodological updates, including bathymetry handling, second-axis representation, and their impact on derived metrics, are presented throughout this manual within each specific analysis section and corresponding technical notes.

1.1 How to cite Interwave Analyzer

If you are referring specifically to the contents, figures, or instructions provided in this manual, please cite it directly as the reference source. However, if you have used the **Interwave Analyzer** software or any of its implemented modules to perform analyses, process data, or generate results, please cite the corresponding scientific publication associated with the software.

All analyses presented in the scientific paper were conducted using Interwave Analyzer version 1.00.3. The citation format is provided below:

> de Carvalho Bueno, R., Bleninger, T. B., Lorke, A. (2021). **Internal wave analyzer for thermally stratified lakes**. *Environmental Modelling and Software*, 136, 104950.

For Latex Users:

```
@article{bueno2021internalwave,
    title={Internal wave analyzer for thermally stratified lakes},
    author={de Carvalho Bueno, R. and Bleninger, T. B. and Lorke, A.},
    journal={Environmental Modelling and Software},
    volume={136},
    year={2021},
    publisher={Elsevier}
}
```

1.2 About Version 2.0

Version 2 represents a significant step forward in the evolution of the Interwave Analyzer, enhancing robustness, modularity, and scientific extensibility. The new *Additional Parameters Framework* provides a dynamic mechanism for incorporating new indices, empirical formulations, or user-defined variables directly through configuration files—without the need to modify the Graphical User Interface (GUI). This flexibility makes Version 2 especially suitable for the implementation of new analysis on future.

In addition to this major structural enhancement, the computational core has been fully refactored to improve numerical consistency, error handling, and overall performance. Data processing routines have been optimized to handle large datasets more efficiently, ensuring faster execution and lower memory usage. The GUI has also been redesigned to facilitate navigation, improve visualization of intermediate and final results, and streamline access to input and output settings.

It is important to note that, due to the methodological refinements introduced in this version, some calculated values may differ slightly from those obtained in earlier releases. These differences stem from algorithmic corrections, improved numerical precision, and better representation of physical processes rather than inconsistencies.

Finally, the static PDF report used in previous versions has been replaced by an interactive HTML dashboard. This dashboard is built using the `Plotly` and `Dash` frameworks. As a consequence, Version 2 no longer depends on the `reportlab` library for report generation. Instead, additional Python packages required for the dashboard functionality must be installed and are listed in the software dependencies section of this manual.

Overall, Version 2 establishes a more robust, extensible, and scientifically reliable platform for the study of internal waves, stratification dynamics, and energy transfer processes in lakes and reservoirs. It provides a foundation for continuous development and collaborative contributions from the research community.

2 Installation

Before installing the software, please read carefully the license agreement presented at the beginning of this manual. The minimum system requirements depend on the execution mode chosen to run the **Interwave Analyzer**: either the *script mode* (executed through a Python interpreter) or the *pre-compiled executable mode*.

These installation instructions apply to **Interwave Analyzer version 2.0.0 or higher**. Older instructions may not be compatible due to significant refactoring of the codebase and the introduction of new dependencies associated with the *Additional Parameters Framework* implemented in Version 2.

To download the Interwave Analyzer, visit our official website at:

https://sites.google.com/view/rafaelbueno/interwave-analyzer

- To use the **pre-compiled executable version**, click on **Executable version**. This option is recommended for users who prefer a ready-to-run graphical interface without configuring a Python environment. However, note that even the script mode also provides a GUI, where users simply need to run the script and can then work directly within the graphical interface, without any additional setup or command-line interaction.

- To access all **Python source scripts**, click on **Code repository**. You will be automatically redirected to our GitHub repository, where the full codebase and auxiliary files are hosted.

For detailed installation and configuration procedures for each mode, refer to the following sections:

Section 2.1: Installation of the pre-compiled executable version;

Section 2.2: Installation and configuration of the Python script version.

2.1 Pre-compiled Mode

The pre-compiled (executable) version is recommended for Windows users. This version is easier to install and run, as it does not require a Python interpreter or any additional packages.

The executable version of Interwave Analyzer requires a minimum system configuration, which may vary depending on the dataset and analysis settings. For the `Milada` example, the requirements are as follows:

- Approximately 1.80 GB for the **interwave.exe** file (size on disk: 470 MB);

- At least 850 MB of RAM;

- Additional disk space of approximately 250 MB for all generated output files.

Note that these values are indicative: larger datasets or more complex configurations may require more RAM and disk space. The memory and storage requirements increase with the number of sensors, the length of time series, the number of isotherms analyzed, and the resolution of generated figures.

The executable version can be downloaded from https://sites.google.com/view/rafaelbueno/interwave-analyzer.

After downloading, create a new folder in a convenient location and save all files there. Do not move or alter the file paths inside the downloaded folder. Navigate to the `dist/interwave` folder and double-click **interwave.exe** to launch the Interwave Analyzer graphical user interface (GUI).

For quicker access, you may create a shortcut to **interwave.exe** on your desktop or in a preferred folder by right-clicking on the file and selecting *Create Shortcut*.

The GUI should appear shortly after launching. Once displayed, you are ready to use the Interwave Analyzer. Note that since the executable mode relies on pre-compiled code, its stability may vary depending on your system specifications.

2.2 Script Mode

The **script mode** allows the Interwave Analyzer to be executed as a standard desktop application through a Python interpreter. No programming knowledge is required. The interpreter is used solely to launch the main program, after which the Graphical User Interface (GUI) is automatically initialized.

Once executed, the system loads all required computational modules and graphical components and presents the user interface without further interaction with the command line.

2.2.1 System Requirements

To execute the Interwave Analyzer in script mode, the following environment is required:

- **Python 3.x** (version 3.8 or higher recommended);
- The following Python libraries: **NumPy**, **SciPy**, **Matplotlib**, **Dash**, **Plotly**, **Tkinter**, and **Datetime**.

All additional dependencies are standard Python libraries automatically included in most Python distributions.

2.2.2 Recommended Environment: Anaconda

The recommended environment for running the Interwave Analyzer is the **Anaconda** Python distribution. Anaconda streamlines installation and dependency management by providing precompiled scientific libraries within an isolated and stable environment structure.

In most cases, the majority of required libraries are already included in a standard Anaconda installation. Typically, only **Plotly** and **Dash** need to be installed manually. Depending on the specific Anaconda version or operating system, additional packages may occasionally be required; however, the installation procedure is straightforward and can be completed using either `conda` or `pip`.

Although Anaconda is recommended, the software can also be executed using any standard Python interpreter, provided that the required libraries are installed manually.

2.2.3 Graphical Backend Compatibility

During initialization, the Interwave Analyzer configures a non-interactive Matplotlib backend to ensure compatibility across operating systems and execution environments. This avoids graphical backend conflicts, particularly when running inside development environments where a Qt session may already be active.

The program automatically manages backend configuration and Qt compatibility, ensuring that the GUI launches correctly without requiring user intervention.

2.2.4 Installation Steps for Anaconda Users

1. Access the official Anaconda website at https://www.anaconda.com/ and download the **Anaconda Distribution** for **Python 3.x**.

2. Select the appropriate installer for your operating system (Windows, macOS, or Linux).

3. Follow the installation wizard and complete the setup using the default recommended settings.

4. After installation, open the **Anaconda Prompt** (administrator privileges are recommended on Windows systems).

5. Install the additional required packages that are not included by default in the standard Anaconda distribution:

   Dash and Plotly   `conda install -c conda-forge dash plotly`

Important: If Anaconda is already installed on your system, verify that:

- The environment uses Python 3.x;

- The required packages listed above are available;

- The environment is activated before running the software.

For users operating outside the Anaconda environment, ensure that compatible versions of the required packages are installed. The packages used by Interwave Analyzer include standard Python modules such as `os`, `sys`, `time`, `random`, `datetime`, `platform`, `subprocess`, and `math`, as well as `numpy`, `numpy.matlib`, `scipy` (including `signal`, `interpolate`, `stats`, `special`, and `optimize`), `matplotlib` (with submodules `pyplot`, `cm`, `colors`, `dates`, `ticker`, `patches`, and `axes_grid1.inset_locator`), `tkinter` (`Tk`, `Text`, `END`), `dash` (including `Dash`, `html`, `dcc`, `Input`, `Output`), `plotly.graph_objects`, and PyQt or PySide packages (`PyQt5` or `PySide6`, including `QtCore`, `QtGui`, `QtWidgets`). Warnings are handled using the `warnings` module.

2.2.5   Running the Interwave Analyzer Scripts

1. Visit the official Interwave Analyzer webpage: https://sites.google.com/view/rafaelbueno/interwave-analyzer

2. Access the **Code Repository** or directly navigate to the associated GitHub repository.

3. Download all required `.py` source files. Additionally, ensure that the following resource files are included in a folder named **assets**:

   - `iwlogo.png`: used in the header of the automatically generated report;

   - `iwcon.png`: used as the graphical interface icon;

   - `style.css`: defines the styling of the dashboard.

4. Place all downloaded files in the same directory to ensure correct module referencing.

5. Open the Anaconda Prompt (or activate your selected Python environment), navigate to the project directory, and execute:

   `python iwgui.py`

6. The graphical interface will initialize automatically within a few seconds.

For first-time users, it is strongly recommended to download the example datasets available on the Interwave Analyzer website under the **Download Example** section. A step-by-step tutorial demonstrating the workflow using these datasets is provided in Section 7.

3 Graphical User Interface and Input Files Format

This section introduces the Interwave Analyzer software interface and explains in detail the structure and format of its required input files. It also provides practical guidance on configuring each analysis tab, interpreting messages, and avoiding common user errors. If your question is not addressed here, please consult the FAQ section on our website or contact us directly.

3.1 Starting Interwave Analyzer

When the `interwave.exe` (or its shortcut) is double-clicked, a black terminal window appears briefly (Figure 1). This window is used to display errors, warnings, and runtime messages. If a crash occurs during execution, the associated error will be displayed in this window. When running the program directly from a Python interpreter (via `iwgui.py`), this window will not appear, and all errors are instead printed to the command line.

Figure 1: Black window of Interwave Analyzer.

After initialization, the main Interwave Analyzer window appears (Figure 2). The interface includes a menu bar with two main items: *File* and *Help*.

The *File* menu provides three options:

- **Open** — Opens a saved configuration file with extension `.set`. When loaded, all settings and paths defined in the saved session are automatically restored.

> ⚠️ Ensure that all file paths saved in the configuration exist and that filenames have not been modified or deleted, otherwise read errors may occur.

- **Save as** — Saves the current configuration (options, variables, and parameters from all four main tabs) into a new `.set` file.
- **Exit** — Closes the Interwave Analyzer application.

The *Help* menu includes: **Manual**, which opens the online documentation of the Interwave Analyzer; **About**, which displays information about the software version, license agreement, and authorship; and **Dashboard**, which prompts the user to select a `dash_data.npz` file in order to load a dashboard from a previous analysis. This file is generated only when the Interwave Analyzer is executed for a specific location and is saved in the same results directory where all PNG figures are stored.
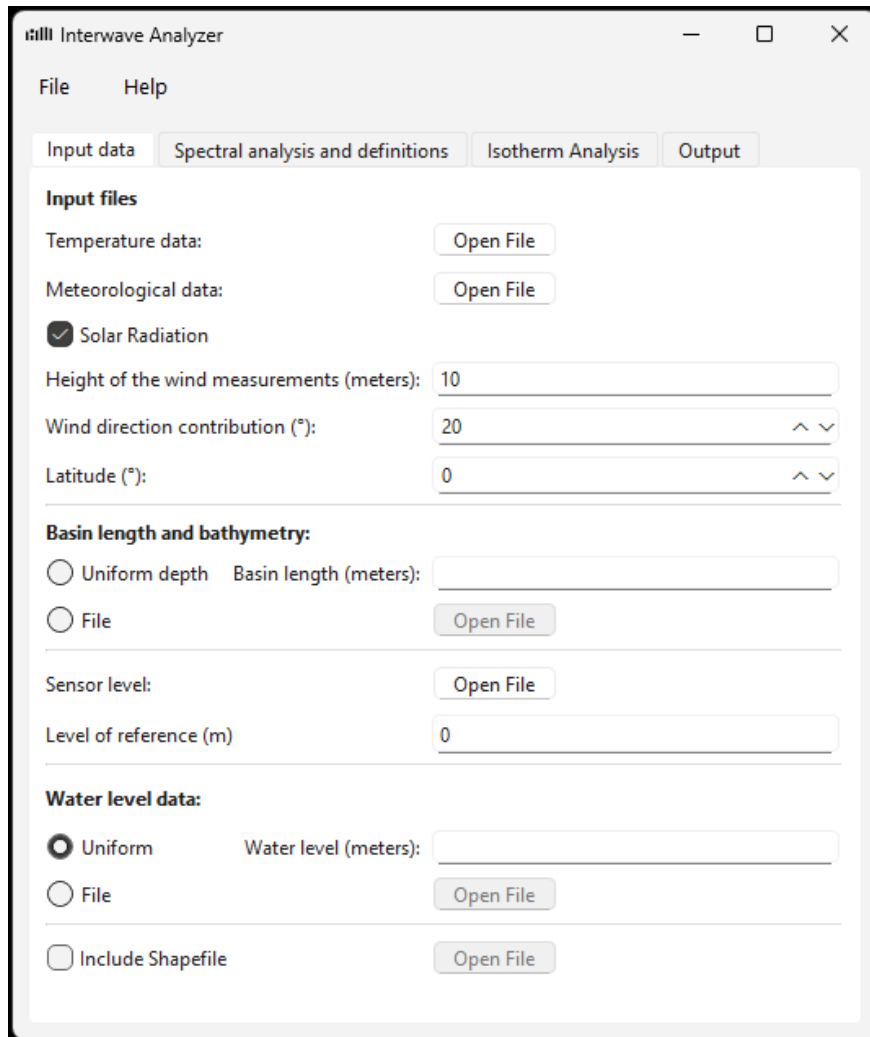
Figure 2: Main window Interwave Analyzer menu.

3.2 Main Configuration Tabs

The Interwave Analyzer interface is organized into four primary tabs: *Input data*, *Spectral analysis and definitions*, *Isotherm analysis*, and *Output and run*. Each tab includes fields that define analysis parameters and data sources. Settings can be saved or loaded using the *File* menu.

3.2.1 Input Data

The *Input data* tab (Figure 2) defines the files and parameters that describe the measurement setup, data structure, and environmental conditions used in the analysis.

Temperature data: A time series of water temperature (in °C) must be provided in a tab-delimited ASCII file with extension `.tem`. Each row represents one timestamp; the first row may contain a user-defined header. The first five columns must correspond to `Year, Month, Day, Hour, Minute`, followed by one column for each temperature sensor. The time step must remain constant throughout the file. An example file is shown in Figure 3.

13

Non-varying initial temperature values: `RuntimeWarning: invalid value encountered in double_scalars Ndeco=int(dt_decom/dt)`

This warning indicates that the first two temperature observations in the input time series are either identical or show no measurable variation over time. Such a condition prevents proper initialization of the temporal decomposition routine, which relies on detecting small variations in temperature to estimate the decomposition interval.

Recommended action: Verify the date and time of the first two records in your temperature file (`<tem>`). Ensure that consecutive timestamps are correctly spaced according to the defined temporal resolution. If the dataset begins with repeated or constant values (e.g., due to logger warm-up or calibration drift), remove or correct those records before running the analysis.

Missing or NaN temperature data: `UnboundLocalError: local variable 'idx' referenced before assignment`

This error occurs when the software encounters missing, non-numeric (`NaN`), or undefined temperature values during processing.

Recommended action: Inspect missing, non-numeric (`NaN`), or undefined values on temperature data provided for analysis.

Year	Month	Day	Hour	Minute	T1	T2	T3	T4	T5	T6	T7
2012	4	7	0	5	23.76	23.15	21.53	17.760	16.53	16.15	15.89
2012	4	7	0	20	23.76	23.02	21.4	17.760	16.53	16.15	15.89
2012	4	7	0	35	23.76	23.02	21.4	17.760	16.53	16.15	15.89
2012	4	7	0	50	23.76	23.02	21.4	17.890	16.53	16.15	15.89
2012	4	7	1	5	23.76	23.02	21.4	17.760	16.66	16.15	15.89

Figure 3: Example of file $<\text{tem}>$ with seven thermistors sampled every 15 min. The sixth column (first temperature column) corresponds to the sensor nearest the surface.

Unstable temperature profile: `ValueError: Digital filter critical frequencies must be 0 < Wn < 1`

This error indicates that the vertical temperature profile provided in the input data exhibits an unstable or non-physical structure, in which deeper sensors record higher temperatures than those closer to the surface. Such a configuration violates the assumption of a stably stratified water column required for spectral decomposition and internal wave modeling. Note, however, that the analysis itself can handle temporary physical instabilities. This error typically occurs when the temperature file has been constructed in the wrong vertical order (i.e., bottom-to-top instead of surface-to-bottom).

Recommended action: Carefully check the order and orientation of the temperature sensors in your input file (`<tem>`) and the corresponding sensor configuration file (`<sen>`). If the data were entered in reverse order (i.e., bottom-to-top), correct the sensor sequence in the input file or update the sensor configuration file accordingly.

Meteorological data: A file containing wind speed, wind direction, and optionally solar radiation, must be specified with extension `.met`. The file must be tab-delimited, with columns: `Year, Month, Day, Hour, Minute, Wind Speed (m/s), Wind Direction (°N)`, and optionally `Shortwave Radiation (W/m²)`. The

temporal resolution does not need to match the temperature data; interpolation is performed automatically. See Figure 4.

```
Year      Month   Day     Hour    Minute  Wind    Direction       Solar Rad.
2012      4       3       17      5       0       245.8   6.287
2012      4       3       17      10      0       232.1   13.146
2012      4       3       17      15      0.9     223.1   7.525
2012      4       3       17      20      0.1     236.8   10.34
2012      4       3       17      25      0       245     6.271
2012      4       3       17      30      0.4     227.9   8.779
2012      4       3       17      35      0.2     250.3   9.673
```

Figure 4: Example of file $<\mathrm{met}>$ with a 5-minute time step.

Incorrect or missing file reference: `ValueError:   could not convert string to float`

This error indicate that a file reference or path is incorrect, causing the program to read header lines or invalid data fields as numerical input.

Recommended action: Inspect the input files name and path.

Height of wind measurements: Height (in meters) above the water surface where wind was measured. Default: $10 \mathrm{~m}$.

Wind Direction Contribution: Defines the maximum allowable angular deviation from the dominant wind direction for a wind event to be considered dynamically coherent and capable of contributing to basin-scale internal wave (BSIW) generation.

By default, $\theta = 20°$, corresponding to an angular window of $\pm 20°$ around the mean wind direction. Only wind directions within this tolerance are considered part of the same homogeneous wind event.

This parameter is used specifically to identify **directionally persistent wind events** within the temporal analysis loop. It does not affect the computation of the Wedderburn number directly, but it determines whether a wind event is considered homogeneous enough to sustain internal seiche growth.

This parameter depends strongly on the geometry and principal axis orientation of the lake or reservoir. Values that are too large may overestimate homogeneous wind persistence, while values that are too small may artificially fragment sustained wind events. Improper configuration may indirectly affect the filtered Wedderburn numbers (filtering parameters). However, this will not affect derived standard stability metrics such as the Wedderburn and Richardson numbers

Latitude: Geographical latitude of the study site ($-90°$ to $+90°$). Used for Coriolis correction in the multi-layer model. Default: $0°$.

Basin Length and Bathymetry : The basin geometry can be specified in one of the following ways:

- **Uniform depth:** The user directly enters a constant depth value in the GUI. This option assumes a vertically uniform basin with constant length along the vertical.

- **File input:** The user provides a bathymetric file with extension `.len`, describing the vertical variation of basin length.

The bathymetry (`.len`) must be provided in a tab-delimited ASCII file with extension `.len`. Each row represents one vertical layer of the basin, ordered from the surface to the bottom. The file must contain three columns: layer depth in meters (H), basin length of the layer in meters (L_S), and the reference horizontal coordinate of the layer (used for slope computation). For clarification see Figure 5.

The first row may optionally contain a user-defined header. Data must be organized in ascending depth order, beginning near the surface and extending to the lake bottom.
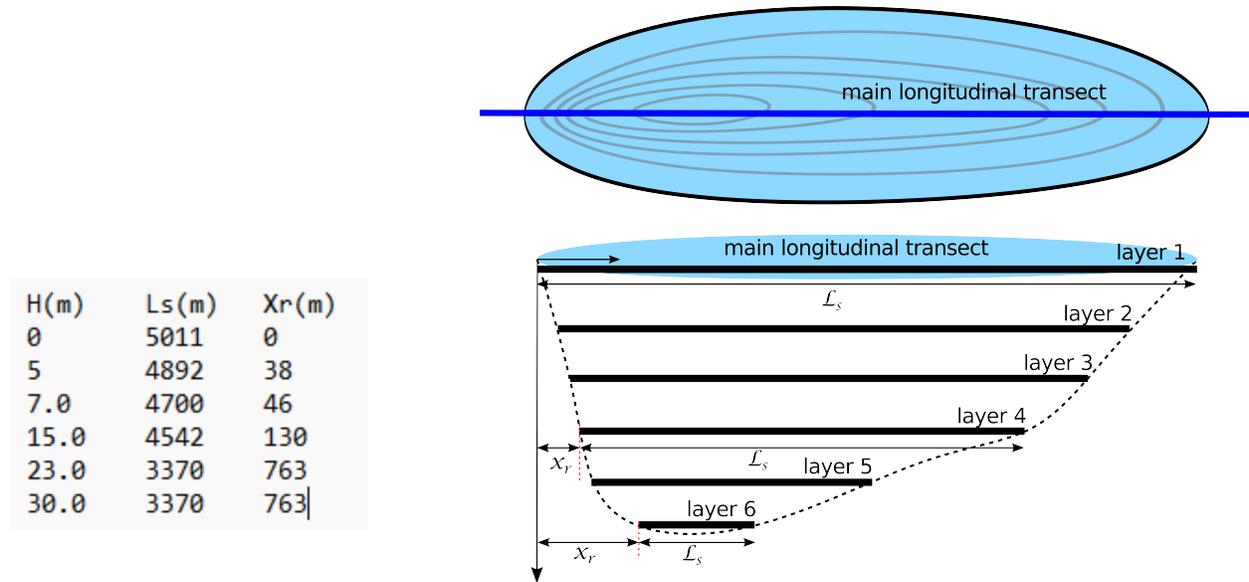


```
H(m)    Ls(m)   Xr(m)
0       5011    0
5       4892    38
7.0     4700    46
15.0    4542    130
23.0    3370    763
30.0    3370    763
```

Figure 5: Example of file $< \mathrm{len} >$ for 6 layers. Illustration and file format does not describe the same system, only similar number of layers.

The bathymetric information provided in the `.len` file is used in several key computations: Determination of the Lake Number, Computation of Schmidt Stability, and estimation of basin slope and geometric asymmetry, which influence internal seiche damping and energy dissipation. The vertical distribution of basin length directly affects the geometric response of the lake to wind forcing and internal wave persistence.

> ⚠️ The bathymetric file must cover the entire water column, from near-surface layers to the lake bottom. The first layer should be located close to the water surface and must represent the full surface basin length. The last layer should be located near the bottom and reflect the minimum basin length at maximum depth. Incomplete or improperly ordered depth coverage may result in inaccurate stability metrics and geometric parameter estimates.

> ⚠️ The computation methodology is conceptually similar to the Lake Analyzer framework; however, the Interwave Analyzer explicitly accounts for basin asymmetry. In this implementation, geometric layers are defined by horizontal lengths rather than areas. Internally, the software converts these lengths into equivalent cross-sectional areas assuming simplified geometries (circular or elliptical when a secondary transect is provided through additional parameters).

Sensor level: The depth information for each temperature sensor must be specified in here. The input must be a tab-delimited ASCII file with the extension `<sen>`. This file contains three columns:

- **Column 1:** Sensor index (integer), ordered from the surface downward.
- **Column 2:** Sensor position (in meters), whose meaning depends on the sensor specification (Column 3).
- **Column 3:** Sensor specification flag.

The first row is a user-defined header and can be customized freely.

Sensor specification flag The sensor specification (Column 3) defines how the sensor is mounted in the buoy chain and determines how its position should be interpreted:

- **Specification = 1 (free-moving sensor)** The sensor moves vertically with changes in water level, maintaining a constant depth *below the water surface*. Consequently, the value in Column 2 must represent the distance from the water surface to the sensor.
- **Specification = 2 (bottom-anchored sensor)** The sensor is fixed relative to the lake or reservoir bottom. In this case, the value in Column 2 must represent the distance from the bottom to the sensor. Because the bottom is the reference, these sensors do not move with water-level fluctuations.

Example: The Figure 6 illustrates an example `<sen>` input file. In this configuration, the buoy contains seven uniformly spaced thermistors (2 m between sensors), all free-moving with water level, plus one bottom-anchored thermistor located 2 m above the lakebed.
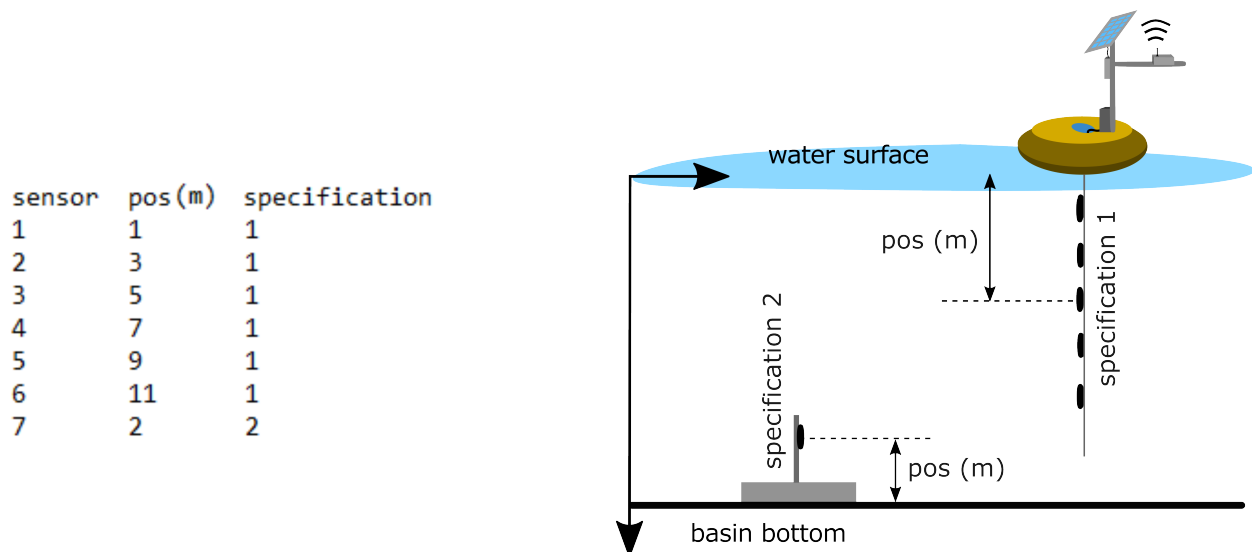


```
sensor  pos(m)  specification
1       1       1
2       3       1
3       5       1
4       7       1
5       9       1
6       11      1
7       2       2
```

Figure 6: Example of file $< sen >$. Illustration and file format does not describe the same thermistor chain.

Level of reference: Reference level (z_0) in meters, typically the lake bottom. Default: 0 m.

> The reference level must be defined consistently with the water level data. When water level variations are provided relative to mean sea level (MSL), the reference elevation may differ from zero. In such cases, the local bottom reference used in field measurements must be specified.

Water Level Data: Specifies the temporal variation of the lake or reservoir free-surface elevation (in meters). This parameter can be defined in two different ways:

- **Uniform value:** The user may enter a single constant value (float, in meters) directly in the GUI. This option assumes that the water level remains constant throughout the analyzed period.

- **File input:** The user provides a time series file with extension `.niv`, containing measured water level data.

The water level time series must be provided in a tab-delimited ASCII file with extension `.niv`. The first five columns must correspond to `Year`, `Month`, `Day`, `Hour`, `Minute`, followed by `Water Level (m)` (Figure 7). Water level values must be expressed in meters and referenced consistently throughout the dataset.

```
Year   Month   Day    Hour    Minute   Water Level
2012   1       1      0       0        814.369
2012   1       1      0       15       814.368
2012   1       1      0       30       814.367
2012   1       1      0       45       814.366
2012   1       1      1       0        814.364
```

Figure 7: Example of file $<\mathrm{niv}>$ using a 15-minute interval.

Water level values must be referenced to the user-defined level of reference. Example: if the total depth is 11 m and the reference level is 799 m, the input level must be $799 + 11 = 810$ m.

Include Shapefile: The current version of the *Interwave Analyzer* does not yet support the direct inclusion of lake shapefiles. This option is reserved for future releases and is displayed for compatibility with planned developments. In forthcoming versions, the integration of georeferenced lake shapefiles (e.g., `.shp` format) will allow a more detailed geometric characterization of the basin. This enhancement will enable spatially explicit computations based on the real shoreline configuration and bathymetric contours.

Shapefile integration is not available in the current release. Users must keep this option unselected. If a `.shp` file is provided, the program will not crash; however, the shapefile will not be loaded or used in any computation, and it will be ignored by the current version of the software.

3.2.2 Spectral Analysis and Definitions

In the *Spectral analysis and definitions* tab (Figure 8), the user specifies all parameters related to spectral analysis, signal filtering, and density structure characterization. These settings control how temperature data are processed and how internal wave dynamics are quantified.

Metalimnion thresholds: This parameter defines the minimum vertical density gradient (in $\mathrm{kg\,m^{-3}\,m^{-1}}$) required for a water layer to be classified as stratified. It is used to identify the upper and lower boundaries of the metalimnion from the computed density profile. The default value is 0.1 $\mathrm{kg\,m^{-3}\,m^{-1}}$. Lower threshold values result in a thicker metalimnion, as weaker density gradients are considered part of the stratified layer. Conversely, higher threshold values restrict the classification to regions of stronger stratification, producing a thinner and more sharply defined metalimnion.
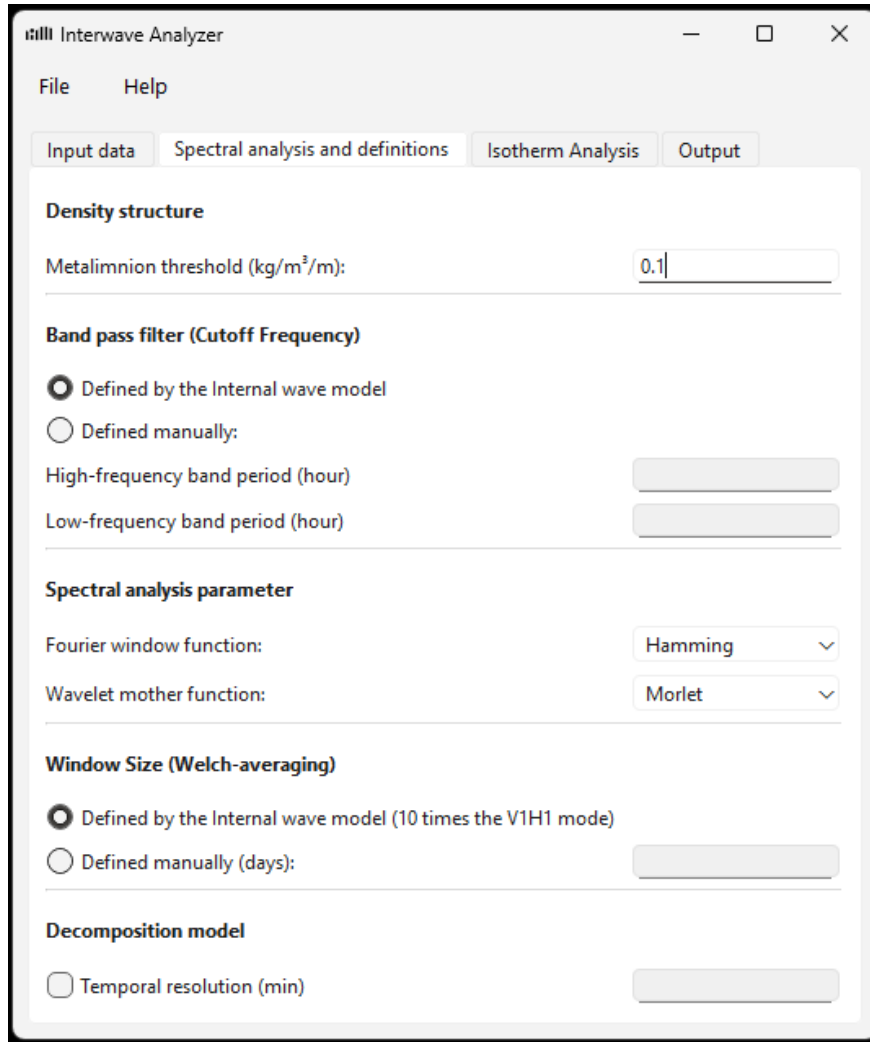
Figure 8: Interwave Analyzer — Spectral analysis and definitions tab.

> ⚠️ This parameter is applied exclusively during the detection of metalimnion thickness from the vertical density gradient. However, because the identified metalimnion limits are subsequently used in additional stability and internal wave calculations, the selected threshold may indirectly influence other derived parameters. In particular, the classification of internal seiche degeneration regimes (internal seiche damping) and the computation of dimensionless stability metrics such as the Lake Number can be sensitive to the chosen metalimnion gradient threshold.

Band-pass filter: The band-pass filter is applied to temperature time series prior to spectral analysis. Two configuration modes are available:

- **Automatic mode:** The cutoff frequencies are computed automatically based on the fundamental internal seiche period estimated from the decomposition model. The model derives the internal seiche period from basin-scale geometry and the dominant wind fetch. The upper and lower cutoff frequencies are then determined using the minimum and maximum wave period computed from the standard deviation of wave period considering the whole period of analysis.

- **Manual mode:** The user specifies both cutoff periods manually (in hours). The high-frequency cutoff must correspond to the smaller period, and the low-frequency cutoff to the larger period.

> ⚠️ The automatic filter assumes that internal waves are dominated by the fundamental baroclinic mode. If higher vertical modes are significant, or if the estimated fundamental period is inaccurate, some internal wave energy may be excluded from the filtered temperature signal. This limitation does not affect the unfiltered power spectral density analysis, only the band-passed time-series.

> ⚠️ When specifying cutoff periods manually, both limits (high and low) must be defined. The high-frequency period must always be shorter than the low-frequency period.

Fourier window function: This option defines the window function used in the Fourier transform, affecting spectral leakage and frequency resolution. Four window types are available: Hamming, Hann, Blackman, and Flattop. Each function offers a different trade-off between main-lobe width and side-lobe attenuation. A detailed comparison and theoretical discussion of these window functions can be found in [1].

Wavelet mother function: This setting selects the mother wavelet used in the continuous wavelet transform. Available options are: Morlet, Paul, and DOG (Derivative of Gaussian). Wavelet analysis extends the time series to the next power of two ($N = 2^n$) by zero-padding. The discrete scale spacing is fixed at 0.25, and the smallest scale is automatically set to twice the sampling interval of the temperature data. These defaults provide good temporal and frequency resolution for detecting internal wave events. For details, consult the *wavelib.py* module.

Window size (Welch-averaging): The window size used for Welch-averaged spectral estimation can also be set in two modes:

- **Automatic mode:** The window length is defined as ten times the fundamental internal seiche period estimated by decomposition model. If the dataset is too short to meet this criterion, only one window is applied (no averaging performed).
- **Manual mode:** The user specifies the window length directly (in days).

Larger windows increase frequency resolution but reduce the number of independent averages. The selected value is reported in the diagnostic file.

Decomposition model: The decomposition model computes the vertical structure of basin-scale internal seiches based on the observed stratification profile and estimates the associated horizontal velocity fields (in arbitrary units) for the first five baroclinic modes. To reduce computational cost, the user may optionally define a coarser temporal grid for the decomposition procedure without modifying the original temperature data resolution.

If desired, the *Temporal resolution* option can be enabled to specify a custom time step (in minutes) for the modal decomposition. When this option is disabled, the model adopts the native temporal resolution of the input temperature dataset. The temporal resolution must be an integer multiple of the sampling interval. If a non-multiple value is entered, the program automatically rounds it to the next valid multiple and reports the adjustment in the *diagnose file*.

Reducing the temporal resolution of the decomposition model directly affects the temporal representation of vertical velocities, modal structures, thermocline depth estimates, and internal seiche periods. For subsequent analyses that rely on these variables, such as internal seiche damping over sloping topography, the internal seiche periods (for different vertical modes) and thermocline depth are linearly interpolated onto the original temperature time grid. Consequently, some output variables may retain the native resolution of the temperature dataset, even though they are derived from decomposition results computed at a coarser temporal resolution. Users should carefully evaluate the trade-off between computational efficiency and temporal accuracy.

If the specified temporal resolution is smaller (i.e., finer) than the sampling interval of the temperature data, the program automatically resets it to the native resolution and records a warning in the *diagnose file*.

3.2.3 Isotherm Analysis

The *Isotherm analysis* tab (Figure 9) defines parameters related to isotherm-based spectral diagnostics and sensor-specific analyses. Here, the user selects which temperature isotherms and thermistor sensors will be included in the analysis, as well as the pairs of isotherms for which phase and coherence relationships are computed.

Isotherm analysis: In this section, the user specifies the isotherms (in $°C$) to be used for spectral, phase, and coherence analyses. Up to four isotherms can be defined simultaneously to reduce computational cost and memory usage. Each selected isotherm corresponds to a constant-temperature contour derived from the temperature–depth profile.

Phase and coherence calculations between the selected isotherms and the meteorological data (e.g., wind speed and direction) are automatically performed using **Isotherm 2** as the reference series. If **Isotherm 2** is not defined, the phase and coherence analysis involving meteorological forcing is skipped automatically.

The user may also specify up to two pairs of isotherms to compute inter-isotherm phase shifts and coherence functions. Both isotherms in each selected pair must be defined in the isotherm list.

If a phase or coherence comparison is requested for an isotherm that has not been defined, the resulting plots will be blank and flagged in the diagnostic file.

Sensor analysis: This option enables spectral or fluctuation analysis based on temperature records from specific sensors at fixed depths. Up to four thermistor sensors can be selected for this purpose. Sensor indices correspond to the order in which they are declared in the input temperature file (`<tem>`). The index starts at *1* for the sensor closest to the water surface, increasing with depth.

Sensor index out of bounds — `IndexError: index [specified sensor number] is out of bounds for axis 0 with size [total number of sensors].`

This error is raised when the user selects a sensor index that does *not* exist in the input `<sen>` file. In other words, the specified sensor number exceeds the total number of sensors loaded into the Interwave Analyzer.

Recommended action: Verify that the sensor index selected in the GUI corresponds to a valid sensor listed in the `<sen>` file. Correcting the sensor numbering or selecting a valid index will resolve the issue.
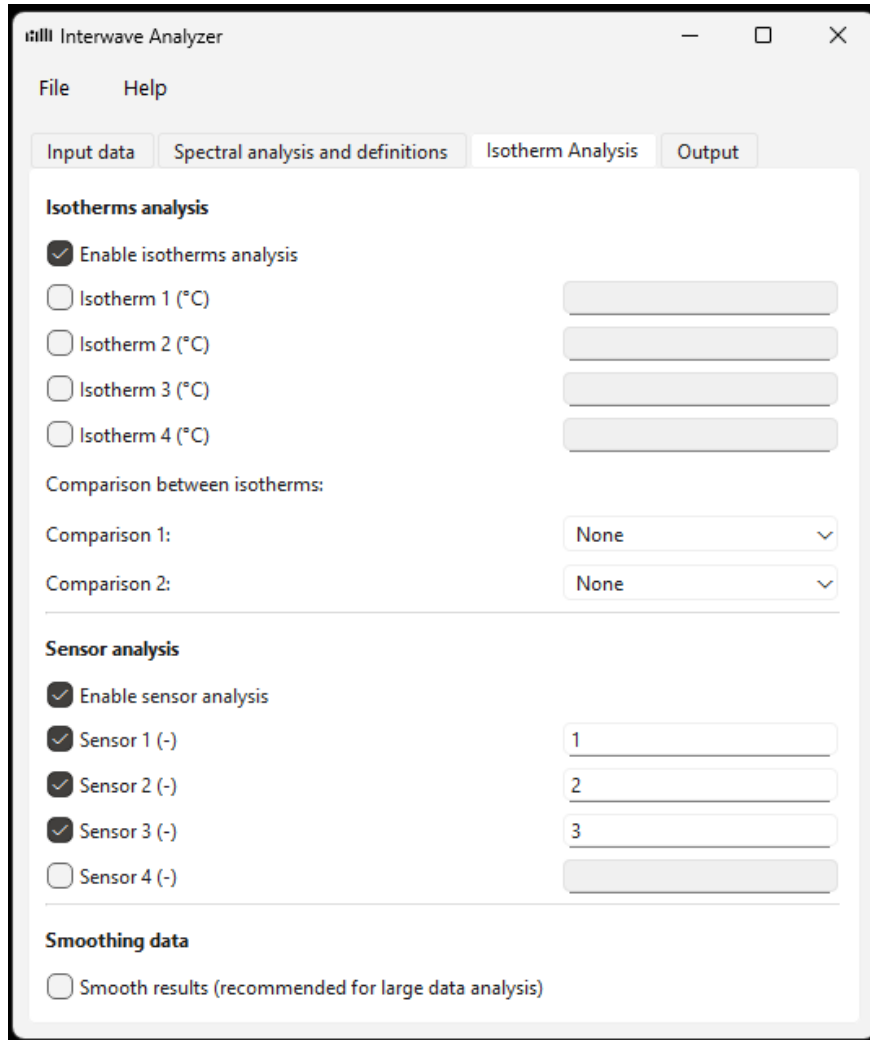
Figure 9: Interwave Analyzer — Isotherm analysis tab.

Smooth results: Activating the *Smooth results* checkbox applies temporal smoothing to the extracted isotherm time series, reducing data length and computational effort for extremely long datasets. However, smoothing may attenuate high-frequency oscillations associated with internal wave dynamics.

> ⚠️ For internal wave and high-frequency spectral analysis, it is recommended **not** to enable smoothing. Use this option only for long-term trend analysis or when computational constraints are significant.

3.2.4 Output and Run

The *Output and Run* tab (Figure 10) allows the user to define the output directory, configure the quality of generated figures, adjust additional model parameters, and finally execute the complete analysis routine. All selected configurations from previous tabs are processed sequentially once the run command is initiated.
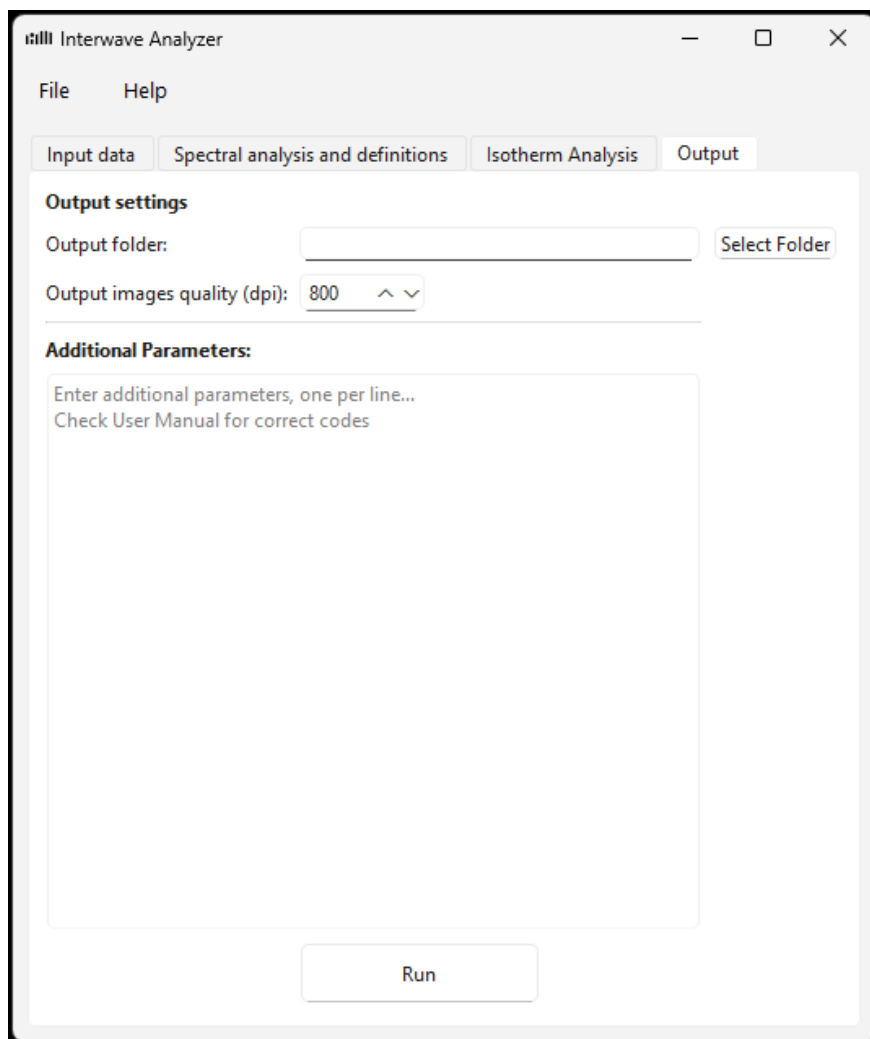
Figure 10: Interwave Analyzer — Output and Run tab.

Output folder: Click on the *Select Folder* button to choose the directory where all output files and subfolders will be saved. The program will automatically create the required folders for figures, text files, and diagnostic reports.

Output image quality (DPI): Here, the user specifies the resolution of the generated plots in Dots Per Inch (DPI). The accepted range is between 50 and 1000 DPI. Higher DPI values yield publication-quality figures but significantly increase processing time and storage size.

> ⚠️ For images with DPI values greater than 250, the computation and rendering time can increase considerably, especially for large datasets.

Additional parameters: This section introduces a flexible framework designed to activate supplementary tools, analysis modules, or diagnostic features without requiring modifications to the graphical user interface. New functionalities implemented in future versions of the Interwave Analyzer will be enabled through this mechanism,

allowing users to selectively activate advanced capabilities while maintaining backward compatibility and interface stability. The list with all currently available additional parameters are available in section 4. Note that this list is not fixed; parameters may be added, removed, or revised in subsequent releases as new modules, analyses, or computational features become available. Each Additional parameter is characterized by a keyword and a value, in which keywords are CASE-sensitive. The value is often the name of an attribute file and must be enclosed between #'s. Some features implemented via keywords may require more than one single keyword

Run: The *Run* button initiates the complete analysis process. Before clicking, verify that all input files, variables, and parameters are correctly defined across all tabs. Once executed, an active progress panel appears (Figure 11, displaying the current stage of computation (e.g., spectral analysis, decomposition, output generation).
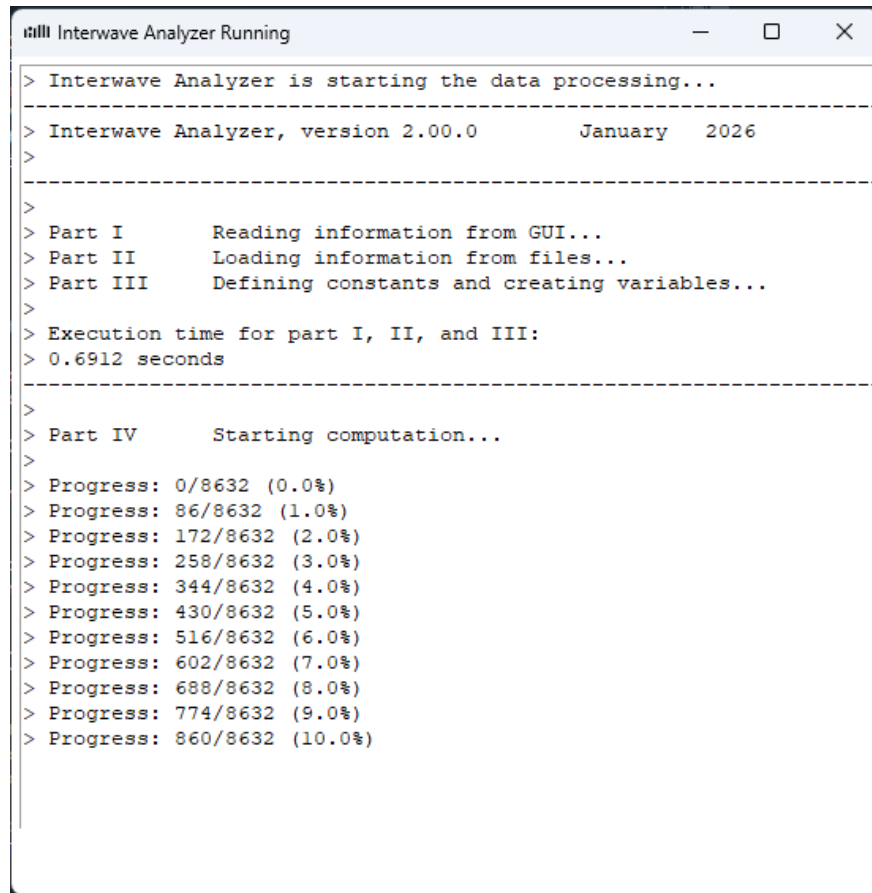

```
> Interwave Analyzer is starting the data processing...
-----------------------------------------------------------------
> Interwave Analyzer, version 2.00.0          January    2026
>
-----------------------------------------------------------------
>
> Part I        Reading information from GUI...
> Part II       Loading information from files...
> Part III      Defining constants and creating variables...
>
> Execution time for part I, II, and III:
> 0.6912 seconds
-----------------------------------------------------------------
>
> Part IV       Starting computation...
>
> Progress: 0/8632 (0.0%)
> Progress: 86/8632 (1.0%)
> Progress: 172/8632 (2.0%)
> Progress: 258/8632 (3.0%)
> Progress: 344/8632 (4.0%)
> Progress: 430/8632 (5.0%)
> Progress: 516/8632 (6.0%)
> Progress: 602/8632 (7.0%)
> Progress: 688/8632 (8.0%)
> Progress: 774/8632 (9.0%)
> Progress: 860/8632 (10.0%)
```

Figure 11: Active progress panel.

During long computations or when using large datasets, the GUI may temporarily appear unresponsive or "frozen." This behavior is normal, the process continues to run in the background. All real-time messages, errors, and warnings are simultaneously printed in the black terminal window.

> ⚠ If the progress window stops updating for an extended period but no error message appears in the black terminal window, the software is still processing normally. Only terminate execution if explicit error messages are displayed.

After successful completion, the software saves:

- All figures in the chosen output folder (in PNG or PDF format);

- Numerical results and diagnostic data in the automatically generated `textfiles` subfolder;

- A summary log of the execution process.

4 Additional Parameters

The *Additional Parameters* section provides optional configuration keywords that allow advanced customization of basin geometry, orientation, and visualization. These parameters are not required for standard model execution; however, they enable enhanced geometric representation and more detailed physical interpretation, particularly in morphologically complex or asymmetric basins.

Additional parameters are defined through keywords specified prior to execution. When not provided, default values are automatically assigned. These options are intended for advanced analyses in which basin asymmetry, directional alignment, or metadata specification may influence internal wave characterization and stability metrics.

Table 2: Additional parameters available in the Interwave Analyzer.

Keyword	Value	Description	Default
nameBasin	#name#	Name of the analyzed lake or reservoir. Displayed in dashboard panels and exported outputs. Does not affect calculations.	"No name"
pathBathy	#file.len#	Optional secondary bathymetric transect file (90° relative to the main transect) used to represent basin asymmetry and enable three-dimensional geometric approximation (elliptical cross-sections). The file must be located in the same directory as the primary .len file specified in the Basin Length tab of the GUI.	None
changeBasin	#angle#	Rotation angle (degrees) applied to the principal basin axis to control directional wind–fetch alignment and geometric orientation.	270°

4.1 nameBasin

The parameter nameBasin defines the name of the lake or reservoir being analyzed. This identifier is displayed exclusively in graphical dashboard panels and exported visual outputs.

This parameter has no influence on numerical computations, stability metrics, or internal wave calculations. If not specified, the system automatically assigns the default label "No name".

4.2 pathBathy

The pathBathy parameter allows inclusion of an additional bathymetric transect (extension .len) oriented 90° relative to the primary transect (Figure 12).

When only a single transect is provided, the basin geometry is treated as vertically variable but horizontally symmetric (plane x-y). In this configuration, each depth layer is internally represented as a circular cross-section, and geometric quantities such as volume, stability, and restoring forces are derived assuming radial symmetry.

When a second transect is specified via pathBathy, the software combines both longitudinal and transverse length profiles to approximate basin asymmetry. In this configuration, each vertical layer is internally represented as an ellipse rather than a circle. This refinement enables a more realistic three-dimensional geometric approximation.

The inclusion of the secondary transect improves the estimation of basin volume distribution, enhances the computation of Schmidt Stability and Lake Number, refines the representation of internal seiche damping influenced by lateral geometry, and modifies effective wind fetch as a function of wind direction.

Under this configuration, wind fetch becomes direction-dependent. Consequently, the effective basin length governing internal seiche dynamics varies with wind orientation. This allows the possibility of transversal internal

```
H(m)    Ls(m)   Xr(m)
0       5011    0
5       4892    38
7.0     4700    46
15.0    4542    130
23.0    3370    763
30.0    3370    763
```

```
H(m)    Ls(m)   Xr(m)
2.5     1000    0
7.0     600     200
15.0    300     350
23.0    200     400
30.0    100     450
```
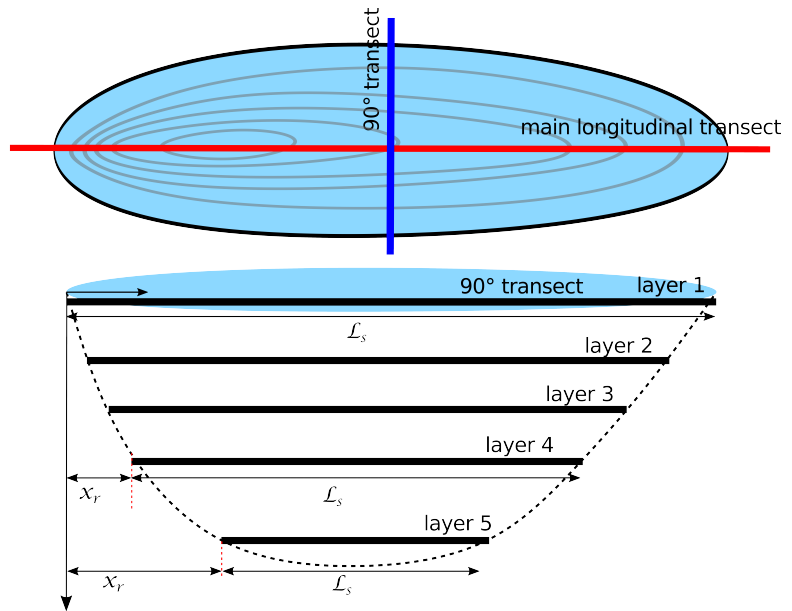
Figure 12: Example of file $< \mathrm{len} >$ for the second transect. Illustration and file format do not represent the same system.

waves, which may exhibit shorter oscillation periods compared to those associated with the principal longitudinal axis.

The use of `pathBathy` is particularly recommended for elongated or morphologically asymmetric reservoirs where cross-basin geometry significantly influences internal wave dynamics and stability behavior.

4.3   changeBasin

The `changeBasin` parameter defines the angular rotation (in degrees) applied to the principal basin axis (Figure 13. This parameter controls the geometric alignment between the main basin axis, the wind direction, and the effective wind fetch used in internal wave and stability calculations.

> This parameter only affects calculations when `pathBathy` is defined. If only a single transect is provided, the basin is internally treated as circular and rotationally symmetric; therefore, axis rotation does not modify the results.

The default value of $270°$ assumes a conventional east–west orientation of the principal basin axis. However, natural lakes and reservoirs frequently present arbitrary orientations relative to geographic north. Adjusting this parameter rotates the internal geometric reference system, ensuring that wind forcing is properly projected onto the dominant longitudinal axis.

This rotation influences effective wind fetch computation, internal wave period estimation, wind direction contribution filtering, homogeneous wind event detection, Wedderburn Number estimation, Lake Number computation, and theoretical classification of mixing regimes and internal seiche degeneration.

Users should define `changeBasin` according to the geographic orientation of the main basin axis relative to true north.
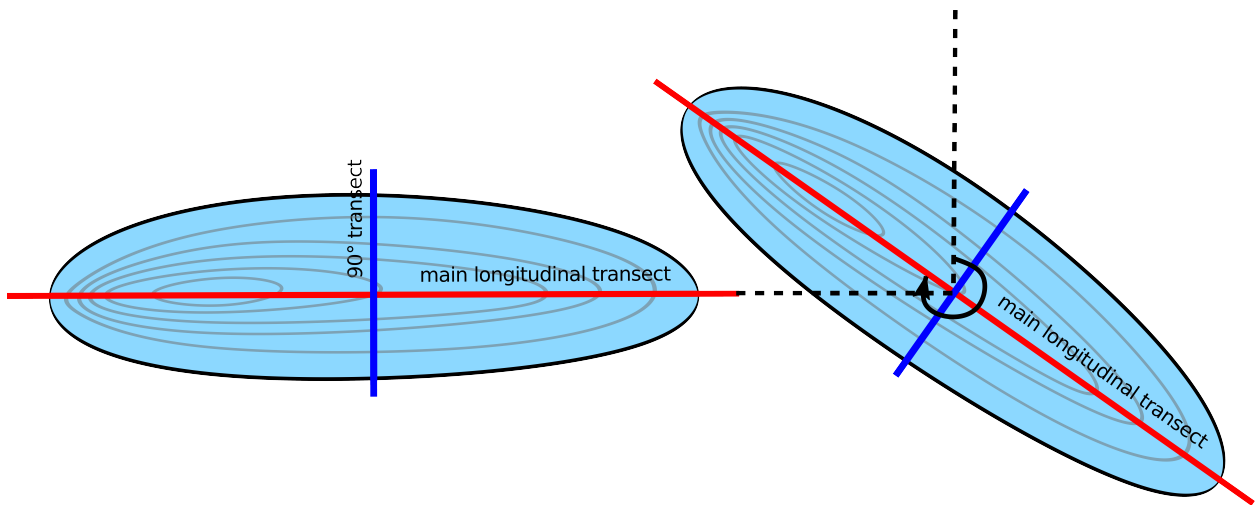
27

Figure 13: Example of basin rotation using the additional parameter `changeBasin`

5 Interwave Analyzer results

The *Interwave Analyzer* generates results in three complementary formats: structured text files, graphical figures (PNG format), and an interactive dashboard interface. These outputs are designed to support both scientific analysis and technical reporting, allowing users to access numerical values, visual diagnostics, and dynamic exploration of internal wave dynamics.

All results are automatically saved in the output directory defined during execution. Text files provide quantitative values suitable for post-processing, while PNG figures summarize diagnostic plots. The dashboard offers an interactive environment for exploratory analysis and rapid visualization.

5.1 Text File Outputs

Text files are exported in tab-delimited ASCII format and contain processed time series, stability parameters, dimensionless numbers, and derived quantities. These files are suitable for further statistical analysis or integration into external modeling frameworks.

Table 3: Text files generated by the Interwave Analyzer.

File Name	Description
bandpass_isoX	Time series of isotherm fluctuations (m) relative to the mean, filtered between cutoff frequencies defined in the GUI or estimated by the decomposition model based on the standard deviation range of the theoretical internal wave period. X denotes the isotherm selected in the GUI.
bandpass_senX	Time series of temperature fluctuations (°C) relative to the mean, filtered between cutoff frequencies defined in the GUI or estimated by the decomposition model. X denotes the sensor number (counted from the surface downward) selected in the GUI.
basin_length	Time series of effective basin length determined from wind direction. This series remains constant when `pathBathy` is not defined in the Additional Parameters.
buoyancy	Time series of mean buoyancy frequency (Hz) computed using two approaches: (1) based on layered mean density and epilimnion thickness; and (2) based on maximum–minimum density contrast and total water depth. See Section 6.1.5 for details.
cpzinho_modeX	Stratification-weighted vertical mode structure (N^2w) at each depth, computed using the refined vertical grid from the decomposition model ($N = 100$). X indicates the vertical mode (V1–V5).
internalseiche_periods	Time series of internal seiche periods (hours) for the first five vertical modes derived from the decomposition model.
isothermsX	Time series of selected isotherm elevations (m above bottom/reference level). X denotes the isotherm defined in the GUI.
mab_decomp	Refined vertical grid (m above bottom) generated by the decomposition model ($N = 100$).
mab_decomp_original	Original vertical grid resolution (m above bottom) corresponding to the sensor depths.
mean_buoyancy	Time-averaged vertical profile (m above bottom) of buoyancy frequency (Hz), including 95% confidence intervals and standard deviation limits.
mean_profile	Time-averaged vertical temperature profile (°C, m above bottom), including 95% confidence intervals and standard deviation limits.
metalimnion_thickness	Time series of metalimnion thickness (m), estimated using the Maximum Density Gradient Method.

File Name	Description
modeX_interfaces	Time series of interface depths (m above bottom) for vertical mode X. Higher modes include additional interface levels (additional columns).
modeX_layers	Time series of layer thicknesses associated with vertical mode X. Higher modes include a greater number of layers.
rednoise_isothermsX	Confidence limits of the power spectral density (m^2/Hz) for isotherm X. The first column contains frequency (Hz).
richardson	Depth-resolved Richardson number (-). Rows correspond to time (hours since the beginning of the simulation), and columns correspond to refined depth levels (m above bottom).
sensorX	Time series of temperature (°C) recorded at sensor X.
spectral_isothermsX	Power spectral density (PSD) of isotherm X. The first column contains frequency (Hz).
spectral_sensorX	Power spectral density (PSD) of temperature at sensor X. The first column contains frequency (Hz).
spectral_wind	Power spectral density (PSD) of wind speed. The first column contains frequency (Hz).
stability	Time series of stability parameters, including Richardson number (Ri), Wedderburn number (W), lower and upper Wedderburn thresholds for internal seiche dominance (Wmin, Wmax), direction-filtered Wedderburn number (Wfilt), Schmidt Stability, and Lake Number.
thermo_psdX	Power spectral density (°C^2/Hz) of temperature at the thermocline depth (identified using the Maximum Density Gradient Method). The first column contains period (h).
thermo_psd_siginificance	Confidence limits of the thermocline PSD (°C^2/Hz). The first column contains frequency (Hz).
thermo_wavelet	Wavelet power spectrum of temperature at the thermocline depth. Columns represent periods (see thermo_wavelet_period.txt), and rows represent time.
thermo_wavelet_period	Periods (h) corresponding to the thermocline wavelet analysis.
thermocline	Time series of thermocline depth (m).
thermocline_temperature	Time series of temperature (°C) at the thermocline depth.
time_decomp	Time array (hours since the beginning of the analysis) corresponding to the decomposition resolution defined in the GUI. If unchanged, it matches the original temperature time grid.
uarbit_decomp_modeX	Time series of horizontal velocity structure for vertical mode X at each refined depth level ($N = 100$). X ranges from V1 to V5.
watercond_mode1	Time series of mean epilimnion and hypolimnion densities (kg/m^3), together with their respective layer thicknesses estimated using the Density Gradient Method.
wd_event	Time series of wind diagnostics related to internal seiche dominance and mixing regimes. "Literature" indicates mean wind direction during moderate Wedderburn regimes ($W < 20$), whereas "Spigel" denotes the same quantity under stricter theoretical limits (see Section 6.5.1). nan indicates periods that do not satisfy the specified criteria. "Homogeneous" denotes persistent wind-direction events (value 357 is used as a continuity flag). fdire represents the directional reduction factor; low values indicate weak directional persistence.
wind	Time series of wind speed and direction interpolated onto the temperature time grid.

5.2 PNG Figure Outputs

Graphical results are automatically exported in PNG format. These figures summarize the main diagnostics of stratification, wind forcing, internal wave response, and spectral characteristics.

Table 4: PNG figures generated by the Interwave Analyzer.

Figure Name	Description
buoyancy	Time series of buoyancy frequency (Hz) over depth. The water surface and thermocline are indicated by blue and red lines, respectively. The thermocline interface is computed using the Maximum Density Gradient Method.
classification_evolution	a) Theoretical relationship between normalized internal seiche amplitude (A/h_e) and the Wedderburn number according to different formulations. The normalized internal seiche amplitude (markers) were computed based on time-averaged epilimnion thickness and maximum band-pass filtered isotherm displacement. The Wedderburn number is averaged over windows corresponding to either one-eighth of the fundamental period (W_{V1H1}) or one-eighth of the wind-event duration (W_{wind}); the minimum averaged value is retained as the critical wind–stratification condition. b) Influence of higher-order h_e/H effects on internal seiche amplitude.
coherence	Magnitude-squared coherence and phase shift between selected isotherms defined in the GUI.
degenera	a) Averaged degeneration regime of internal seiches in the parameter space defined by h_e/H and $1/W$. Theoretical instability limits (e.g., dissipative steepening, bore limit, Kelvin–Helmholtz) are shown as reference curves. Ellipses represent the mean state and 95% variability for three subperiods (P1–P3). b–d) Theoretical lake mixing regimes for each subperiod.
degeneration_evolution	Temporal evolution of the degeneration regime in the h_e/H versus $1/W$ parameter space, shown as a time series relative to theoretical instability limits for selected subperiods.
depth_bandpass	Band-pass filtered temperature fluctuations (°C) relative to the mean, using frequency limits defined in the GUI or estimated from the decomposition model.
iso_bandpass	Band-pass filtered isotherm displacements (m) relative to the mean, using user-defined or model-estimated frequency limits.
isoX	a) Time series of isotherm X, b) corresponding wavelet spectrum. The y-axis represents oscillation period (h), and the x-axis represents time.
isotherms	Time series of selected isotherm elevations (m above bottom or reference level).
mean_temperature	Time-averaged a) temperature and b) buoyancy frequency profiles, including standard deviation and 95% confidence intervals. Negative buoyancy frequency values indicate locally unstable stratification.
meteo_spectra	Power spectral density (PSD) of wind speed.
mode_period	Time series of theoretical internal seiche periods for the first five vertical modes (V1–V5) estimated with the decomposition model.
psd	a) Power spectral density (PSD) and b) variance-preserving PSD of isotherms with 95% confidence limits. Vertical bars indicate theoretical modal periods. Shaded widths represent temporal variability. Dashed lines denote Coriolis (low-frequency) and mean buoyancy frequency (high-frequency) limits.

31

Figure Name	Description
psd_coriolis_depth	PSD of temperature fluctuations with 95% confidence limits. a) Theoretical modal periods, b) modal periods corrected for Coriolis effects. Dashed lines denote Coriolis (low-frequency) and mean buoyancy frequency (high-frequency) limits.
psd_hydro_coriois	PSD of isotherms with 95% confidence limits. a) Theoretical modal periods, b) modal periods including Coriolis correction. Dashed lines denote Coriolis (low-frequency) and mean buoyancy frequency (high-frequency) limits.
psd_multi	Vertical distribution of temperature PSD as a function of frequency and depth. The contour map shows spectral energy, and vertical lines indicate forcing, buoyancy, and theoretical modal frequencies (V1H1 and V2H1).
psd_nonhydro	a) PSD of isotherms with 95% confidence limits and theoretical modal periods (V1–V3). b) Coherence between wind spectra and the second selected isotherm, indicating potential wind–seiche resonance.
richardson	a) Time series of the standard Wedderburn number, with the shaded region indicating the internal seiche dominance range. b) Local Richardson number with thermocline and surface references.
schmidt	Time series of Schmidt Stability (J m^{-2}).
sensitivity_fundamental	Two-layer sensitivity analysis of the fundamental internal seiche period (V1H1) to variations in ρ_e, ρ_h, h_e, and h_h, showing the period response to controlled perturbations around the mean state.
sensitivity_parameters	Sensitivity of the fundamental period to dimensionless depth and density parameters. Theoretical curves are shown with shaded regions representing admissible modal ranges (green) and 99% confidence intervals (gray).
sensorX	a) Temperature time series for sensor X. b) Corresponding wavelet spectrum. The y-axis represents oscillation period (h).
stability	Time series of a) wind stress and b) Wedderburn (blue) and Lake Number (red).
structure_thermo	Time series of mean epilimnion and hypolimnion densities, include maximum (water bottom) and minimum (water surface) water densities.
temperature_depth	Time series of temperature for all sensors, highlighted sensors correspond to those selected in the GUI. The legend indicates height above bottom.
temporal_analysis	Wind diagnostics related to internal seiche dominance and mixing regimes. Green lines represent mean wind direction within moderate Wedderburn ranges, red lines indicate stricter theoretical limits, and blue bars denote persistent directional events.
tempstructure	Time–depth diagram of water temperature. The black line indicates thermocline depth, and gray lines represent metalimnion boundaries derived from the decomposition model.
tempstructure-multi	Time–depth temperature diagram with thermocline depth computed using both the decomposition model (black) and the Maximum Density Gradient Method (red).
thermocline_analysis	Analysis of temperature at thermocline depth, including a) time series, b) wavelet spectrum, and c) PSD.
thorpe_scale	Time series of a) Thorpe scale and b) Thorpe displacement.
velocity_arbitrary_modeX	Time series of horizontal velocity structure for vertical mode X at each refined depth ($N = 100$). The theoretical mean modal period is indicated.
wedd_filtering	Time series of the standard and directionally filtered Wedderburn numbers. The shaded region indicates the internal seiche dominance range.
wind	Time series of wind speed and direction interpolated onto the temperature time grid.

Figure Name	Description
wind_resonance	Wavelet transform of wind speed. Black and red lines indicate theoretical internal seiche periods for vertical modes 1 and 2, respectively, used to identify resonance conditions.

5.3   Interactive Dashboard

In addition to static outputs, the Interwave Analyzer provides an interactive dashboard developed using Plotly visualization framework. Although the dashboard does not have all results generated by Interwave Analyzer, the dashboard enables dynamic exploration of stratification dynamics, wind forcing, and internal wave behavior without requiring post-processing of exported files.

The dashboard is automatically launched upon completion of the analysis and typically opens in the system's default web browser. For subsequent access, all processed data required to reconstruct the interface are automatically stored in a file named `dash_data.npz`, located in the same directory as the generated PNG figures. The dashboard can be reopened at any time through the GUI menu via:

`Help > Dashboard`

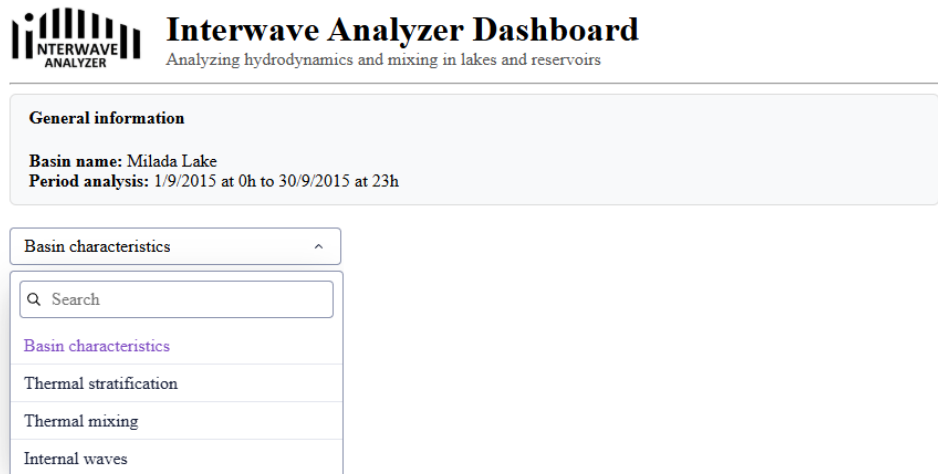The interface is organized into four primary tabs (Figure 14), each dedicated to a specific analysis domain.

Figure 14: Main interface of the Interactive Dashboard, illustrating the four primary analysis tabs: Basin Characteristics, Thermal Stratification, Thermal Mixing, and Internal Waves.

1. Basin Characteristics

This tab presents the geometric representation and morphometric properties of the studied basin. The left panel displays the two-dimensional longitudinal transect, illustrating depth variation along the principal axis. The right panel provides a three-dimensional visualization of basin geometry (Figure 15). When only a single transect is available, the basin is internally approximated using circular layers; if a secondary transect is supplied via `pathBathy`, an elliptical representation is adopted to account for transversal asymmetry.

Below the geometric panels, the time series of effective wind fetch (basin length) is presented (Figure 16). If a secondary transect is defined, fetch dynamically varies with wind direction; otherwise, it remains constant. When a time step is selected in the fetch time series, the corresponding wind direction is displayed in the 2D basin map above.
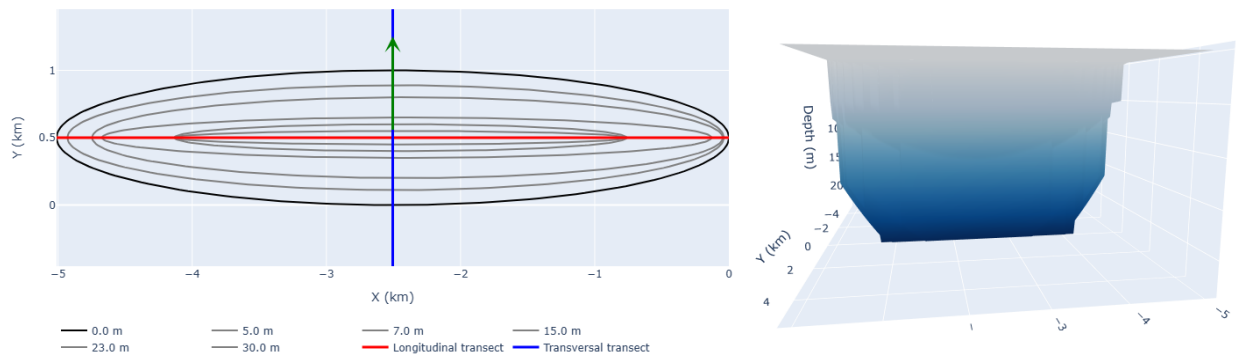
Figure 15: Basin geometry visualization. Left: two-dimensional longitudinal transect of depth. Right: three-dimensional representation of basin morphology. When a secondary transect is provided, the 3D geometry accounts for transversal asymmetry.

The tab concludes with quantitative slope indicators for both longitudinal and transversal directions. These slopes are derived from bathymetric gradients and are relevant for assessing theoretical internal seiche damping and energy dissipation associated with sloping boundaries.
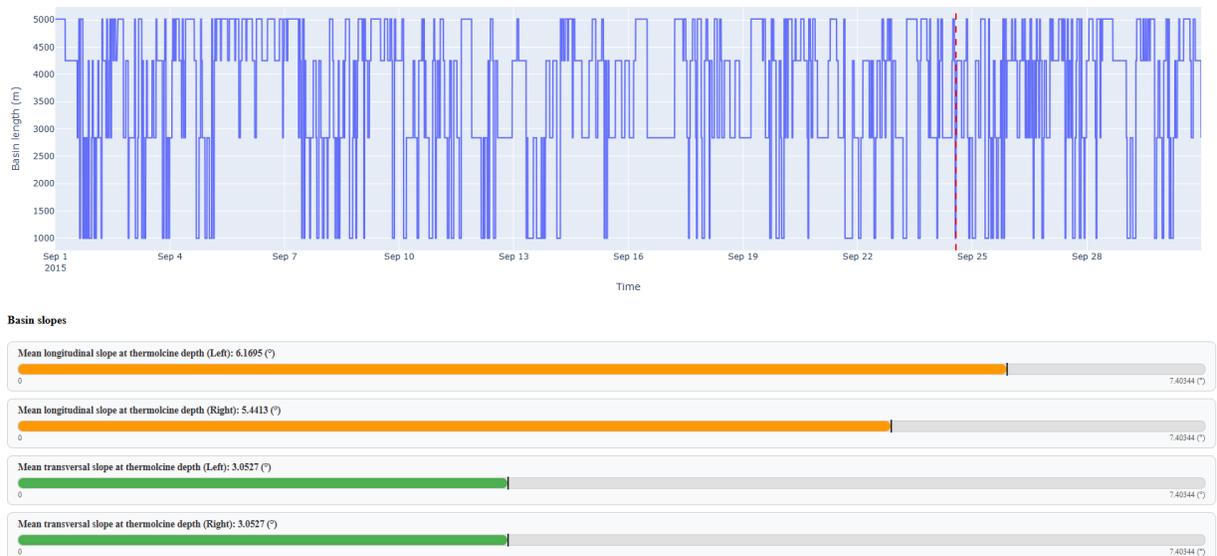

Figure 16: Basin metrics. Top: time series of effective wind fetch (basin length) as a function of wind direction. Bottom: longitudinal and transversal slope indicators derived from bathymetry.

2. Thermal Stratification

This tab provides a comprehensive assessment of the lake's thermal structure and stratification dynamics.

The "Isotherms" panel displays the temporal evolution of selected isotherm depths, enabling identification of internal wave signatures and thermocline oscillations (Figure 17). The "Temperature Variation" section presents temperature time series at selected sensor depths together with the corresponding instantaneous vertical temperature and buoyancy frequency profiles for a chosen time step. This combined representation allows simultaneous

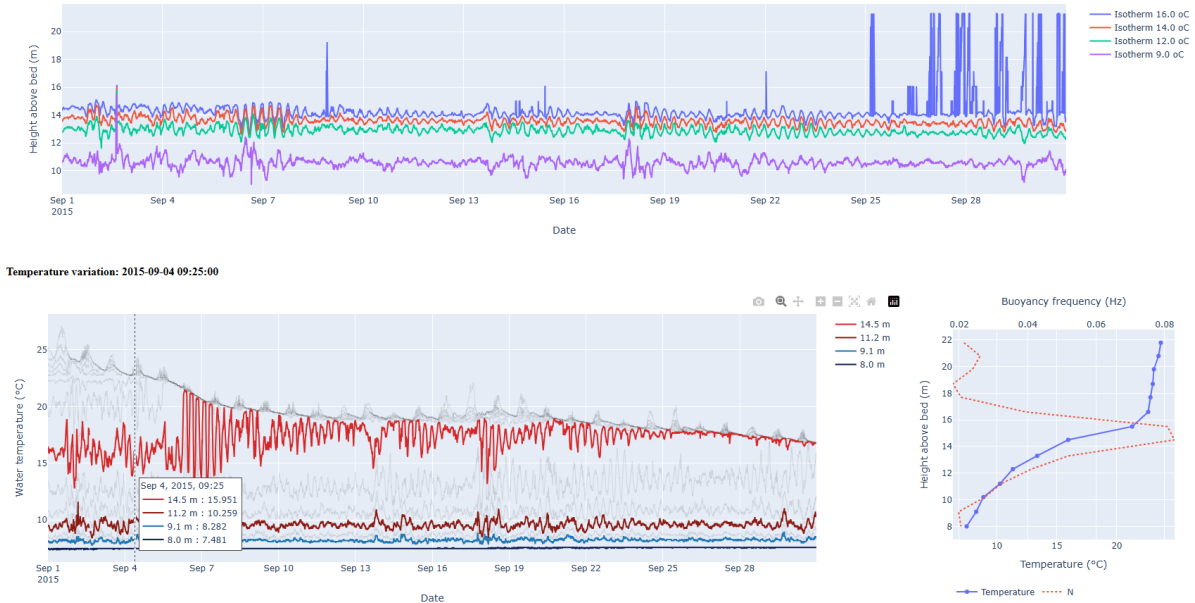evaluation of temporal variability and vertical stratification structure.

Figure 17: Thermal stratification overview. Top: temporal evolution of selected isotherms. Bottom-left: temperature time series at selected depths. Bottom-right: vertical profiles of temperature and buoyancy frequency for a selected time step.

The "Thermal Structure" panel shows the time series of thermocline depth and metalimnion boundaries estimated using the decomposition model (Figure 18). These metrics quantify vertical layer organization and its temporal evolution.

Figure 18: Temporal evolution of thermocline depth (solid line) and metalimnion upper and lower boundaries (dashed lines) estimated using the decomposition model.

Additional panels display the time series of Schmidt Stability and depth-averaged buoyancy frequency, which quantify resistance to mixing and overall stratification strength. The mean buoyancy frequency is estimated from the maximum–minimum density contrast and total water depth.

The tab concludes with "Thermal Summary Indicators," reporting time-averaged layer thicknesses, mean densities, and associated 95% confidence intervals. These indicators synthesize the principal physical characteristics of the stratified water column.

3. Thermal Mixing

This tab evaluates wind forcing and its influence on mixing processes and regime transitions. The upper panel combines wind forcing and stability diagnostics (Figure 19). Wind speed and wind stress are displayed together with the Wedderburn number, facilitating identification of periods favorable to internal seiche dominance, upwelling events, or potential mixing conditions. A zoomed isotherm panel provides detailed visualization of thermocline displacement during selected intervals.

A Richardson regime signal bar summarizes temporal classification of lake mixing based on local Richardson number thresholds, highlighting transitions between stable, transitional, and mixing-prone conditions.
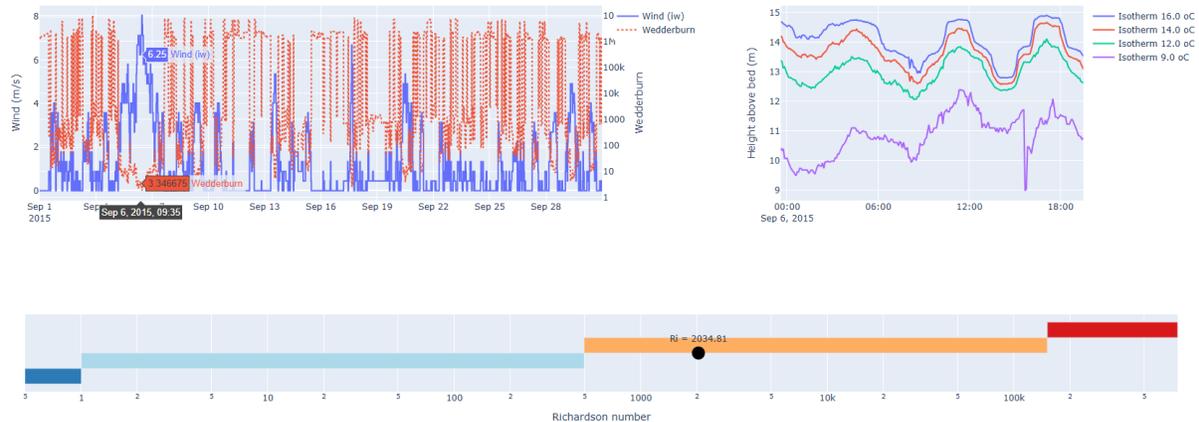

Figure 19: Wind forcing and mixing diagnostics. Top-left: wind speed and Wedderburn number. Top-right: zoomed isotherm displacement. Bottom: Richardson regime classification and Lake Number time series.

The Lake Number time series is also presented, quantifying whole-basin stability and the balance between stabilizing buoyancy forces and destabilizing wind stress.

The tab concludes with "Mixing Summary Indicators," which synthesize key metrics including wind friction velocity, Wedderburn thresholds, wind-event duration, directional persistence, and reduction factors accounting for directional variability in internal seiche development.
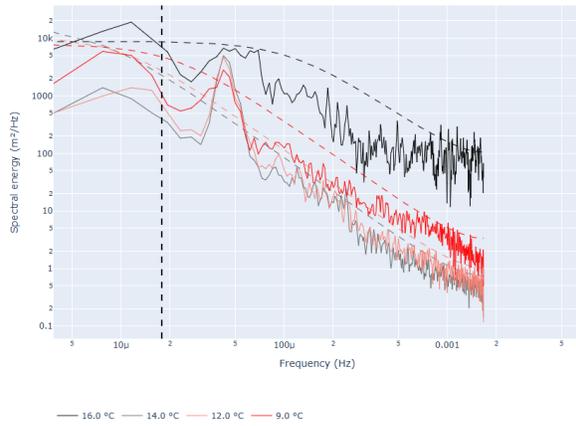
4. Internal Wave

This tab focuses on spectral and modal characterization of internal wave dynamics. The primary panel presents the power spectral density (PSD) of selected isotherms (Figure 20), allowing identification of dominant oscillatory modes and comparison with theoretical internal seiche frequencies. Statistical confidence limits are included to assess spectral significance.

Theoretical internal seiche periods for multiple vertical modes are summarized alongside wind duration and directional persistence metrics.

Band-pass filtered isotherm time series are displayed using frequency limits defined in the GUI or derived from theoretical modal periods, isolating oscillations within the expected internal wave range.

The lower panels present full isotherm time series together with degeneration regime diagnostics and damping analysis associated with sloping bathymetry (Figure 21). These visualizations support evaluation of internal seiche decay mechanisms and the potential influence of topographic control on modal dominance.
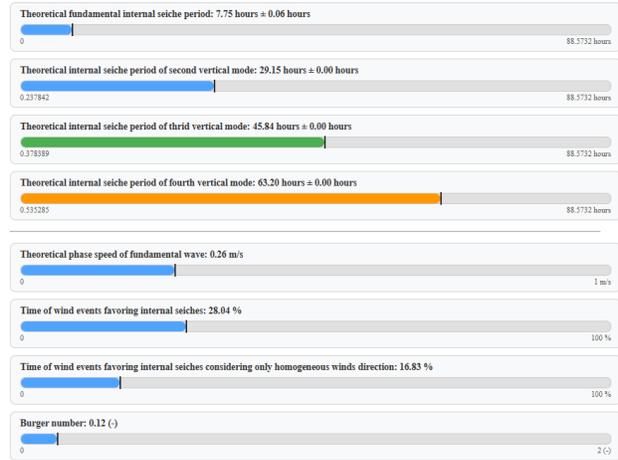
Figure 20: Spectral analysis of internal waves. Left: power spectral density (PSD) of selected isotherms with confidence limits and theoretical modal frequencies. Right: theoretical internal seiche periods and wind-related metrics.
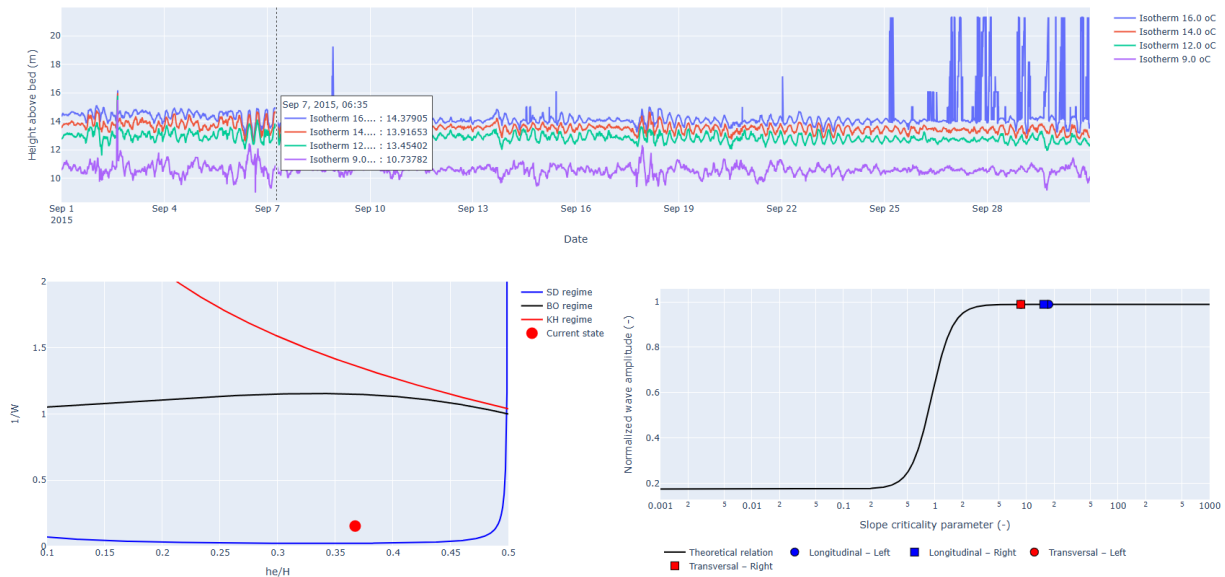

Figure 21: Internal wave degeneration and damping diagnostics. Panels illustrate isotherm evolution, degeneration regime in the h_e/H versus $1/W$ parameter space, and theoretical limits for instability and topographic damping.

6 Interwave Analyzer Computation

This section describes how the Interwave Analyzer computes physical parameters, mathematical variables, spectral diagnostics, and system classifications. For the analyzed time window, the program generates textual summaries, numerical outputs, data files, and graphical products. The software estimates the reservoir's thermal structure and evaluates how wind forcing contributes to baroclinic activity, providing detailed information on thermal stratification, wind statistics, and indicators relevant to internal-wave stability. In addition, the program classifies mixing regimes and basin-scale internal wave generation and decay.

The Interwave Analyzer also performs spectral analyses of selected isotherms and meteorological variables using both Fourier and Wavelet methods, including phase-shift and coherence diagnostics. These results can be compared with theoretical expectations, which are also computed by the software. Furthermore, the program estimates internal seiche periods for the first three vertical modes using a decomposition model and includes an optional model-sensitivity analysis.

6.1 Thermal stratification and meteorological forcing

6.1.1 Water density

The computation of water density is performed using the Tait equation [2], a polynomial approximation for freshwater density, formulation for temperatures between 0 and $40°\mathrm{C}$. For each depth index z, the software evaluates the water density $\rho(z)$ directly from the temperature field $\tau(z)$ using a polynomial representation of the freshwater equation of state:

$$\rho(z) = a_0\, \tau(z)^5 + a_1\, \tau(z)^4 + a_2\, \tau(z)^3 + a_3\, \tau(z)^2 + a_4\, \tau(z) + a_5, \tag{1}$$

where $\tau(z)$ is the water temperature (in $°\mathrm{C}$) at depth index z, and the coefficients $\{a_i\}$ correspond to the standard polynomial constants for freshwater:

$$
\begin{aligned}
a_0 &= 6.536336 \times 10^{-9}, \\
a_1 &= -1.120083 \times 10^{-6}, \\
a_2 &= 1.001685 \times 10^{-4}, \\
a_3 &= -9.09529 \times 10^{-3}, \\
a_4 &= 6.793952 \times 10^{-2}, \\
a_5 &= 999.842592.
\end{aligned}
\tag{2}
$$

Water density is given in $\mathrm{kg\,m^{-3}}$ for each temperature input, allowing the thermal stability module to compute depth-dependent buoyancy, stratification metrics, and related quantities.

6.1.2 Thermocline Depth

The thermocline represents the depth at which the vertical density gradient reaches its maximum intensity or, alternatively, the depth of zero crossing of the first baroclinic mode. Two independent methods are implemented for its evaluation: the maximum density gradient method, based on discrete vertical derivatives [3], and the decomposition-model method, based on Sturm–Liouville modal analysis (Figure 22). Both approaches provide complementary physical insight, and their agreement indicates a robust thermocline identification.

Maximum Density Gradient Method

This method identifies the thermocline as the depth at which the vertical density gradient is most pronounced. Water density is first estimated from temperature using a standard freshwater equation of state [2]. From the resulting density profile, the epilimnion, metalimnion, and hypolimnion are conceptually defined according to the intensity and structure of density gradients [3].
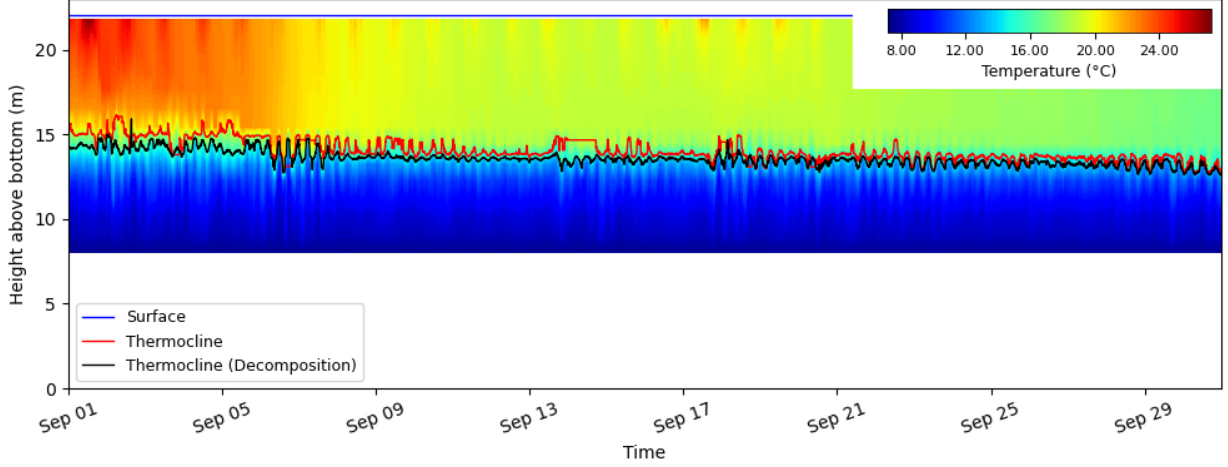
Figure 22: Temperature contour plot showing the thermocline depth time series estimated by the maximum density gradient method (red solid line) and by the decomposition-model approach (black solid line.

To obtain a continuous thermocline estimate from discrete measurements, a weighted-gradient interpolation is performed around the depth index j where the maximum density gradient occurs [3]. The thermocline depth is determined by:

$$Z_{\text{thermo}} = z_{j+1} \left(\frac{\Delta \rho_+}{\Delta \rho_- + \Delta \rho_+} \right) + z_j \left(\frac{\Delta \rho_-}{\Delta \rho_- + \Delta \rho_+} \right), \tag{3}$$

where the forward and backward density-increment predictors are

$$\Delta \rho_+ = \frac{z_j - z_{j+2}}{2 \left[\frac{\rho_{j+1} - \rho_j}{z_j - z_{j+1}} - \frac{\rho_{j+2} - \rho_{j+1}}{z_{j+1} - z_{j+2}} \right]}, \tag{4}$$

$$\Delta \rho_- = \frac{z_{j-1} - z_{j+1}}{2 \left[\frac{\rho_{j+1} - \rho_j}{z_j - z_{j+1}} - \frac{\rho_j - \rho_{j-1}}{z_{j-1} - z_j} \right]}. \tag{5}$$

Here, ρ_j and z_j represent density and depth at the j-th measurement, while Z_{thermo} is the final estimate of the thermocline depth.

Decomposition Model

A second and physically independent method determines the thermocline depth using the vertical structure of internal wave modes. This approach is based on linear internal wave theory and solves the vertical eigenvalue problem associated with stratified basin-scale oscillations [4, 5].

First, the observed density profile is converted into a buoyancy frequency profile $N^2(z)$, defined as

$$N^2(z) = -\frac{g}{\rho_0} \frac{\partial \rho}{\partial z}, \tag{6}$$

where g is gravitational acceleration, ρ_0 a reference density, and $\partial \rho / \partial z$ the vertical density gradient. The buoyancy frequency is interpolated onto a refined vertical grid. The vertical structure of internal waves is then obtained by solving the Sturm–Liouville eigenvalue problem:

$$\frac{\mathrm{d}^2 w}{\mathrm{d}z^2} + k^2 \left(\frac{N^2(z)}{\omega^2} - 1 \right) w = 0, \tag{7}$$

where $w(z)$ is the vertical velocity structure function, $k = \pi/L$ is the horizontal wavenumber for a basin of effective length L, and ω is the angular frequency associated with each vertical mode. Boundary conditions impose zero vertical velocity at the surface and bottom.

The equation is solved numerically using a finite-difference formulation on the refined grid. For each vertical mode, the eigenfrequency ω_m (or equivalently the modal period T_m) is determined iteratively by enforcing the boundary condition at the lower boundary. A bracketing and interval-halving (bisection) procedure ensures convergence of the eigenvalue solution [4].

The resulting eigenfunctions $w_m(z)$ are normalized according to the stratification-weighted inner product:

$$\int_0^H N^2(z)\, w_m^2(z)\, \mathrm{d}z = 1, \tag{8}$$

which guarantees energetic consistency between modes.

The thermocline depth is identified as the nodal depth of the first baroclinic mode:

$$w_1(z_{\text{thermo}}) = 0. \tag{9}$$

This definition is consistent with the theoretical interpretation of the thermocline as the interface separating counter-rotating layers in the dominant internal oscillation [6, 7].

In addition to thermocline detection, the decomposition model provides the thickness of dynamically consistent layers for higher vertical modes, determined from successive nodal depths of $w_m(z)$, the stratification-weighted modal structure, computed as

$$c_p^{(m)}(z) = N^2(z)\, w_m(z), \tag{10}$$

which represents the vertical distribution of potential energy associated with each mode.

In addition, the corresponding horizontal velocity structure are obtained, proportional to the vertical gradient of the modal function:

$$u_m(z) \propto \frac{\partial w_m}{\partial z}, \tag{11}$$

which describes the shear distribution induced by internal seiche motions.

The stratification-weighted modal structure and the corresponding horizontal velocity structure are provided by user in text-file formats, and can be used externally, in combination with velocity measurements, to estimate the horizontal velocity associated to each internal seiche mode. See https://github.com/buenorc/decomp-interwave for more details.

> ⚠️ The decomposition model does not only determine thermocline depth. Its modal structure is also used to define dynamically consistent layer thicknesses for higher vertical modes, to compute stratification-weighted modal amplitudes (c_p), and to derive the corresponding horizontal velocity structure. Consequently, any limitation in vertical resolution or stratification quality will propagate consistently into all modal diagnostics derived from this method.

> ⚠️ The time resolution of the decomposition model can be adjusted by the user to accelerate the analysis. If a coarser temporal resolution is selected, variables computed by the decomposition model (e.g., wave period and layer thicknesses) are interpolated back onto the original time grid. This interpolation procedure may introduce additional uncertainty into the derived quantities.

6.1.3 Metalimnion Boundaries

Maximum Density Gradient Method

The boundaries of the metalimnion are defined using threshold values of the absolute buoyancy (or density) gradient [3]. Let $d\rho/dz$ denote the vertical density gradient. The upper and lower boundaries of the metalimnion, z_1 and z_2, are given by

$$z_i = h[j], \tag{12}$$

where $i = 1$ corresponds to the epilimnion–metalimnion interface and $i = 2$ to the metalimnion–hypolimnion interface. The depth index j is defined as

$$j = \min\left\{ z \ : \ \frac{d\rho}{dz} > \text{minval} \right\}, \tag{13}$$

with minval being a prescribed gradient threshold.

If gradient-based detection is unsuccessful (e.g., under weak or ambiguous stratification), a fallback criterion is applied:

$$z_i = \frac{gH}{3}, \tag{14}$$

where H is the total water depth and $g = 2$ for the upper boundary $(i = 1)$ and $g = 1$ for the lower boundary $(i = 2)$.

Decomposition Model

In the decomposition-based approach, the metalimnion corresponds to the region of maximum curvature of the mode-1 eigenfunction $w_1(z)$ or, equivalently, the depth interval surrounding the zero crossing of $w_1(z)$ (Figure 23). Since $w_1(z)$ represents the vertical velocity structure of the dominant internal mode, the region where its curvature intensifies or changes sign naturally aligns with the physical transition layer between the epilimnion and hypolimnion.

6.1.4 Buoyancy Frequency

The squared buoyancy frequency $N^2(z)$ quantifies the strength of vertical stratification and represents the restoring force acting on vertically displaced water parcels under stable density conditions. It is derived from the vertical density gradient according to

$$N^2(z) = -\frac{g}{\rho_0} \frac{\partial \rho}{\partial z}, \tag{15}$$

where g is gravitational acceleration and ρ_0 is a reference density. In the discrete form adopted by the Interwave Analyzer, the buoyancy frequency is approximated between consecutive measurement depths as

$$N(z) = \sqrt{\frac{g}{\rho_{z+1}} \frac{\rho_{z+1} - \rho_z}{h_{z+1} - h_z}}, \tag{16}$$
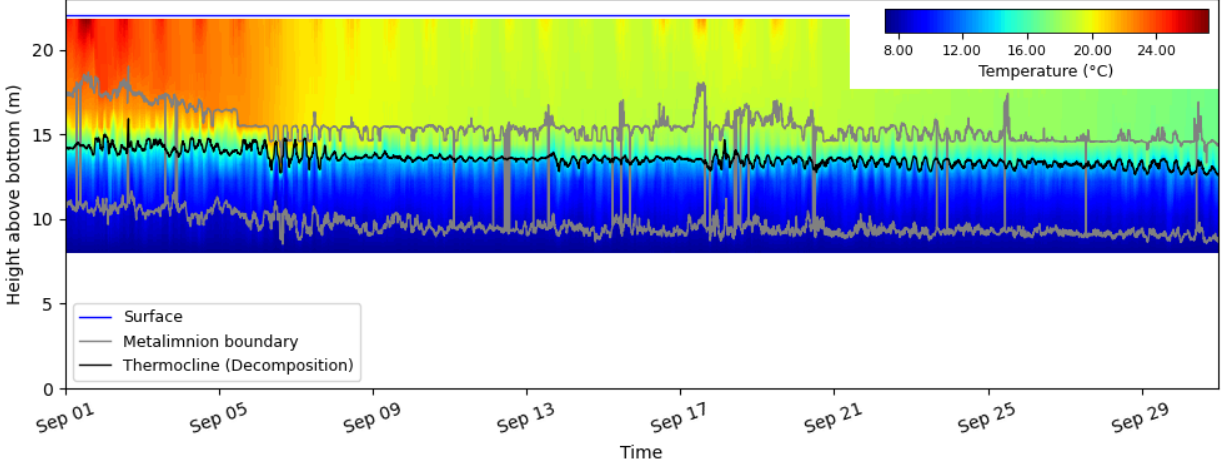
Figure 23: Temperature contour plot showing the thermocline and metalimnion boundaries the time series estimated by the maximum density gradient method (red solid line) and by the decomposition-model approach (black solid line.

where ρ_z and ρ_{z+1} are densities at successive depths, and h_z and h_{z+1} are the corresponding vertical coordinates. Positive values of N^2 indicate stable stratification, whereas negative values denote gravitational instability (Figure 24).

6.1.5 Mean Buoyancy Frequency

In addition to the depth-resolved profile, the Interwave Analyzer computes a representative depth-averaged buoyancy frequency using two complementary approaches.

Bulk Density Contrast Method

The first approach estimates a bulk buoyancy frequency from the density difference between near-surface and near-bottom waters [8]:

$$\bar{N} = \sqrt{\frac{g \, |\rho_{\mathrm{bot}} - \rho_{\mathrm{up}}|}{\rho_{\mathrm{up}} H}}, \tag{17}$$

where ρ_{bot} and ρ_{up} are the bottom and surface densities, respectively, and H is the total water depth.

Two-Layer Reduced Gravity Method

The second approach is based on an idealized two-layer representation of the water column. The density structure is reduced to an epilimnion (thickness h_e, density ρ_e) and a hypolimnion (thickness h_h, density ρ_h). The reduced gravity is defined as

$$g' = g \frac{\rho_h - \rho_e}{\rho_h}, \tag{18}$$

which represents the effective gravitational acceleration acting at the density interface.
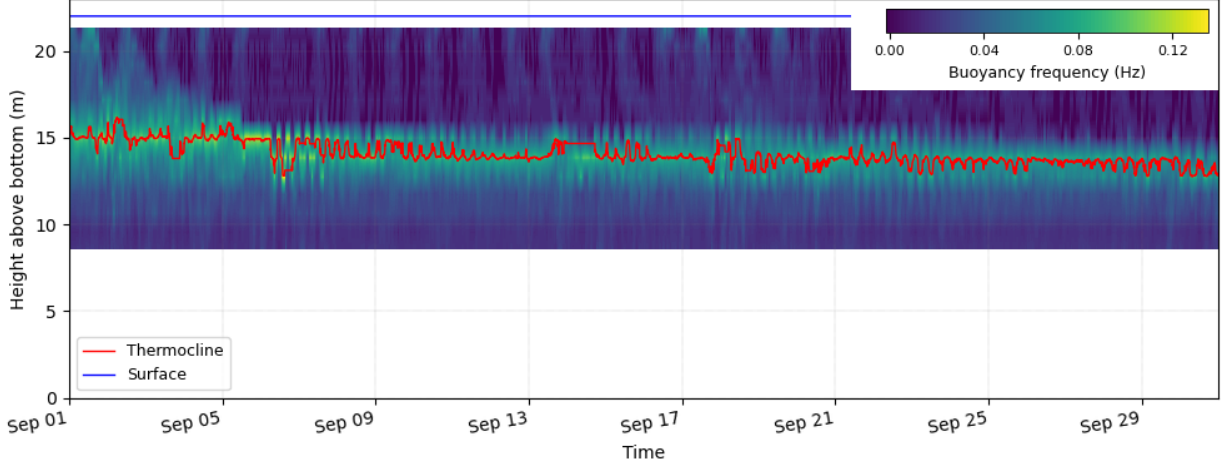
Figure 24: Temperature contour plot showing the thermocline and metalimnion boundaries the time series estimated by the maximum density gradient method (red solid line) and by the decomposition-model approach (black solid line.

Assuming a sharp interface and linear internal wave theory, the characteristic buoyancy frequency of the upper layer is then estimated as

$$\bar{N} = \sqrt{\frac{g'}{h_e}}. \tag{19}$$

6.1.6 Mean Temperature and Buoyancy Profiles

Vertical profiles of temperature and buoyancy-related quantities are frequently summarized using temporal averages (Figure 25). Given a generic field $\xi(t, z)$, where ξ may represent temperature, buoyancy frequency, or any other depth-resolved variable, the temporal mean profile is computed as

$$\bar{\xi}(z) = \frac{1}{N} \sum_{t=1}^{N} \xi(t, z), \tag{20}$$

where N is the number of available time steps. The mean profile provides a baseline representation of the vertically stratified state, filtering out transient oscillations such as internal waves or short-lived mixing events.

To quantify the variability around the mean, the standard deviation at each depth level is computed as

$$\sigma_\xi(z) = \sqrt{\frac{1}{N-1} \sum_{t=1}^{N} \left[\xi(t, z) - \bar{\xi}(z) \right]^2}. \tag{21}$$

From this, a 95% confidence interval of the mean is estimated under the assumption of normally distributed fluctuations:

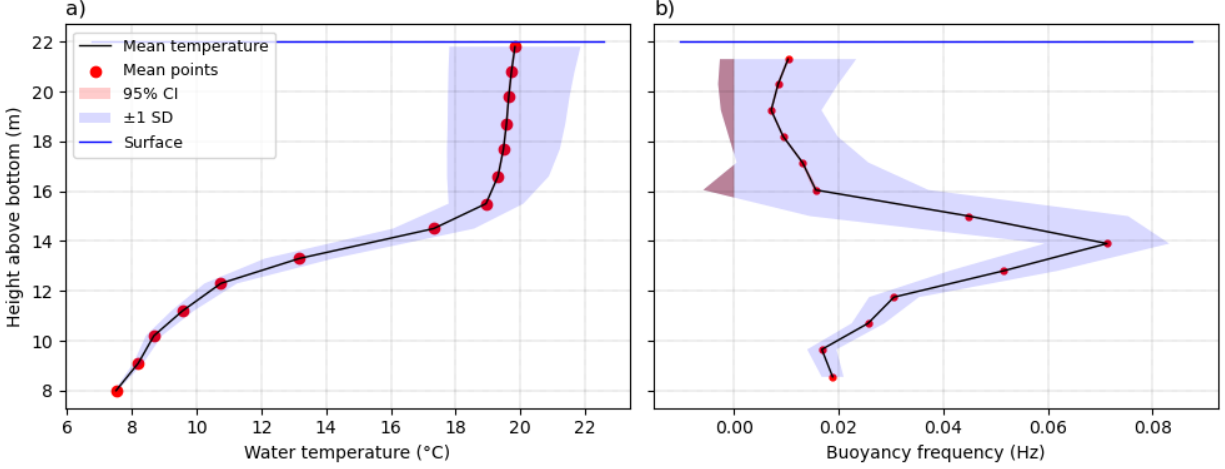$$CI_{95}(z) = 1.96 \frac{\sigma_\xi(z)}{\sqrt{N}}. \tag{22}$$

43

Figure 25: Time-averaged a) temperature and b) buoyancy frequency profiles, including standard deviation and 95% confidence intervals. Negative buoyancy frequency values indicate locally unstable stratification.

6.1.7 Isotherms

Isotherms represent the depths at which the water temperature equals a specified target value T_0 at each time step (Figure 26). They provide a compact description of thermal stratification dynamics, since it describe the movements on density interfaces.

Isotherms are obtained by identifying all depths h that satisfy $T(h, t) = T_0$, for each time t. Because discrete temperature sensors rarely align exactly with the target isotherm value, linear interpolation is applied between adjacent measurement levels.

If $T(h_i, t)$ and $T(h_{i+1}, t)$ straddle T_0, the isotherm depth is estimated as

$$h(T_0, t) = h_i + \left(\frac{T_0 - T(h_i, t)}{T(h_{i+1}, t) - T(h_i, t)} \right) [h_{i+1} - h_i]. \tag{23}$$

6.1.8 Thorpe Scale and Displacement

Thorpe analysis provides a quantitative measure of turbulent overturning intensity in stratified waters [9]. The method compares the observed vertical temperature profile to a statically stable version of itself, obtained by sorting the temperature values into a monotonically decreasing sequence.

Let $T(z)$ be the measured temperature profile at a given time step. After sorting $T(z)$ to produce a stable reference profile $T_s(z)$, the Thorpe displacement at each depth level i is defined as

$$d_i = h_s(i) - h(i), \tag{24}$$

where $h(i)$ is the original depth of sample i and $h_s(i)$ is the depth that the same water parcel would occupy in the sorted, gravitationally stable profile. The displacement d_i thus quantifies the vertical reordering required to eliminate static instability.

The characteristic overturning scale, or Thorpe scale, is then computed as the root-mean-square of the displacements:

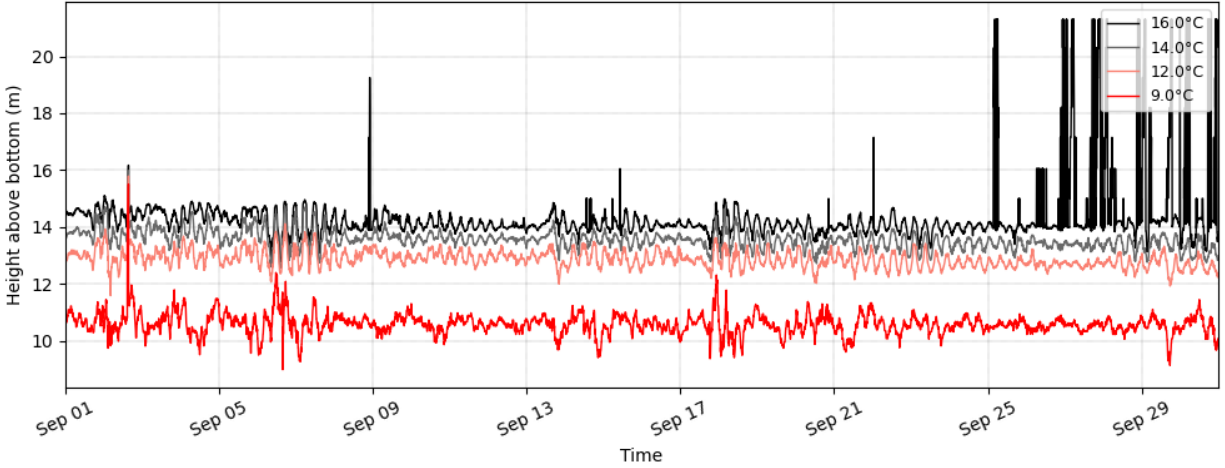$$L_T = \sqrt{\frac{1}{N} \sum_{i=1}^{N} d_i^2}, \tag{25}$$

44

Figure 26: Time series of selected isotherm elevations (reference from the lake bottom).

where N is the number of vertical samples in the profile.

The Thorpe scale provides a proxy for turbulence intensity. Larger values of L_T indicate stronger overturning motions and enhanced mixing, whereas small values indicate a more stably stratified, weakly turbulent environment.

> ⚠️ Although this metric is widely used for estimating turbulent diffusivity, diagnosing mixing hotspots, and identifying internal wave breaking events, when temperature measurements are acquired at low temporal frequency or with coarse vertical spacing, the interpretation of L_T requires caution. Limited resolution can smooth or entirely miss small-scale overturns, biasing L_T toward larger, low-frequency structures. Under such conditions, the Thorpe scale may predominantly reflect diurnal stratification cycles or large-scale internal wave motions rather than true turbulence-driven overturns. Consequently, L_T-based mixing estimates in low-resolution datasets should be interpreted as qualitative indicators of instability rather than precise measures of turbulent fluxes.

6.2 Wave Periods

6.2.1 Decomposition Model for Fundamental and Higher Vertical Modes

The decomposition model computes vertical mode shapes and corresponding internal–wave periods by numerically solving a discrete form of the Taylor–Goldstein equation on a refined, uniformly spaced vertical grid [5]. This approach provides a physically consistent representation of continuous stratification and supports the extraction of the first several baroclinic vertical modes.

A refined grid of $N = 100$ levels is constructed according to

$$z_i = i\,\Delta z, \qquad \Delta z = \frac{H}{N-1}, \tag{26}$$

where H is the total water depth.

The buoyancy frequency is interpolated onto this grid and expressed in SI units as

$$N^2(z_i) = \frac{b_v(z_i)^2}{3600}, \tag{27}$$

45

where b_v is the buoyancy frequency originally provided in min^{-1}.

The vertical structure function $w(z)$ satisfies the Taylor–Goldstein eigenvalue problem,

$$\frac{d^2w}{dz^2} + k^2\left(\frac{N^2(z)}{\omega^2} - 1\right)w = 0, \tag{28}$$

where $k = \pi/L$ is the horizontal wavenumber associated with the fundamental mode and ω is the internal–wave angular frequency.

A second–order central–difference representation is used for the interior points, yielding the recurrence relation

$$w_i = -w_{i-2} + \left[2 - k^2\Delta z^2\left(\frac{N^2(z_{i-1})p^2}{(2\pi)^2} - 1\right)\right]w_{i-1}, \tag{29}$$

where p is a trial wave period (in seconds) used iteratively in the root–finding procedure.

Boundary conditions impose a rigid–lid constraint at the surface and define a scale for the eigenfunction:

$$w_0 = 0, \qquad w_1 = 1. \tag{30}$$

The model searches for the value of p that forces $w_N = 0$ at the bottom boundary. A bracketing procedure based on sign changes of the boundary residual is used to isolate a root, followed by bisection:

$$p_{\mathsf{new}} = \frac{p_{\mathsf{low}} + p_{\mathsf{high}}}{2}, \tag{31}$$

until the interval meets the tolerance

$$\left|p_{\mathsf{high}} - p_{\mathsf{low}}\right| < 0.1 \text{ s}. \tag{32}$$

The corresponding mode period (in hours) is then

$$T_m = \frac{p}{3600}. \tag{33}$$

Finally, the mode shape is normalized through

$$\mathsf{norm} = \sqrt{\sum_{i=0}^{N-1} N^2(z_i)\,w_i^2}, \tag{34}$$

and

$$\tilde{w}_i = \frac{w_i}{\mathsf{norm}}, \tag{35}$$

yielding the final vertical mode structure for each modal index m.

Interwave Analyzer computes for each time the internal seiche period of the first five vertical modes (Figure 27)

⚠ | The time resolution of the decomposition model can be adjusted by the user to accelerate the analysis. If a coarser temporal resolution is selected, variables computed by the decomposition model (e.g., wave period and layer thicknesses) are interpolated back onto the original time grid. This interpolation procedure may introduce additional uncertainty into the derived quantities.
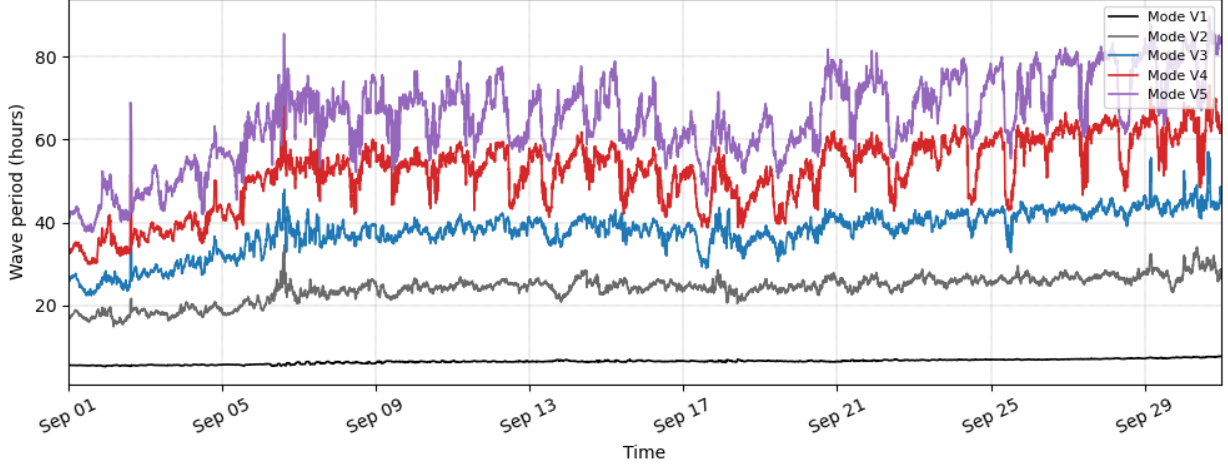
Figure 27: Time series of theoretical internal seiche periods for the first five vertical modes (V1–V5) estimated with the decomposition model.

6.2.2 Analytical Layered Models

For systems that can be approximated by a finite number of homogeneous layers [6, 10], analytical solutions provide an efficient alternative to the continuous decomposition model. These layered formulations explicitly capture the physics of interfacial internal waves and yield closed-form expressions for the wave period. Consider a basin composed of an epilimnion of thickness h_e and density ρ_e overlying a hypolimnion of thickness h_h and density ρ_h. The density ratio is defined as

$$\gamma = \frac{\rho_e}{\rho_h}. \tag{36}$$

The horizontal wavenumber for mode m is

$$k = \frac{m\pi}{L}. \tag{37}$$

Introduce the hyperbolic tangent factors

$$t_i = \tanh(kh_i), \qquad i \in \{e, h\}. \tag{38}$$

The dispersion relation reduces to a biquadratic equation in the wave frequency ω,

$$p\,\omega^4 + q\,\omega^2 + r = 0, \tag{39}$$

with coefficients

$$p = \frac{\gamma\, t_e t_h + 1}{k\, t_h}, \qquad q = -g\,\frac{t_h + t_e}{t_h}, \qquad r = -g^2(\gamma - 1)\, k\, t_e. \tag{40}$$

The discriminant is

$$\Delta = q^2 - 4pr, \tag{41}$$

and the physically relevant root for the internal–wave mode is

$$\omega = \sqrt{\frac{-q - \sqrt{\Delta}}{2p}}. \tag{42}$$

The wave period is finally given by

$$T = \frac{2\pi}{\omega}. \tag{43}$$

47

6.2.3 Coriolis Correction to Wave Period

Large-scale internal motions in natural lakes and reservoirs are weakly influenced by Earth's rotation. Although the Coriolis effect is typically small in basins with horizontal scales of a few kilometers, its contribution becomes increasingly relevant for long-period motions and higher latitudes. To account for rotational effects, the internal–wave period can be corrected by incorporating the Coriolis parameter.

The Coriolis parameter at latitude ϕ is defined as

$$f = 2\Omega \sin \phi, \tag{44}$$

where $\Omega = 7.292115 \times 10^{-5} \text{ s}^{-1}$ is Earth's angular velocity.

Given an uncorrected wave period T_0, the corresponding angular frequency is

$$\omega_0 = \frac{2\pi}{T_0}. \tag{45}$$

In the presence of rotation, the dispersion relation for long internal waves is modified, and the effective frequency becomes

$$\omega = \sqrt{\omega_0^2 + f^2}, \tag{46}$$

which reflects the stabilizing contribution of the Coriolis term.

The rotation-corrected internal–wave period is therefore

$$T_{\text{cor}} = \frac{2\pi}{\omega}. \tag{47}$$

6.2.4 Sensitivity Analysis of Layered Internal-Wave Models

Internal seiche periods derived from layered models depend directly on how the water column is partitioned into vertical layers. Because lake stratification is inherently time-variable, any procedure based on a fixed threshold—such as a temperature or buoyancy criterion defining the metalimnion—may introduce uncertainty into the estimated layer thicknesses. When the stratification regime fluctuates rapidly or lacks a well-defined metalimnetic structure, the resulting layer-averaged properties may not be representative of the full variability. In such cases, internal seiche periods must be interpreted with caution, and subdividing the temporal analysis window is recommended.

To quantify this structural uncertainty, the *Interwave Analyzer* incorporates a comprehensive sensitivity analysis that evaluates how internal seiche periods vary when the underlying layer parameters are perturbed.

The sensitivity analysis of the wave period is performed exclusively using estimates derived from the two-layer system obtained via the Maximum Density Gradient Method. This analysis is not applied to wave periods estimated by the decomposition model.

For two-layer hydrostatic models, the periods of internal seiches depend primarily on epilimnion thickness h_e, hypolimnion thickness h_h, epilimnion density ρ_e, and hypolimnion density ρ_h. A useful nondimensional indicator of structural variability is the thickness parameter

$$\bar{H} = \frac{h_e h_h}{H}, \tag{48}$$

which expresses the relative partition of the water column. Variations in $\bar{H}$ summarize the temporal changes in layer division and reflect how sensitive the system is to the assumed metalimnetic boundary.

> ⚠️ A thicker gray bar in Figure 28 indicates stronger structural variability during the analyzed interval, whereas the green bar represents variability primarily induced by changes in wind fetch (effective basin length). Note that when the effective basin length varies with wind direction (elliptical basin analysis), the variability represented by the green area may become relatively large due to the inclusion of transverse internal seiche components.

For each parameter $x \in \{h_e, h_h, \rho_e, \rho_h\}$, the sensitivity analysis samples a symmetric perturbation interval centered on the mean value:

$$x_j = x_{\text{mean}} - \Delta x + j \frac{2\Delta x}{N-1}, \qquad j = 0, \dots, N-1, \tag{49}$$

where Δx defines the perturbation amplitude. For every sampled parameter value, the internal-wave period is recomputed:

$$T(x_j) = T_{\text{layered}}(x_j), \tag{50}$$

with T_{layered} representing either the analytical two-layer solution or the extended multi-layer dispersion model. Final results are expressed in hours as

$$T_j^{(\text{hours})} = \frac{T(x_j)}{3600}. \tag{51}$$

Figure 28 illustrates the sensitivity ranges in layer thickness and density gradient. The vertical gray bar indicates the natural variability detected within the analysis interval, while the horizontal green bar shows the wave-period variability associated with changes in basin length resulting from the predominant wind direction.
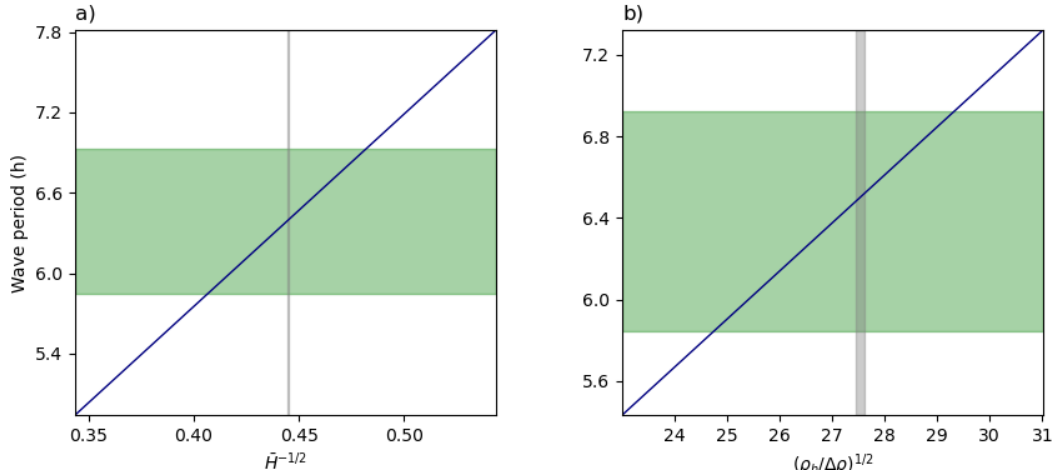

Figure 28: Sensitivity analysis performed by the *Interwave Analyzer*. a) Sensitivity of the multi-layer hydrostatic model to variations in layer thicknesses, measured through the thickness parameter $\bar{H}$ (Eq. 48). b) Equivalent sensitivity assessment for the density gradient $\rho_h - \rho_e$. The vertical gray box illustrates the natural variability detected during the analysis period, while the horizontal green bar shows the variability in wave periods resulting from the possible range of effective basin lengths associated with wind direction.

6.3 Spectral analysis

To highlight the periodic evolution in meteorological and temperature data, the Interwave Analyzer uses two spectral analysis (based on Fourier and Wavelet analyses) for internal wave identifications. The spectral analysis is applied on isotherms, water surface elevation, meteorological data, and is used to determine the number of

standing wave modes, the depth variation of each mode, the energy distribution, the presence of higher vertical modes, and the occurrence of wind-resonance.

6.3.1 Fourier Analysis

The Interwave Analyzer applies a Short-Time Fourier Transform (STFT) to resolve the temporal evolution of harmonic components in the thermal and meteorological time series [11]. This method is normalized by the spectral resolution to ensure that energy density is consistent across different window sizes. The STFT allows the detection of transient periodicities such as internal seiche oscillations, which are often non-stationary in nature.

In the algorithm, the signal $f(t)$ is divided into partially overlapping segments defined by a selected window function $w(t)$. The user can select among *Hamming*, *Hanning (Hann)*, *Blackman*, or *Flattop* windows [1]. The purpose of the window function is to minimize spectral leakage at segment boundaries by tapering the edges of the signal. Mathematically, the windowed segment is given by

$$f_k(t) = f(t)\,w(t - k\Delta), \tag{52}$$

where Δ is the step (overlap) between adjacent windows.

The default window length Wf_{size} is dynamically linked to the fundamental basin-scale internal seiche period, ensuring that the frequency resolution is matched to the physical oscillation of interest. The relation is defined as

$$Wf_{size} = 10\,T_{V1H1}, \tag{53}$$

where T_{V1H1} represents the fundamental internal seiche period obtained from the decomposition or analytical model. When the signal length is shorter than $10T_{V1H1}$, the program automatically redefines Wf_{size} to equal the total signal duration. For sensor time series, a fixed window of $72\,\mathrm{h}$ is adopted by default to capture diurnal and sub-basin oscillations.

Before the transform, all input data are linearly detrended to remove low-frequency bias that could distort the power spectral estimate. Each segment is then processed using the Welch algorithm, which performs a Fourier transform of each windowed segment and averages the resulting power spectra to reduce variance. The general form of the STFT for a signal $f(t)$ is expressed as

$$F(\omega, \tau) = \int_{-\infty}^{+\infty} f(t)\,w(t - \tau)\,e^{-i\omega t}\,dt, \tag{54}$$

where τ is the temporal position of the window and ω is the angular frequency.

The resulting Power Spectral Density (PSD) represents the energy distribution of the signal per unit frequency. In the discrete implementation, the PSD for each segment is calculated as

$$\phi_{ff}(\omega) = \frac{\delta t}{N_{\text{window}}}\,|F\{f(n)\}|^2\,, \tag{55}$$

where $\phi_{ff}(\omega)$ is the spectral energy density, $F\{f(n)\}$ is the discrete Fourier transform of the windowed segment $f(n)$, δt is the sampling period, and N_{window} is the window length in samples. The factor $\delta t/N_{\text{window}}$ ensures proper normalization with respect to both time resolution and window duration.

Finally, the Interwave Analyzer normalizes each PSD by the spectrum resolution $\Delta f = 1/Wf_{size}$, such that

$$P(\omega) = \frac{\phi_{ff}(\omega)}{\Delta f}, \tag{56}$$

yielding a dimensionally consistent representation of power per unit frequency.

The Fourier transform routine enables harmonic analysis of the signal (Figure 29a). Comparing the power spectral density (PSD) of the isotherms with the theoretical internal seiche periods (Figure 29a) allows discrimination

between general oscillatory thermocline motions and those specifically associated with internal seiches [1]. The amplitude and phase of each frequency component are computed from the complex Fourier coefficients and subsequently used in cross-spectral and coherence analyses described in later sections.

> ⚠️ The power spectral density (PSD) only resolves internal waves whose periods are shorter than the selected window size. When the window length is tied to the internal seiche period T_{V1H1}, the analysis emphasizes the fundamental basin-scale mode, and higher vertical modes may be underrepresented or filtered out.

6.3.2 Confidence of spectral peaks

The Interwave Analyzer quantifies the statistical significance of spectral peaks to help distinguish physically meaningful oscillations (e.g., internal seiches or inertial motions) from stochastic background noise (Figure 29). To accomplish this, the program estimates a red-noise background spectrum and applies a Chi-square test to identify frequency bands where the observed power exceeds the red-noise expectation at a specified confidence level.

The red-noise model is derived from a first-order autoregressive (AR(1)) process estimated from the time series itself [1]. Given a one-lag autocorrelation coefficient r_1, the theoretical red-noise power spectral density (PSD) can be computed as

$$P_{\text{red}}(\omega) = \frac{1 - r_1^2}{1 - 2r_1 \cos(\omega \delta t) + r_1^2}, \tag{57}$$

where δt is the sampling interval and ω the angular frequency. This analytical form represents the expected spectral energy distribution of a red-noise process with the same autocorrelation characteristics as the observed data.

To assess whether a spectral peak at frequency ω_i is statistically significant, the observed PSD $\phi_{ff}(\omega_i)$ is compared against the red-noise background scaled by the Chi-square distribution. The Interwave Analyzer performs a χ^2 test at the 95% confidence level, following the approach of [12] and [13]. The degrees of freedom (dof) for the test are calculated as

$$\text{dof} = 2\, k_{\text{over}} \left(\frac{2.5164\, N_{\text{zero}}}{N_{\text{window}}} \right), \tag{58}$$

where N_{window} is the window size (in samples) used in the spectral estimation, N_{zero} is the effective window length after zero-padding, and $k_{\text{over}} = 1.2$ is a correction factor compensating for spectral leakage and overlap effects associated with the Welch method. This correction is particularly recommended for 50% overlapping Hamming windows [12].

The 95% significance level for each frequency is then determined from the Chi-square quantile:

$$P_{\text{sig}}(\omega_i) = P_{\text{red}}(\omega_i) \frac{\chi^2_{0.95,\,\text{dof}}}{\text{dof}}, \tag{59}$$

where $\chi^2_{0.95,\,\text{dof}}$ is the 95th percentile of the Chi-square distribution with dof degrees of freedom.

Spectral peaks exceeding $P_{\text{sig}}(\omega_i)$ are considered statistically significant and interpreted as representing coherent physical oscillations rather than stochastic variability [1]. This statistical screening is visualized in the Interwave Analyzer output plots (e.g., Figure 29a), where significant frequencies are highlighted above the red-noise confidence curve.

6.3.3 Variance-Preserving Power Spectral Density for Isotherms

To accurately interpret the temporal dynamics of internal waves in a stratified lake, it is essential to quantify how temperature fluctuations at specific isotherms contribute to the overall energy variance of the system. The
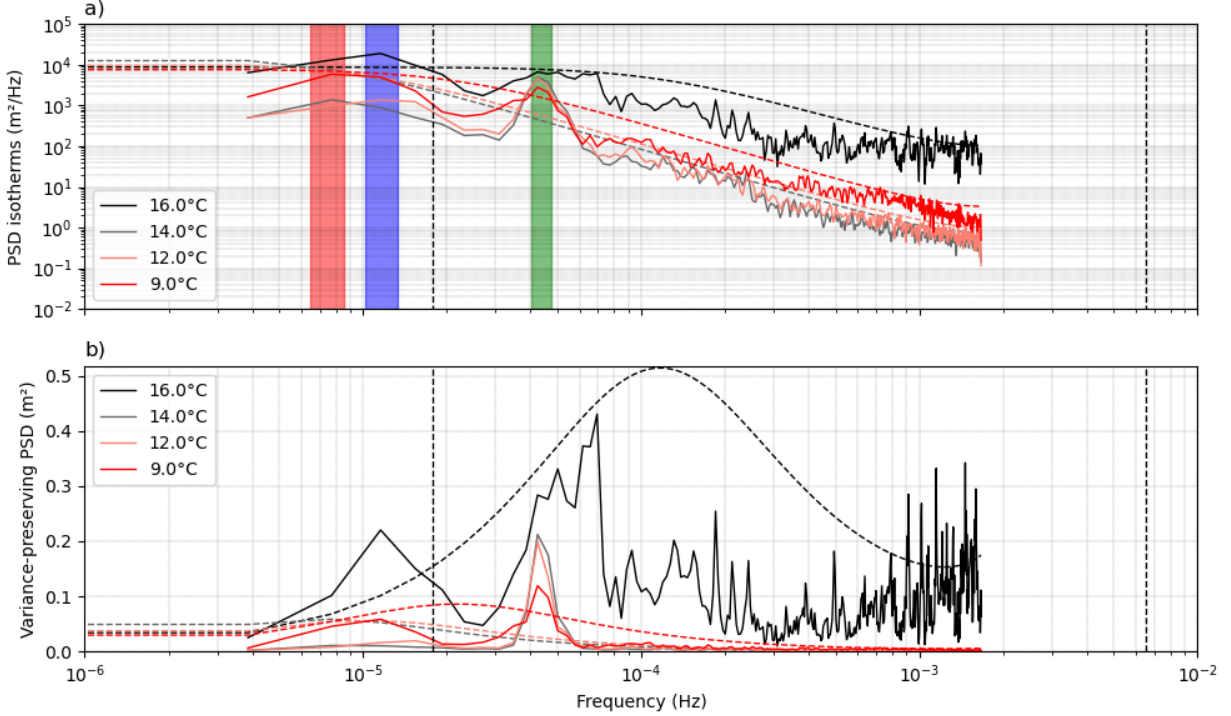
Figure 29: a) Power spectral density (PSD) and variance-preserving power spectral density of isotherm displacements for the four isotherms. The vertical red, green, and blue bars in the spectrum mark the frequencies of basin-scale internal waves estimated by the decomposition model for first, second, third vertical mode, respectively. The width of the colored boxes indicate the time variability of the estimated internal wave periods. Note that, indirectly it considers the direction of internal seiche formation taking into account transversal internal seiches. The dashed lines indicate the mean red noise spectrum for the time series at a 95% confidence level.

Interwave Analyzer computes the variance-preserving power spectral density (PSD) for selected isotherms (e.g., Figure 29b). This diagnostic method transforms classical power spectra into a form that directly reflects the contribution of each frequency band to the total signal variance.

A traditional PSD $S(f)$ represents the distribution of signal energy as a function of frequency f (in Hz). However, because the PSD is typically displayed in logarithmic frequency space, low-frequency oscillations dominate visually, making it difficult to assess the relative importance of higher-frequency processes. To resolve this, a variance-preserving transformation is applied:

$$S_v(f) = f\, S(f), \tag{60}$$

where $S_v(f)$ has units of variance per logarithmic frequency interval. The integral of $S_v(f)$ over $\log f$ directly corresponds to the signal variance:

$$\sigma^2 = \int_{\log f_{\min}}^{\log f_{\max}} S_v(f)\, d(\log f). \tag{61}$$

Thus, peaks in $S_v(f)$ identify frequencies (or periods) that most effectively contribute to the observed temperature variance at a given isotherm.

Confidence limits, computed via the Chi-square method (Eq. 59), are superimposed to identify statistically significant spectral peaks. Isotherm frequencies exceeding these thresholds are interpreted as physically coherent internal oscillations rather than random variability.

6.3.4 Coherence and Phase-Shift Analysis

The Interwave Analyzer evaluates the dynamical coupling between pairs of isotherm signals through the coherence and phase-shift analyses (Figure 30). These tools quantify the linear correlation and relative phase delay between oscillations at different depths, enabling the detection of baroclinic wave propagation, standing internal seiches, and resonance between wind forcing and internal modes [1].
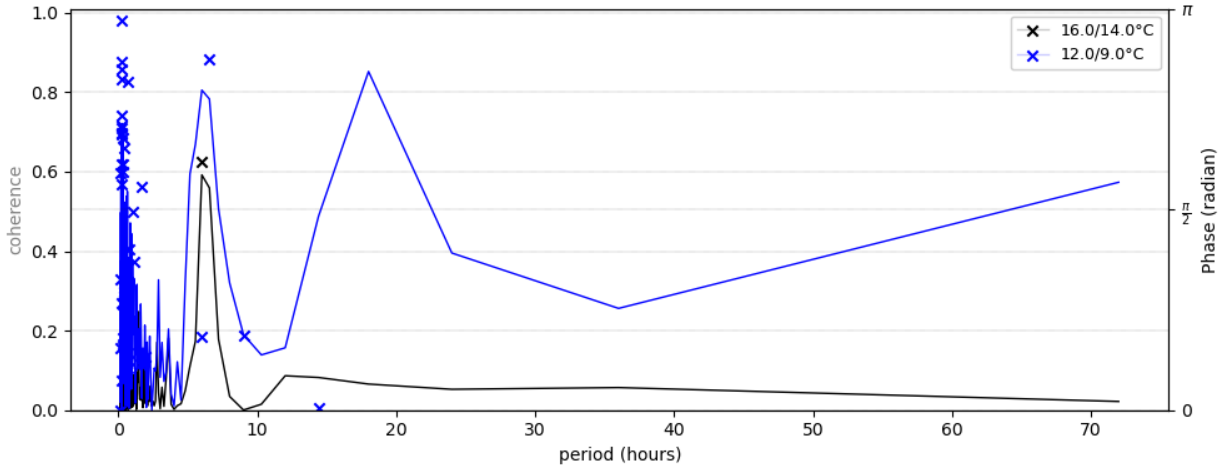

Figure 30: Magnitude-squared coherence and phase shift between selected isotherms defined in the GUI.

The coherence analysis is based on the relationship between the mean-square power spectra of two time series, $f(t)$ and $g(t)$, and their cross-power spectrum $\phi^*_{fg}(\omega)$. The cross-spectrum represents the shared variance between both signals at each frequency, and is obtained from the Fourier transform of their cross-covariance function:

$$\phi^*_{fg}(\omega) = \sum_{k=-\infty}^{\infty} \frac{1}{N-1} \sum_{n=1}^{N} (f_n - \bar{\mu}_f)(g_n - \bar{\mu}_g) e^{-i\omega k}, \qquad \omega \in [-1/2, 1/2], \tag{62}$$

where $\bar{\mu}_f$ and $\bar{\mu}_g$ denote the temporal means of f and g, respectively, and N is the total number of samples. The algorithm computes ϕ^*_{fg} internally using Fast Fourier Transform (FFT) operations on detrended signals.

The magnitude-squared coherence function is then defined as:

$$C_{fg}(\omega) = \left| \frac{\phi^*_{fg}(\omega)}{\sqrt{\phi^*_{ff}(\omega)\,\phi^*_{gg}(\omega)}} \right|^2, \qquad C_{fg}(\omega) \in [0, 1], \tag{63}$$

where ϕ^*_{ff} and ϕ^*_{gg} are the individual power spectral densities (PSDs) of f and g, respectively. Coherence values approaching unity $(C_{fg} \to 1)$ indicate strong phase-locked oscillations at frequency ω, implying that both signals share a consistent periodic component, such as a common internal seiche mode.

For isotherm temperature records, high coherence values identify depth levels that oscillate synchronously under the influence of a basin-scale standing wave. Coherence peaks between isotherms and wind could indicate forced internal seiches or, if oscillations occurs at the fundamental internal seiche period, indicate resonance between wind-induced surface forcing and the natural baroclinic response of the lake.

To complement the coherence analysis, the Interwave Analyzer computes the relative phase shift (or lag) between signals f and g at each frequency. The complex phase angle is derived from the real and imaginary parts of the

cross-spectrum:

$$P_{fg}(\omega) = \tan^{-1}\left(\frac{\mathrm{Im}\{\phi_{fg}^*(\omega)\}}{\mathrm{Re}\{\phi_{fg}^*(\omega)\}}\right), \qquad P_{fg}(\omega) \in [-\pi, \pi], \tag{64}$$

where Im and Re denote the imaginary and real components, respectively. A phase shift of 0 indicates synchronous motion, while π or $-\pi$ indicates antiphase behavior (e.g., one isotherm rising while the other sinks). Intermediate phase angles reveal propagating internal waves, with the sign of $P_{fg}(\omega)$ indicating the direction of energy propagation (upward or downward through the water column), which can be used to detect internal seiche with higher vertical modes.

6.3.5 Band–Pass Filtering

The Interwave Analyzer applies Butterworth band–pass filters to isolate frequency bands associated with dominant internal seiche oscillations in selected isotherm and temperature sensor time series (Figure 31). This method enables separation of large-scale baroclinic oscillations from background turbulence and high-frequency noise, improving the interpretation of energy contained within specific wave modes [1].
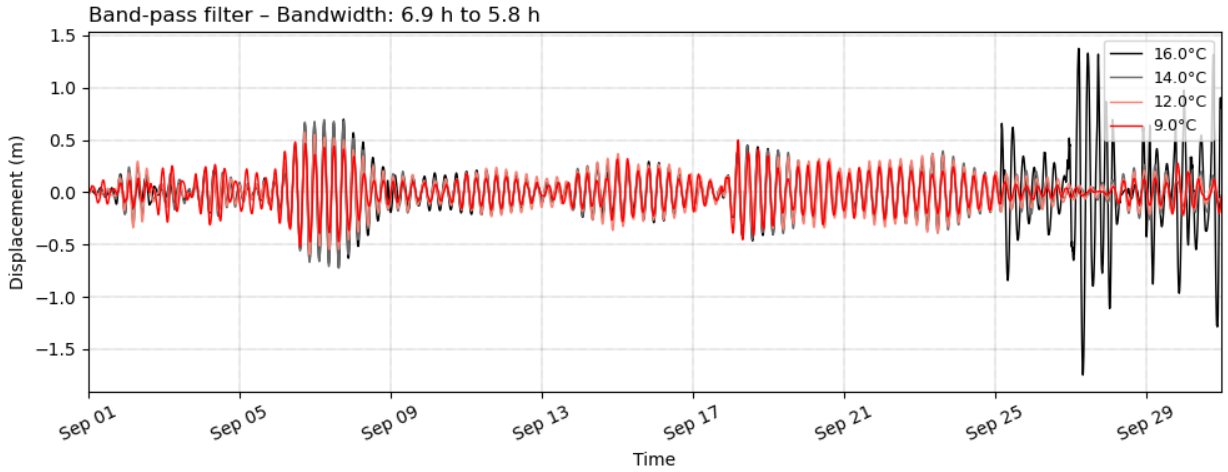

Figure 31: Band-pass filtered isotherm displacements (m) relative to the mean, using user-defined or model-estimated frequency limits.

A band–pass filter passes only those signal components whose frequencies lie between two cutoff frequencies: the lower cutoff f_{low} and upper cutoff f_{high}. The Butterworth design was chosen for its maximally flat response in the passband, minimizing amplitude distortion. The normalized filter coefficients are determined by solving the classical Butterworth polynomial in the frequency domain:

$$H(\omega) = \frac{1}{\sqrt{1 + \left(\frac{\omega}{\omega_c}\right)^{2n}}}, \tag{65}$$

where ω_c is the cutoff angular frequency and n is the filter order. The transfer function $H(\omega)$ defines how input amplitudes are attenuated across frequencies. In the Interwave Analyzer, the implementation uses the digital equivalent with second–order sections (SOS) for numerical stability:

$$\mathrm{sos} = \mathrm{butter}(n, [f_{\mathrm{low}}/f_{\mathrm{Nyq}}, f_{\mathrm{high}}/f_{\mathrm{Nyq}}], \texttt{btype='band'}), \tag{66}$$

where $f_{\mathrm{Nyq}} = 0.5\, f_s$ is the Nyquist frequency, and f_s is the sampling frequency.

The band–pass filter is applied to temperature fluctuations at selected isotherms, and raw temperature signals from submerged thermistors. By selecting frequency bands that correspond to the theoretical periods of fundamental and higher–order internal seiche modes (computed from the decomposition model), the filtering procedure extracts the oscillatory response associated with these modes.

After filtering, the amplitude of the oscillatory component for each isotherm is estimated as:

$$A_i = \max(|f_{\text{filtered},i}(t)|), \tag{67}$$

where A_i is the maximum absolute deviation of the filtered signal for the i–th isotherm.

The overall maximum amplitude among all isotherms is then identified as:

$$A_{\max} = \max_i(\text{banda}_i), \qquad \tau_{\max} = \tau_i \text{ where } A_i = A_{\max}. \tag{68}$$

This amplitude corresponds to the isotherm with the strongest oscillatory motion and is subsequently used in the theoretical classification of internal seiche generation and degeneration.

6.3.6 Wavelet Analysis

The Interwave Analyzer applies a time–frequency localized spectral analysis to resolve non–stationary oscillations in temperature and meteorological data [14]. Unlike the Fourier transform, which assumes signal stationarity, the wavelet transform adapts its window length dynamically with frequency, enabling simultaneous temporal and frequency resolution (Figure 32b). This makes it especially effective for detecting **wind–resonant internal waves** and transient seiche events in stratified lakes [14].
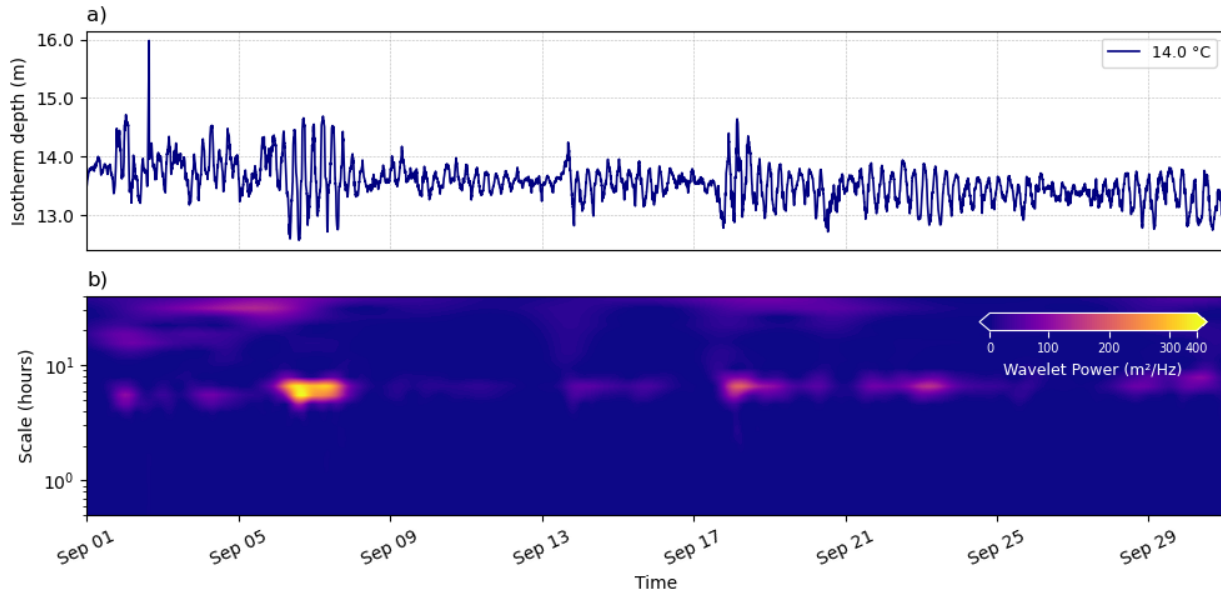

Figure 32: a) Time series of 14 °C isotherm, b) corresponding wavelet spectrum. The y-axis represents oscillation period (h), and the x-axis represents time

The continuous wavelet transform (CWT) of a time series $f(t)$ is defined as

$$W_f(v, s) = \frac{1}{\sqrt{s}} \int_{-\infty}^{+\infty} f(t)\, \psi^*\left(\frac{t-v}{s}\right)\, dt, \tag{69}$$

where s is the scale parameter controlling frequency dilation, υ is the translation parameter determining the time localization, and $\psi(t)$ is the chosen mother wavelet. The transform decomposes $f(t)$ into a two–dimensional time–scale space (υ, s) that captures both amplitude and phase variations of oscillatory components.

All input time series are zero–padded at both ends to reduce border distortions due to edge effects. The distance between successive scales is fixed to $\Delta s = 0.10$, providing a balance between computational cost and scale resolution (smaller values improve precision but increase computation time). The smallest wavelet scale is defined as four times the sampling period Δt:

$$s_{\min} = 4\,\Delta t. \tag{70}$$

This ensures that the highest–frequency oscillations are well resolved without violating the Nyquist criterion.

The wavelet power spectrum quantifies the variance of the signal at each scale and time:

$$P(\upsilon, s) = \frac{|W_f(\upsilon, s)|^2}{\sigma^2}, \tag{71}$$

where σ^2 is the variance of the original time series. This normalization allows the power at each scale to be expressed as a proportion of the total variance, facilitating comparison between different isotherms or datasets.

The Interwave Analyzer provides three selectable mother wavelets: Morlet wavelet, Paul wavelet, and Derivative of Gaussian (DOG) wavelet. The choice of wavelet depends on the analysis goal. For identifying wind–driven resonances, the Morlet function is typically preferred; for transient thermocline displacements, DOG is more effective.

When applied to isotherm temperature fluctuations, wavelet analysis reveals the time–varying energy distribution of internal waves. Because the frequency of internal seiches often evolves under changing wind forcing, CWT provides superior temporal tracking compared to Fourier methods. Regions of high normalized power in the (υ, s) space indicate episodes of strong oscillatory activity, frequently coinciding with peaks in wind speed.

6.4 Meteorological and stability parameters

6.4.1 Averaged Wind Direction

To determine the prevailing direction of meteorological forcing acting on the lake surface, the Interwave Analyzer computes an intensity–weighted mean wind direction based on the approach described by [15]. This method avoids the discontinuity problem inherent to circular data (e.g., averaging 359° and 1° should yield 0°, not 180°) by performing the averaging in vector space rather than directly on angular values.

Given instantaneous wind direction θ_i (in degrees) and corresponding wind speed u_i (in $\mathrm{m\,s^{-1}}$), the zonal and meridional components of the wind are first computed by converting directions to radians:

$$u_{\mathrm{east}} = u_i \sin\theta_i, \tag{72}$$
$$u_{\mathrm{north}} = u_i \cos\theta_i. \tag{73}$$

Each component is weighted by the wind speed magnitude to account for the relative strength of different wind events. The mean vector components are obtained as:

$$\bar{u}_{\mathrm{east}} = \frac{1}{N}\sum_{i=1}^{N} u_i \sin\theta_i, \tag{74}$$

$$\bar{u}_{\mathrm{north}} = \frac{1}{N}\sum_{i=1}^{N} u_i \cos\theta_i. \tag{75}$$

The resulting mean wind direction $\bar{\theta}$ (in degrees) is calculated using the four–quadrant inverse tangent function to preserve correct directional orientation:

$$\bar{\theta} = \arctan 2(\bar{u}_{\text{east}}, \bar{u}_{\text{north}}) \times \frac{180}{\pi} \bmod 360. \tag{76}$$

This ensures that $\bar{\theta}$ is expressed in the full circular range of $0°$ to $360°$ measured clockwise from the north.

The averaged wind direction represents the dominant direction of energy input to the lake surface over a selected time window. Because the computation is weighted by wind intensity, it reflects the direction of the most dynamically influential winds, rather than a simple arithmetic mean of directions.

6.4.2 Wind Speed at 10 m Height

In meteorological and limnological applications, wind speed is commonly standardized to a reference height of 10 m above the surface to ensure consistency in comparing datasets and estimating momentum fluxes. However, field measurements are frequently obtained at other elevations depending on the location of weather stations or instrumentation. To account for this, the Interwave Analyzer converts wind speed measured at height z (u_z) to the equivalent 10 m reference speed (u_{10}) using a logarithmic wind profile formulation derived from the surface-layer similarity theory.

Under horizontally homogeneous and neutrally stable atmospheric conditions, the vertical profile of horizontal wind velocity near the surface can be described by:

$$u(z) = \frac{u_*}{k} \ln\left(\frac{z}{z_0}\right), \tag{77}$$

where u_* is the friction velocity (m s^{-1}), $k = 0.4$ is the von Kármán constant, z_0 is the aerodynamic roughness length of the surface. This logarithmic law expresses the vertical decay of mean wind velocity toward the surface due to turbulent shear stress.

The Interwave Analyzer implements a simplified form of Eq. 77 to relate the measured velocity at height z to the equivalent velocity at the 10–m reference height. The relationship is expressed as:

$$u_{10} = u_z \left[1 - \frac{\sqrt{C_d}}{k} \ln\left(\frac{10}{z}\right)\right]^{-1}, \tag{78}$$

where C_d is the air–water drag coefficient, which quantifies surface frictional resistance and $\ln(10/z)$ represents the logarithmic correction between the two elevations.

In the Interwave Analyzer source routine, C_d is parameterized according to wind speed:

$$C_d = \begin{cases} 0.0010, & u_z < 5 \text{ m s}^{-1}, \\ 0.0015, & u_z \geq 5 \text{ m s}^{-1}. \end{cases} \tag{79}$$

This empirical formulation captures the increase in aerodynamic drag with rising wind velocity due to enhanced surface roughness and wave formation.

6.4.3 Wind Stress

The Interwave Analyzer estimates the surface wind stress τ (in N m^{-2} or Pa) to quantify the mechanical forcing exerted by atmospheric flow over the lake surface (Figure 33). This stress represents the rate of momentum transfer from air to water and provides the primary energy source for generating surface currents and internal seiches.
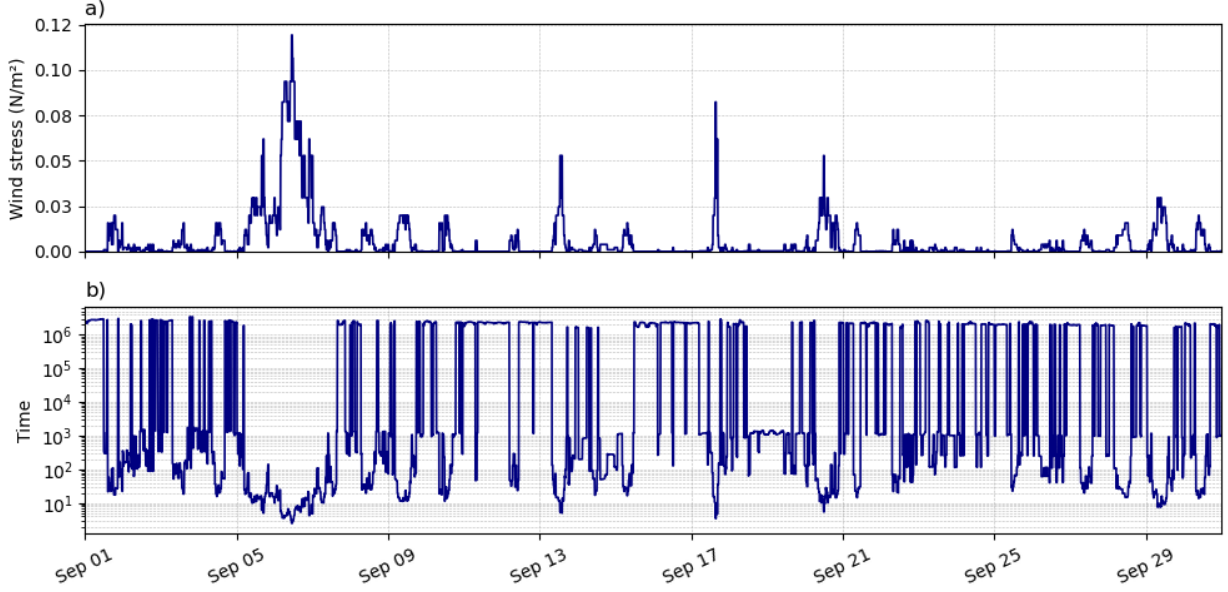
Figure 33: Time series of a) wind shear stress and Wedderburn number.

Wind stress is calculated using the classical quadratic drag law:

$$\tau = \rho_{\text{air}}\, C_d\, u^2, \tag{80}$$

where τ is the wind stress $(\text{N}\,\text{m}^{-2})$, $\rho_{\text{air}} = 1.225\ \text{kg}\,\text{m}^{-3}$ is the air density at standard conditions, C_d is the air–water drag coefficient (dimensionless), u is the wind velocity $(\text{m}\,\text{s}^{-1})$.

The computed τ values are subsequently used to derive the Wedderburn number and Richardson number in lake stability analyses, and forcing inputs to internal seiche generation models. Thus, τ acts as the quantitative link between atmospheric forcing and internal hydrodynamic response.

6.4.4 Homogeneous Wind Events

The Interwave Analyzer identifies periods of homogeneous wind direction, intervals during which wind forcing maintains a consistent direction aligned with the lake's principal axis (Figure 34, horizontal bars above the graph). Such events are crucial for establishing sustained surface setup and for effectively transferring momentum to excite internal seiches [1, 16].

Homogeneous events are detected within the temporal loop by tracking consecutive time steps where the wind direction remains within an angular tolerance $\Delta\theta$ of the dominant lake axis (tolerance prescribed by user as wind direction contribution).

For each time step t, the software compute the mean wind direction $\bar{\theta}_t$ over a sliding window of width W_{win} using intensity-weighted averaging:

$$\bar{\theta}_t = \arctan\left(\sum iw_i \sin\theta_i, \sum iw_i \cos\theta_i\right) \times \frac{180}{\pi} \bmod 360 \tag{81}$$

The software determine the allowable angular limits $(\theta_{\min}, \theta_{\max})$ based on $\bar{\theta}_t$ and the tolerance $\Delta\theta$. If the current wind direction θ_t lies within these bounds, increment the directional persistence counter N_{dir}; otherwise, reset it. The longest consecutive sequence satisfying this condition defines $T_{\text{direction}}$.
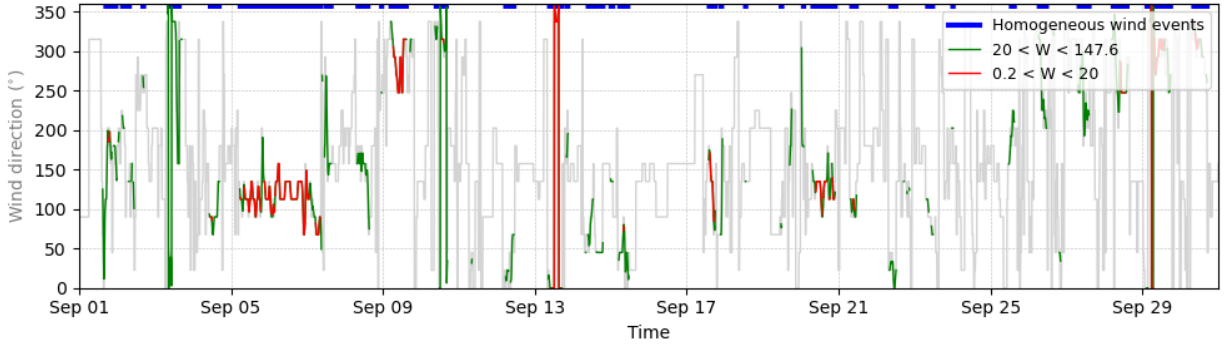
58

Figure 34: Wind diagnostics related to internal seiche dominance and mixing regimes. Green lines represent mean wind direction within moderate Wedderburn ranges, red lines indicate stricter theoretical limits, and blue bars denote persistent wind directional events.

Homogeneous winds generate consistent surface shear stress in a single direction, maximizing the horizontal displacement of the surface layer and promoting the growth of basin-scale standing internal waves. In contrast, variable winds redistribute momentum across multiple directions, dispersing energy and preventing coherent thermocline oscillation.

6.4.5 Reduction Factors

The reduction factors quantify how the effective wind energy available for internal seiche generation is diminished by limited wind persistence and directional variability [16]. Even under strong wind stress, short-duration or inconsistent winds may fail to impart sufficient energy for establishing basin-scale internal seiches. Thus, two coefficients, duration and direction reduction factors, are applied to normalize the Wedderburn number W.

The duration-based reduction factor is defined as:

$$f_{\text{duration}} = \min\left(1, \sqrt{\frac{4T_{\text{duration}}}{T_{V1H1}}}\right), \tag{82}$$

and the direction-based reduction factor as:

$$f_{\text{direction}} = \min\left(1, \sqrt{\frac{4T_{\text{direction}}}{T_{V1H1}}}\right), \tag{83}$$

where T_{V1H1} is the fundamental basin-scale internal wave period, computed from the internal seiche decomposition model, T_{duration} is the duration of the longest continuous wind event consistent with the BSIW dominance regime (Wedderburn number within dynamic limits), and $T_{\text{direction}}$ is the duration of the longest episode of homogeneous wind direction.

Each factor scales between 0 and 1, acting as a filtering coefficient that reduces the effective Wedderburn number:

$$W_{\text{eff}} = W \, f_{\text{duration}} \, f_{\text{direction}}. \tag{84}$$

This ensures that only winds with sufficient persistence and directional coherence are considered capable of generating basin-scale internal motions. For example, when $T_{\text{duration}} < 0.25 \, T_{V1H1}$, the duration factor strongly attenuates W_{eff}, preventing spurious classification of transient gusts as seiche-generating events.

59

6.4.6 Schmidt Stability

Schmidt Stability (S_t) quantifies the mechanical stability of a stratified water column by measuring the amount of work per unit surface area required to fully mix the water body to uniform density without adding or removing heat [17]. It represents the resistance of the stratification to wind-induced mixing and depends both on the density structure and basin geometry (Figure 35).
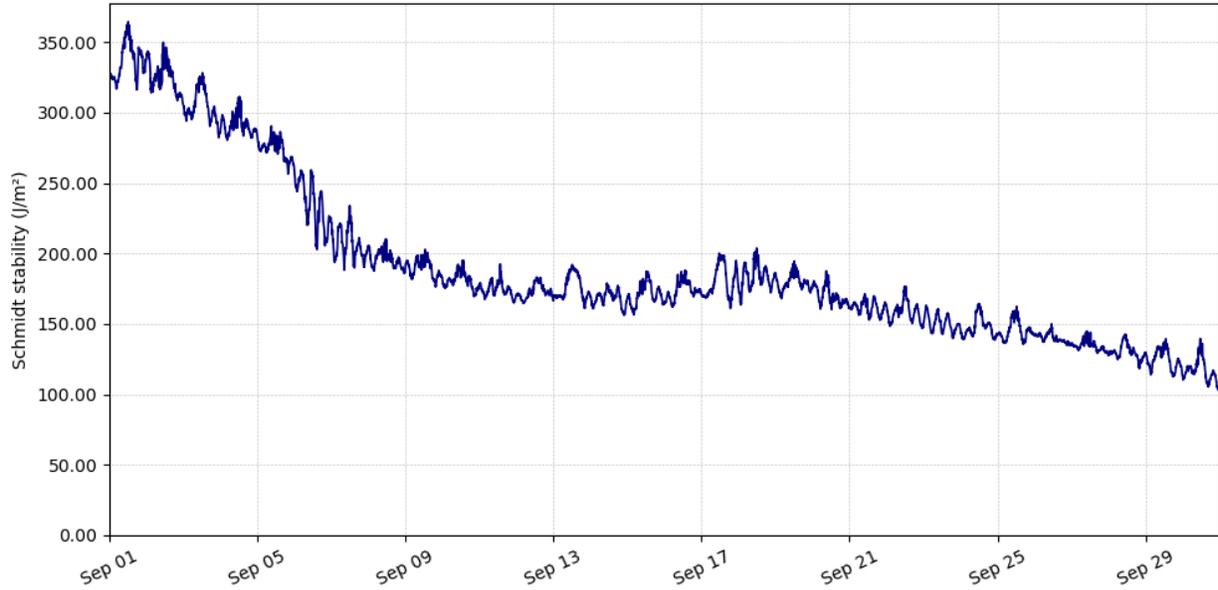

Figure 35: Time series of Schmidt Stability (J/m^2).

The Interwave Analyzer reconstructs the basin hypsography internally from longitudinal and, when available, transverse bathymetric transects.

Two geometric configurations are supported:

Circular basin approximation (when only longitudinal data are available):

$$A(z) = \pi \left(\frac{L_{\text{long}}(z)}{2} \right)^2. \tag{85}$$

Elliptical basin approximation (when both longitudinal and transverse data are available):

$$A(z) = \pi \left(\frac{L_{\text{long}}(z)}{2} \right) \left(\frac{L_{\text{trans}}(z)}{2} \right). \tag{86}$$

where z be the vertical coordinate (positive downward), $A(z)$ the horizontal cross-sectional area at depth z, $L_{\text{long}}(z)$ the longitudinal width at depth z, and $L_{\text{trans}}(z)$ the transverse width (if available). Bathymetric distances for constant vertical a refined vertical grid with spacing $\Delta z = 0.1$ m to ensure accurate numerical integration.

The temperature profile $T(z)$ is interpolated onto the same refined vertical grid. Water density $\rho(z)$ is then computed using the equation of state (Eq. 1). The vertical position of the center of volume Z_{cv} is computed as

$$Z_{cv} = \frac{\int z A(z) \, dz}{\int A(z) \, dz}, \tag{87}$$

which represents the geometric centroid of the basin volume.

Schmidt Stability ($J\,m^{-2}$) is defined as

$$S_t = \frac{g}{A_0} \sum \left[-(Z_{cv} - z_i)\,\rho_i\,A_i\,\Delta z \right].$$ (88)

where g is gravitational acceleration, A_0 is the lake surface area, and $z_{\min}$ and $z_{\max}$ define the vertical domain.

> ⚠️ Accurate Schmidt Stability estimation requires consistent bathymetric reconstruction and correct sensor depth ordering (depths must increase positively downward). Errors in basin geometry or temperature interpolation directly affect the computed stability. The method assumes horizontal homogeneity of temperature at each depth and does not account for lateral density gradients.

6.4.7 Richardson Number

The Richardson number (Ri) is a non-dimensional parameter that quantifies the balance between stabilizing buoyancy and destabilizing shear in a stratified fluid. In the Interwave Analyzer, it is used to diagnose the dynamic stability of the water column in relation to wind shear and to determine whether wind-induced shear can overcome stratification to promote vertical mixing or internal wave generation.

The Interwave Analyzer computes both a depth-resolved (Figure 36b) and a bulk (Ri_{1D}) Richardson number at each time step.
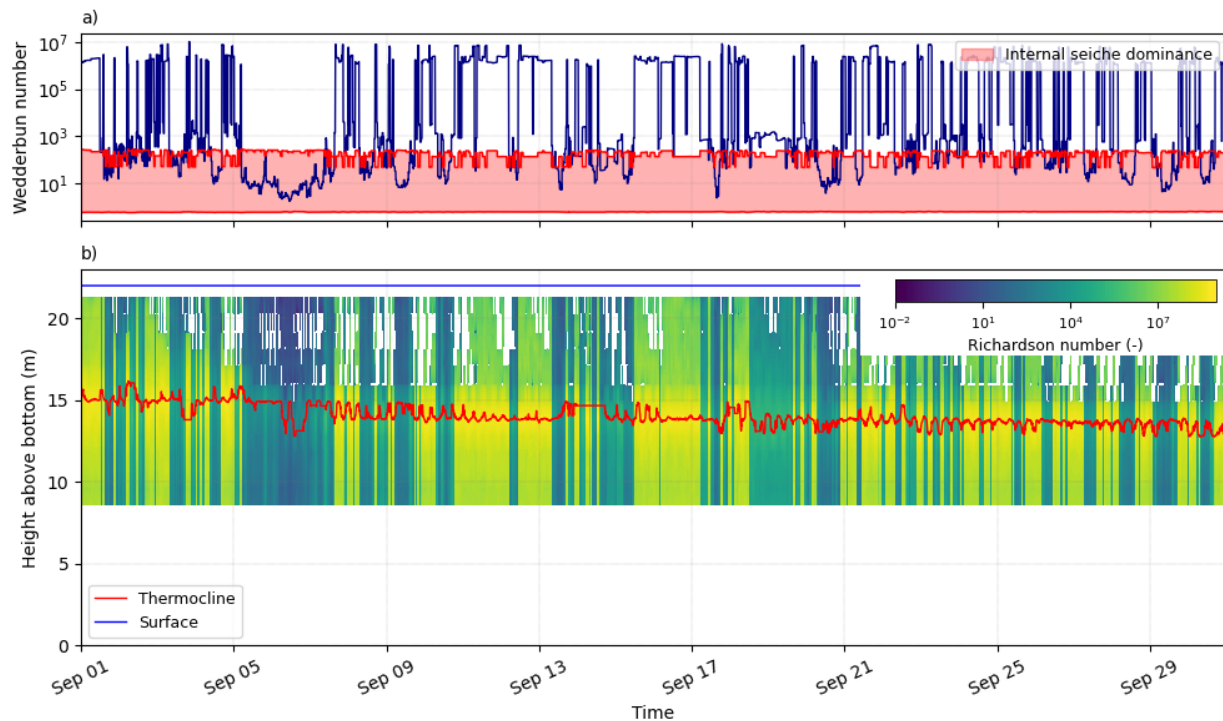

Figure 36: a) Time series of the standard Wedderburn number, with the shaded region indicating the internal seiche dominance range. b) Local Richardson number with thermocline and surface references.

For each vertical layer, the software estimates the velocity shear associated with wind stress and computes the Depth-Resolved Richardson Number (Ri_{2D}) as

$$Ri(z_i) = \frac{g_{\text{lin}}(z_i)\left(H - h_{\text{mid}}(z_i)\right)}{u_*^2},\tag{89}$$

where $g_{\text{lin}}(z_i)$ is the local buoyancy gradient (s^{-2}), H is the total lake depth (m), $h_{\text{mid}}(z_i)$ is the mid-layer depth, $u_* = \sqrt{\tau/\rho}$ is the friction velocity of the wind $(\text{m}\,\text{s}^{-1})$, and τ is the surface wind stress $(\text{N}\,\text{m}^{-2})$.

The density between layers is averaged to define ρ_{mean}:

$$\rho_{\text{mean}} = \left|\frac{\rho_i + \rho_{i+1}}{2}\right|.\tag{90}$$

The friction velocity is computed as:

$$u_* = \sqrt{\frac{\tau}{\rho_{\text{mean}}}}.\tag{91}$$

Equation 89 is evaluated for all layers (z_1 to z_{qt-1}), producing a vertical Richardson number profile.

The bulk, or layer-integrated, Richardson number provides a single value that characterizes the potential for shear instability across the entire water column or mixing layer [18]:

$$Ri_{\text{bulk}} = \frac{g_{\text{lin}}\,h_e}{u_*^2},\tag{92}$$

where g_{lin} is the bulk buoyancy gradient, and h_e is the effective mixed-layer or shear depth.

The Interwave Analyzer evaluates these criteria at every time step to classify lake stability regimes and to identify events of potential internal seiche degeneration or turbulence generation, according to lake mixing classification [18] (classification that is illustrated in Figure 19, from dashboard results)

6.4.8 Wedderburn Number

The Wedderburn number (W) is a non-dimensional parameter describing the balance between wind-induced shear and buoyancy forces in a stratified lake (Figure 36a). It represents the relative importance of stabilizing stratification to destabilizing wind stress and is a fundamental diagnostic for predicting the onset of basin-scale internal seiches and vertical mixing.

The Wedderburn number was introduced by [18] to quantify the deformation of the thermocline due to sustained wind forcing. It can be expressed as:

$$W = \frac{g'h_e^2}{L_S\,u_*^2},\tag{93}$$

where g' is the reduced gravity $(\text{m}\,\text{s}^{-2})$, h_e is the epilimnion depth (m), L_S is the characteristic fetch length or lake length in the direction of the wind (m), u_* is the wind friction velocity $(\text{m}\,\text{s}^{-1})$, and τ is the surface wind stress.

The parameter W thus represents the ratio between potential energy associated with stratification and the kinetic energy input from wind forcing. A high W value (> 1) indicates a stable regime where wind forcing is insufficient to significantly tilt the thermocline, while a low W value (< 1) indicates that the thermocline can be displaced or even overturned by wind stress.

The Interwave Analyzer implements Eq. 93 directly, computing the instantaneous Wedderburn number at each time step from modeled and measured quantities (Figure 36a). The function includes safeguards to avoid division by zero or undefined results when input values are non-physical (e.g., negative or zero). The lake mixing regime and the dominance of internal seiche activity can be predicted by the Wedderburn number (Eq. 93) and theoretical

mixing regimes index from [18] (see section 6.5.1). This classification to identify internal seiche dominance period is illustrated in Figure 36a.

The Wedderburn number is also filtered by reduction factors based on the wind homogeneity and wind duration to support the formation of BSIW (Figure 37):

$$W_{filtered} = W_{standard} \, f_{factor},$$ (94)
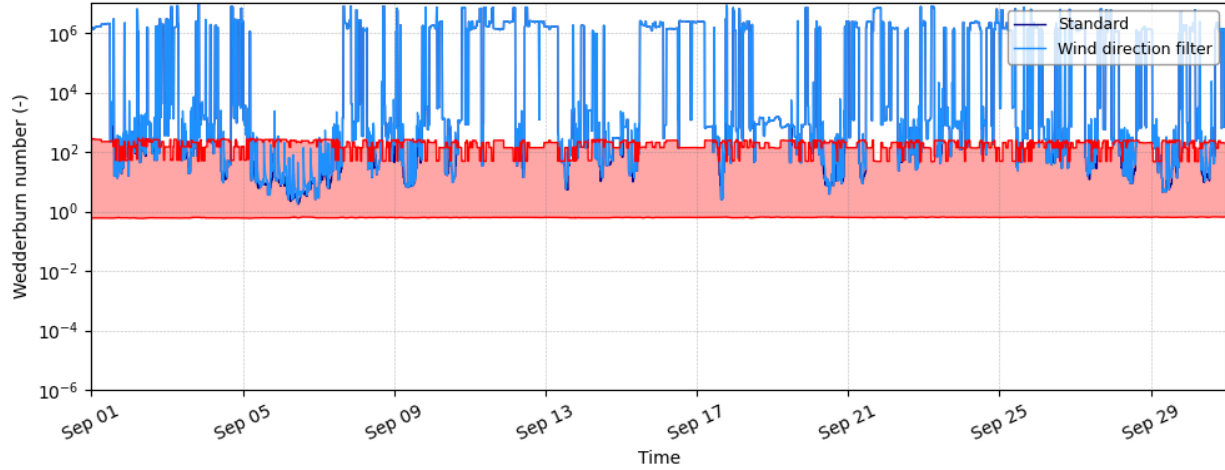
in which f_{fector} are the filtered factors.

Figure 37: Time series of the standard and directionally filtered Wedderburn numbers. The shaded region indicates the internal seiche dominance range [18].

6.4.9 Lake Number

The Lake Number (L_n) is a dimensionless stability index that quantifies the balance between stratification strength and wind forcing [19]. It compares the stabilizing potential energy of stratification with the destabilizing shear stress exerted by wind at the lake surface.

The volumetric stability is first reconstructed as

$$S_v = \frac{S_t A_0}{g},$$ (95)

which represents the total potential energy anomaly of the water column.

The Lake Number is then computed as

$$L_n = \frac{g S_v (h_e + h_h)}{2 \rho_h u_*^2 A_0^{3/2} Z_{cv}}.$$ (96)

This formulation expresses the ratio between restoring buoyancy forces and wind-driven tilting forces acting on the stratified water column. Because L_n depends on both stratification (S_t) and wind forcing (u_*), it provides a dynamically integrated indicator of mixing potential.

⚠️ Lake Number estimation is sensitive to uncertainties in Schmidt Stability, friction velocity (u_*), and layer thickness determination. Errors in thermocline depth directly affect h_e and h_h, while inaccuracies in wind stress parameterization propagate quadratically through u_*^2. Additionally, the formulation assumes horizontal homogeneity and neglects Coriolis effects and three-dimensional circulation patterns. Therefore, L_n should be interpreted as a basin-integrated diagnostic index.

6.5 Theories and classification

The lake mixing classification and theoretical prediction of the basin-scale internal seiches amplitude and degeneration are based on well established theories described by [18, 20, 21, 8], and presented in more details in this section.

6.5.1 Lake classification

The lake classification is based on theory proposed by [18], which classify the lake mixing according to lake conditions, including the Wedderburn Number calculated at the thermocline depth (Eq. 93). According to [18], a prediction of internal seiche generation can be done by comparing the Wedderburn number or Richardson number with the aspect ratio between the reservoir length that is aligned with the wind, L and the epilimnion thickness, h_e (Figure 38b-d).
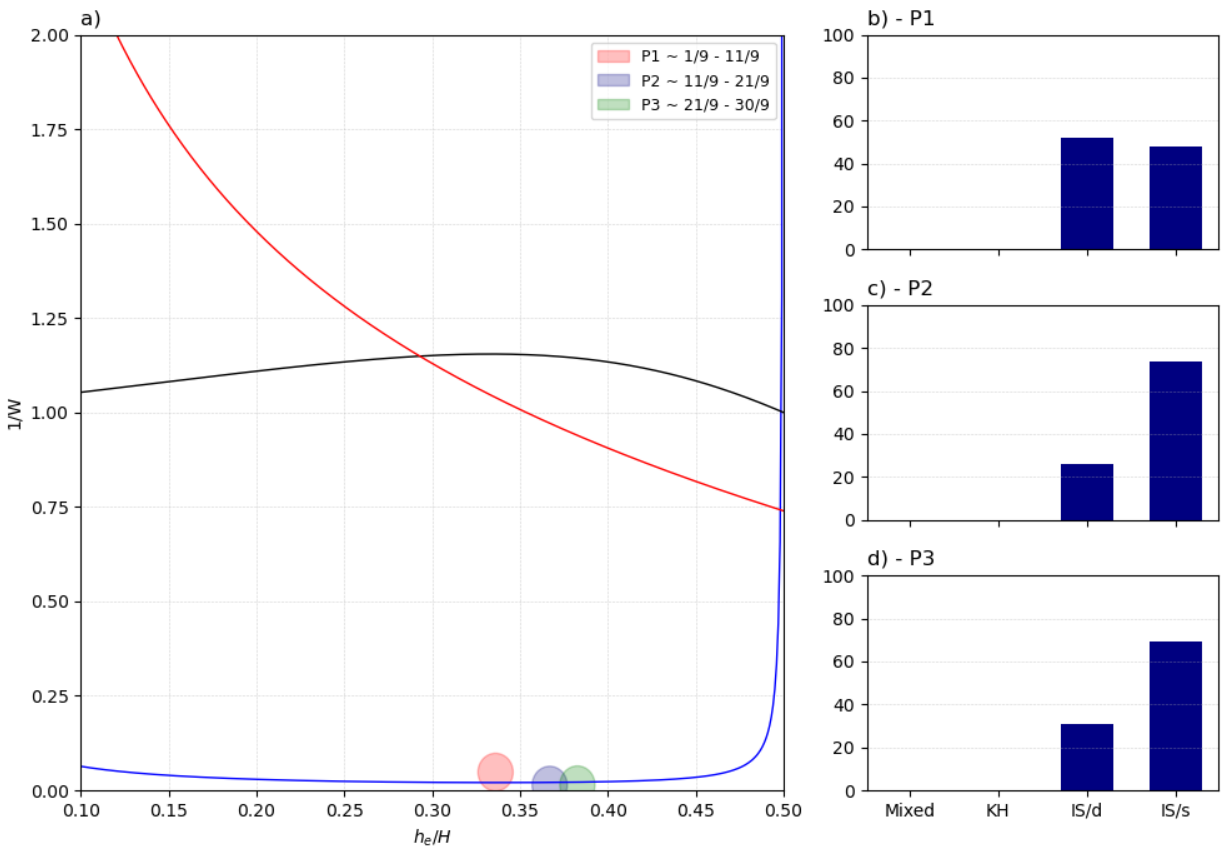

Figure 38: a) Averaged degeneration regime of internal seiches in the parameter space defined by h_e/H and $1/W$. Theoretical instability limits (e.g., dissipative steepening, bore limit, Kelvin–Helmholtz) are shown as reference curves. Ellipses represent the mean state and 95% variability for three subperiods (P1–P3). b–d) Theoretical lake mixing regimes for each subperiod.

Note that the Wedderburn number and the Richardson number are closely related and can both be used to describe lake mixing regimes ($W = Ri \, h_e/L$). Although the presence of L may appear to introduce an additional dependency, the regime classification based solely on Ri also implicitly depends on the basin length scale. The Interwave Analyzer typically presents mixing regimes according to the Richardson number definition (e.g., Figure 19).

When $W < h_e/L$ (Regime 1), the disturbance frequency is higher than the stratification frequency, resulting in a complete mixing of the lake (*Mixed*). In spite of baroclinic shear could occur, the intensity of the wind is so strong compared to the stratification that the stratification is broken down by mixing.

When $h_e/L < W < 0.5 \, ((h_e + h_h)/h_h)^{1/2}$ (Regime 2), a large interface displacement occurs and is accompanied by interface shear and Kelvin-Helmholtz billows (*KH*). As stated by [22], Kelvin-Helmholtz billow is a kind of wave that develops when the destabilizing effect overcomes a little the stabilizing density stratification effect, occurring a shear flow effect. In this regime, internal seiches are usually not observed because the perturbation frequency normally is higher than the Brunt–Väisälä. A complete vertical mixing can occur during a single wind episode and thickness of the metalimnion can be $> 0.3 \, h_e$.

When $0.5 \, ((h_e + h_h)/h_h)^{1/2} < W < L/(4h_e) \, ((h_e + h_h)/h_h)^{1/2}$ (Regime 3), internal seiche is dominant within the system interior (*IS/d*). Although the buoyancy effect is strong compared to the disturbances caused by wind stress, winds are strong enough to cause significant interface displacements. According to [18], two-dimensional effects can be disregarded for most of the range of W in this regime, and a complete vertical mixing is unlikely to occur.

When $W > L/(4h_e) \, ((h_e + h_h)/h_h)^{1/2}$ (Regime 4), the buoyancy dominates all processes. Internal seiches still may be generated, but normally they present short periods and small amplitudes (*IS/s*). Although low W is frequently associated with less stable system and mixing, the shear flow caused by internal waves in deep water presents instabilities even for large W. The waves grow by extracting energy from the background shear flow. As the system becomes less stable, linear theory fails to reproduce the real motion. However, as stated by [23], nonlinear simulations have demonstrated that if W is sufficiently large, the disturbance saturates at finite amplitude. In a weak stratified system, the interface wraps, forming Kelvin-Helmholtz billows.

6.5.2 Initial Basin-Scale Internal Wave Amplitude

The initial amplitude of basin-scale internal waves (BSIW) is estimated using two complementary theoretical approaches: classical linear two-layer theory and a higher-order parametrization derived from numerical simulations. There results is compared to measurements data using band-pass filtered isotherms and estimated Wedderburn number and epilimnion thickness (Figure 39).

Linear Two-Layer Theory

According to linear internal wave theory for a two-layer system composed of immiscible fluids [19], the initial displacement of the interface induced by wind forcing is inversely proportional to the Wedderburn number W. The predicted fundamental-mode amplitude is

$$\zeta_0 = \frac{h_e}{2W},$$

(97)

where ζ_0 is the basin-scale internal wave amplitude and h_e is the epilimnion thickness.

This expression assumes, small-amplitude oscillations, sharp density interface, uniform wind forcing, and linear restoring dynamics. Equation 97 represents the theoretical interface displacement associated with the fundamental internal seiche (V1H1 mode).
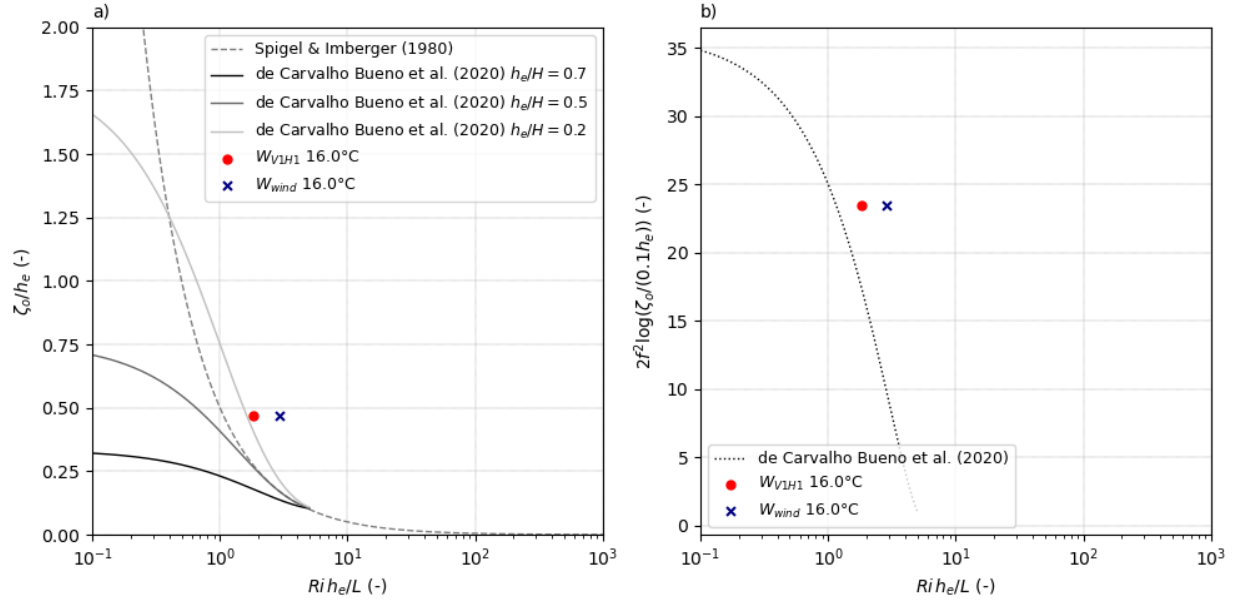
Figure 39: a) Theoretical relationship between normalized internal seiche amplitude (A/h_e) and the Wedderburn number according to different formulations. The normalized internal seiche amplitude (markers) were computed based on time-averaged epilimnion thickness and maximum band-pass filtered isotherm displacement. The Wedderburn number is averaged over windows corresponding to either one-eighth of the fundamental period (W_{V1H1}) or one-eighth of the wind-event duration (W_{wind}); the minimum averaged value is retained as the critical wind–stratification condition. b) Influence of higher-order he/H effects on internal seiche amplitude.

Higher-Order Parametrization for Miscible Fluids

Recognizing that natural lakes exhibit continuous stratification and boundary effects, [21] proposed a semi-empirical parametrization that accounts for miscibility and finite-depth geometry. The normalized amplitude is expressed as

$$\frac{\zeta_0}{h_e} = \xi \exp\left[\frac{-(Ri\,h_e - k_2 L)^2}{2(Lf)^2}\right], \tag{98}$$

where Ri is the bulk Richardson number, L is the effective basin length (fetch), $\xi = 0.1$ defines the minimum internal wave energy level captured by the parametrization, $k_2 = 0.125$ is an empirical constant, and f is a non-dimensional function of h_e/H.

The higher-order dependence on relative layer thickness is given by

$$f\left(\frac{h_e}{H}\right) = g\left(\frac{h_e}{H}\right)\exp\left(\frac{(h_e/H)^2}{k_3}\right), \tag{99}$$

with

$$g\left(\frac{h_e}{H}\right) = 12.156\left(\frac{h_e}{H}\right)^3 - 15.714\left(\frac{h_e}{H}\right)^2 + 2.8426\left(\frac{h_e}{H}\right) + 2.0846. \tag{100}$$

This parametrization was validated for $0.1 \leq h_e/H \leq 0.8$ and incorporates nonlinear and geometric effects not captured by linear theory.

Observed Amplitude Estimation

The Interwave Analyzer estimates observed internal seiche amplitude from band-pass filtered isotherm displacements (Figure 39, red and blue markers). For each selected isotherm, the signal is filtered within the internal-wave frequency band using a Butterworth filter. The maximum absolute displacement during the analyzed period is extracted:

$$\zeta_{\mathrm{max}} = \max |\zeta_{\mathsf{band}}(t)|, \tag{101}$$

where $\zeta_{\mathsf{band}}(t)$ is the band-pass filtered isotherm displacement. The representative normalized amplitude is then

$$\frac{\zeta_{\mathrm{max}}}{h_e}. \tag{102}$$

> ⚠️ The observed internal seiche amplitude estimated from band-pass filtered isotherm displacements is subject to several methodological limitations. The estimation depends strongly on the location of the thermistor chain relative to the basin-scale modal structure. Locations near antinodes provide more representative amplitudes. In addition, butterworth band-pass filtering introduces edge effects at the beginning and end of the time series. and the choice of frequency band directly affects the extracted amplitude. Therefore, the reported normalized amplitude ζ_{max}/h_e should be interpreted as an indicator of potential internal wave activity rather than an exact measure of the true basin-scale modal amplitude.

Wedderburn Number Averaging Strategies

Because W varies in time due to fluctuating wind forcing and stratification, two representative Wedderburn indices are computed (Figure 39):

1. W_{V1H1}: obtained by averaging W over windows proportional to one-eighth of the fundamental internal seiche period T_{V1H1}, and retaining the minimum averaged value:

$$W_{V1H1} = \min \left(\overline{W}_{\Delta t = T_{V1H1}/8} \right). \tag{103}$$

2. W_{wind}: obtained by averaging W over windows proportional to one-eighth of the wind-event duration T_{wind}, again retaining the minimum averaged value:

$$W_{\mathsf{wind}} = \min \left(\overline{W}_{\Delta t = T_{\mathsf{wind}}/8} \right). \tag{104}$$

The use of the minimum window-averaged value represents the most critical wind–stratification balance condition responsible for internal seiche excitation.

Duration and Direction Filtering

To account for finite wind-event duration and directional persistence, correction factors are applied:

- A duration factor proportional to $\sqrt{4T_{\text{wind}}/T_{V1H1}}$,

- A direction factor based on cumulative wind alignment relative to modal velocity structure.

These filters reduce the effective Wedderburn number when wind events are short or directionally inconsistent, preventing overestimation of predicted amplitudes.

6.5.3 Degeneration Classification

The degeneration of basin-scale internal waves (BSIW) is primarily controlled by nonlinear steepening, boundary-layer dissipation, shear instability, and hydraulic transitions. The theoretical framework describing these mechanisms is presented in detail by [24, 25, 20]. The Interwave Analyzer implements this framework to classify internal seiche behavior into five dynamical regimes (Figure 38a):

- Damped linear wave,

- Degeneration into propagating solitary internal waves,

- Kelvin–Helmholtz instability,

- Bore and billow formation,

- Supercritical flow.

The classification is performed in the parameter space defined by the relative epilimnion thickness h_e/H and the inverse Wedderburn number $1/W$. The Wedderburn number is computed as

$$W = \frac{g'h_e^2}{u_*^2 L},$$
(105)

where g' is the reduced gravity, h_e the epilimnion thickness, u_* the wind friction velocity, and L the effective fetch. The inverse Wedderburn number $(1/W)$ represents the relative importance of wind forcing compared to stratification.

For each time step, W and h_e/H are calculated using dynamically consistent layer properties derived from the two-layer or decomposition model. The full time series is then divided into three equal subperiods (P1–P3) to assess temporal variability of degeneration regimes. For each subperiod, confidence intervals (typically 95%) are computed for both h_e/H and $1/W$, providing statistically robust regime characterization.

> For the dashboard plots, the degeneration computation may differ from the values presented here, as it is calculated at each time step using time-varying variables.

Dissipative–Steepening Transition

When wave amplitude is small, basin-scale internal waves are damped by viscous dissipation and weak nonlinear effects. The transition from purely damped oscillations to nonlinear steepening occurs when the dissipative timescale becomes comparable to the nonlinear steepening timescale. This condition yields

$$\frac{\zeta_0}{h_e} < \frac{\nu T_{V1H1}}{3H\gamma_h}\left[\sqrt{\frac{\pi}{\nu T_{V1H1}}}\left(1-\frac{h_e}{H}\right)^2 + \frac{1}{\Delta_h}\right],$$
(106)

where ζ_0 is the internal wave amplitude, ν is the kinematic viscosity of water ($\nu \approx 1.1 \times 10^{-6}$ m^2 s^{-1}), T_{V1H1} is the fundamental internal seiche period, and

$$\gamma_h = \frac{h_e}{H}\left(1 - 2\frac{h_e}{H}\right). \tag{107}$$

If this inequality is satisfied, oscillations remain in the damped linear regime. **Bore (Supercritical) Formation**

For sufficiently large amplitudes, internal waves may transition to supercritical flow, producing hydraulic jumps (bores) and strong mixing. This occurs when

$$\frac{\zeta_0}{h_e} > \sqrt{\frac{(1 - h_e/H)^2}{(h_e/H)^3 + (1 - h_e/H)^3}}. \tag{108}$$

This condition indicates that nonlinear advection dominates dispersive and restoring effects. **Kelvin–Helmholtz Instability**

When shear across the thermocline becomes sufficiently strong, Kelvin–Helmholtz billows may form. This regime is reached when

$$\frac{\zeta_0}{h_e} > 2\sqrt{\frac{\Delta_h}{H}\left(\frac{H}{h_e} - 1\right)}. \tag{109}$$

This condition compares the instability growth timescale to the internal seiche period and reflects the onset of shear-driven overturning. **Combined Regimes and Solitary Wave Formation**

If both conditions in Equations 108 and 109 are satisfied, bore formation and Kelvin–Helmholtz instabilities may occur simultaneously. When neither threshold is exceeded but nonlinear steepening is significant, basin-scale oscillations may degenerate into trains of propagating solitary internal waves. **Implementation Procedure**

The Interwave Analyzer evaluates these theoretical boundaries using mean layer properties (densities, thicknesses, and total depth) and effective fetch. Theoretical regime curves are computed as continuous functions of h_e/H, while observational data $(h_e/H,\ 1/W)$ are overlaid using statistically averaged values for each subperiod.

Temporal evolution of degeneration is assessed by smoothing the time series of h_e/H and $1/W$ and comparing instantaneous states with the theoretical regime boundaries.

6.5.4 Slope Criticality Parameter

The slope criticality parameter evaluates whether internal waves propagating within the stratified water column are likely to reflect, transmit, or break upon encountering basin boundaries [8]. It compares the characteristic internal wave slope to the local bathymetric slope at thermocline depth.

For a stratified system, the characteristic propagation angle θ of a linear internal wave relative to the horizontal is governed by dispersion theory. For a wave with angular frequency ω and buoyancy frequency N, the internal wave slope satisfies

the wave slope angle (in degrees) is defined as

$$\theta = \arcsin\left(\frac{2\pi}{N\,T_{\text{wave}}}\right). \tag{110}$$

where N is the depth-averaged buoyancy frequency (Eq. 17). The angle θ represents the theoretical propagation inclination of internal wave energy rays within the stratified fluid.

At each time step, the thermocline depth is determined from the dynamically estimated epilimnion thickness. The local bathymetric slopes (α) are then computed at that depth along:

- the longitudinal transect (left and right margins),

- the transverse transect (if a two-dimensional geometry is provided).

These slopes are obtained from the derivative of the interpolated bathymetric profile evaluated at the instantaneous thermocline depth.

The slope criticality parameter is defined as the ratio between the local bottom slope (α) and the internal wave slope (θ):

$$A_t = \frac{\alpha}{\theta}. \tag{111}$$

Separate values are computed for:

- Longitudinal left and right margins,

- Transverse left and right margins (when available).

This parameter therefore identifies regions where topographic interaction may enhance boundary mixing and internal wave dissipation. When $A_t < 1$ (subcritical condition), the interaction between internal seiche and sloping topography induces enhanced turbulent mixing and bottom boundary layer separation with transport of water from the slope to the lake interior, inhibiting the formation of internal seiches. When $A_t < 1$ (supercritical condition), the bottom slope is steeper than the internal seiche. The energy is reflected and internal seiche form is preserved, presenting small damping rate (Figure 21).

> ⚠️ The slope criticality parameter assumes linear internal wave theory and uniform stratification. It is sensitive to errors in thermocline depth estimation and to local bathymetric resolution. Additionally, the method does not account for Coriolis effects, which may alter actual propagation angles in large basins.

7 Tutorial

In this tutorial, we guide you through the process of performing a simple analysis using example files available on the Interwave Analyzer webpage, under the **Download Examples** section. The present tutorial is based on the dataset provided in `Example 1 - Milada Lake`. Therefore, before proceeding, download the entire `lake.rar` under the button **Download Example 1 (.rar)**. More examples can be available in this page in future.

Inside the selected folder, there are five attribute files with distinct extensions (Table 5), each containing specific input data required for the analysis, such as water temperature profiles and meteorological forcing. Users may modify the file names if necessary; however, the file extensions are mandatory and must remain unchanged, as they are used by the software to correctly identify and process each input file.

Table 5: Overview of attribute files.

Attribute Files	File Name and Extension	Mandatory Extansion
Basin length and bathymetry	bathymetry.len	<.LEN>
Underwater temperature data	temperature.tem	<.TEM>
Meteorological data	wind.met	<.MET>
Specification of sensors depth and type	sensor.sen	<.SEN>
Basin length and bathymetry for a second transect	transect.sen	<.LEN>

This tutorial is intended for users working with the script-based version of the Interwave Analyzer. However, apart from the initial execution procedure and the steps required to launch the graphical user interface (GUI), the workflow described below is identical to that of users running the standalone executable version.

7.1 Graphical User Interface

To start the Interwave Analyzer, first complete the installation procedure (available at: [link]). Once the environment is properly configured, open *Spyder* or another Python interpreter and execute the script `iwgui.py`. The Interwave Analyzer GUI should then be displayed.

In the first tab (*Input Data*), you are required to load the necessary attribute files.

Click on the first *Open File* button (Temperature Data) and select the file `<temperature.tem>`. Then, click on the second *Open File* button (Meteorological Data) and select `<wind.met>`.

Since the file `<wind.met>` contains only wind speed and wind direction (an additional column for solar radiation could also be included), uncheck the *Solar Radiation* option.

> ⚠️ Interwave Analyzer is configured to recognize specific ASCII file extensions. When browsing a folder, only compatible files are displayed. If a file does not appear, it either has an incorrect extension or does not correspond to the expected data type.

> ⚠️ Clicking on *Open File* does not immediately load the data into memory; it only specifies the file path to be accessed during execution. Any modification to the file name or extension after it has been defined may result in an error when the program is executed.

The program then requests the height of the wind measurements (in meters). Keep the default value (10 m).

For *Wind Direction Contribution*, select a value between 20 and 30.

In the *Latitude* field, enter a latitude of 50 °.

In the section below, *Basin Length and Bathymetry*, select the option *File*. This action disables the manual input field and enables the corresponding *Open File* button. Click *Open File* and select <bathymetry.len>.

Next, specify the *Sensor Level* file. Click the respective *Open File* button and select <sensor.sen>. Below this field, the program requests the *Level of Reference*, defined as the vertical reference corresponding to the lake bottom. Enter a value of 0 m.

> ⚠️ The level of reference must be consistent with the water level data. If water level is referenced to a different datum (e.g., mean sea level), the level of reference must correspond to the elevation of the lake bottom relative to that same datum.

The water level must then be defined. Select *Uniform*. This option disables the *Open File* button. In the corresponding input field (Water Level, meters), specify a constant water of 22 m.

> ⚠️ If the water level varies over time, select *File* and provide a time series of water level data (see required format in previous section). Ensure that these values are referenced to the same level of reference defined previously.

The final option in this section allows the user to load a shapefile. This functionality is currently unavailable; therefore, leave this option unchecked.

> ⚠️ If *Include Shapefile* option is selected and a shapefile is provided, the program will run normally; however, the shapefile will not be loaded, as this functionality has not yet been implemented internally.

Now, click on the tab *Spectral Analysis and Definitions* and specify the following parameters in their respective input fields:

- Metalimnion threshold: 0.1 kg/m^4 (default value)
- Band-pass filter option: *Defined by Internal Wave Model*
- Fourier window function: *Hamming*
- Wavelet mother function: *Morlet*

> ⚠️ After the initial test, you may manually define the band-pass filter periods. Note that the *High-Frequency Band Period* must always be smaller than the *Low-Frequency Band Period*. Only the band-pass filtered results will be affected, corresponding to oscillations within the specified frequency range.

The final parameter to be defined in this tab is the window size for Welch's method. Select *Defined manually (days)*, which enables the input field, and specify a value of 3 days.

The window size should be chosen according to the maximum wave period of interest and the total length of the dataset. A shorter window reduces spectral variance and improves peak resolution, but limits the analysis of low-frequency (long-period) oscillations. A longer window allows the inclusion of lower-frequency oscillations; however, it increases spectral variance, particularly at higher-frequency bands.

Next, click on the *Isotherm Analysis* tab and select *Enable Isotherm Analysis*. Activate *Isotherm 1*, *Isotherm 2*, *Isotherm 3*, and *Isotherm 4* to enable their respective input fields. Enter the following isotherms to be analyzed: $16\ ^{\circ}\mathrm{C}$, $14\ ^{\circ}\mathrm{C}$, $12\ ^{\circ}\mathrm{C}$, and $9\ ^{\circ}\mathrm{C}$, respectively.

Below, select *Iso. 1–2* in *Comparison 1* and *Iso. 3–4* in *Comparison 2*. Then, enable *Sensor Analysis* and select all sensors: *Sensor 1*, *Sensor 2*, *Sensor 3*, and *Sensor 4*. Subsequently, specify the sensor numbers (from surface to bottom) corresponding to each selected sensor: 8, 11, 13, and 14, respectively.

In the final tab (*Output and Run*), click the *Open File* button to define the directory where output files will be saved.

Set the image resolution to 200 DPI. You may optionally save the current configuration for future analyses by clicking *File* in the upper menu and selecting *Save As*. This procedure stores all defined parameters, including the paths to the attribute files.

Only the file paths are saved during this process. The attribute file names must not be changed, nor can the files be moved to a different directory, otherwise errors may occur during execution.

To start the analysis, click the *Run* button. The simulation status and informational messages are displayed in the active (white) window, while warnings and errors are shown in the Python interpreter console.

For a second run, you may include additional parameters. This optional feature allows users to refine, extend, or modify calculations, interpretations, and results. The complete list of available additional parameters is provided in Section 4. This list may expand in future versions as new functionalities are implemented.

For a second run, include the following additional parameters:

- First line: *nameBasin = #Milada Lake#*
- Second line: *pathBathymetry = #transect.len#*

Run the analyzer again.

pathBathymetry modifies the basin geometry by incorporating an additional bathymetric transect (oriented at 90° relative to the main transect), resulting in ellipsoidal rather than purely circular layer representations. The additional bathymetry file must be located in the same directory as the main transect file, have the same extension, and match the name specified in the *pathBathymetry* parameter. This modification significantly affects the results, as it introduces a variable effective basin length, influencing wave periods, nondimensional numbers, Schmidt stability, and all dependent variables.

7.2   Result Files

The results generated by the Interwave Analyzer are stored in the user-defined output directory and are organized into three main file types, all described in Section 5:

- Graphical outputs: <name.png>

- Dashboard <dash_data.npz>

- Text files: <name.txt>

All text-file outputs are saved in an automatically created subfolder named **textfiles** within the specified output directory. In addition, a separate text file named diagnosis.txt is generated in the main output folder.

> Once the analysis is completed, the dashboard is automatically displayed. If the dashboard window is closed, it can only be restored by re-running the simulation or, preferably, by reopening the <dash_data.npz> file using the Interwave Analyzer interface. To do so, go to the main menu and select *Help > Dashboard*. The program will prompt you to select a file; choose the corresponding <dash_data.npz> file.

The file diagnosis.txt contains warning messages and diagnostic information related to the analysis. For example, if the thermocline is too shallow or too deep and cannot be identified using the weighted method (based on neighboring measurements), the program automatically applies a simplified approach, assuming that the thermocline is located at the mid-depth between the sensors exhibiting the largest temperature gradient.

The number of instances in which the weighted method could not be applied is reported in the diagnosis.txt file, allowing the user to assess the reliability and robustness of the thermocline detection throughout the dataset.

References

[1] Rafael de Carvalho Bueno, Tobias Bleninger, and Andreas Lorke. Internal wave analyzer for thermally stratified lakes. *Environmental Modelling \& Software*, 2020.

[2] P G Tait. Voy. Challenger Rep. 2 (Phys. and Chem.). IV. Report on some of the physical properties of fresh and sea water, 1888.

[3] Jordan S Read, David P Hamilton, Ian D Jones, Kohji Muraoka, Luke A Winslow, Ryan Kroiss, Chin H Wu, and Evelyn Gaiser. Derivation of lake mixing and stratification indices from high-resolution lake buoy data. *Environmental Modelling \& Software*, 26(11):1325–1336, 2011.

[4] Bertram Boehrer. Modal response of a deep stratified lake: western Lake Constance. *Journal of Geophysical Research: Oceans*, 105(C12):28837–28845, 2000.

[5] Bertram Boehrer, Johann Ilmberger, and Karl Otto Münnich. Vertical structure of currents in western Lake Constance. *Journal of Geophysical Research: Oceans*, 105(C12):28823–28835, 2000.

[6] Matthias Münnich, Alfred Wüest, and Dieter M Imboden. Observations of the second vertical mode of the internal seiche in an alpine lake. *Limnology and oceanography*, 37(8):1705–1719, 1992.

[7] Rafael de Carvalho Bueno, Tobias Bleninger, Bertram Boehrer, and Andreas Lorke. Physical mechanisms of internal seiche attenuation for non-ideal stratification and basin topography. *Environmental Fluid Mechanics*, 5 2023.

[8] Rafael de Carvalho Bueno, Tobias Bleninger, and Andreas Lorke. Internal seiche damping on sloping topography. *Limnology and Oceanography*, 71(2):e70340, 2 2026.

[9] S A Thorpe. A method of producing a shear flow in a stratified fluid. *Journal of Fluid Mechanics*, 32(4):693–704, 1968.

[10] Rafael de Carvalho Bueno. *Wind-induced internal waves in closed basins: A laboratory experiment and field study*. PhD thesis, Graduate Program in Environmental Engineering of the Federal University of Paraná., 2019.

[11] Peter Welch. The use of fast Fourier transform for the estimation of power spectra: a method based on time averaging over short, modified periodograms. *IEEE Transactions on audio and electroacoustics*, 15(2):70–73, 1967.

[12] Juliane Bernhardt and Georgiy Kirillin. Seasonal pattern of rotation-affected internal seiches in a small temperate lake. *Limnology and oceanography*, 58(4):1344–1360, 2013.

[13] Richard E Thomson and William J Emery. *Data analysis methods in physical oceanography*. Newnes, 2014.

[14] Christopher Torrence and Gilbert P Compo. A practical guide to wavelet analysis. *Bulletin of the American Meteorological society*, 79(1):61–78, 1998.

[15] Stuart Grange. Averaging wind speeds and directions. *no. October*, page 12, 2014.

[16] Adrien Gaudard, Robert Schwefel, Love Råman Vinnå, Martin Schmid, Alfred Wüest, and Damien Bouffard. Optimizing the parameterization of deep mixing and internal seiches in one-dimensional hydrodynamic models: a case study with Simstrat v1. 3. *Geoscientific Model Development*, 10(9):3411–3423, 2017.

[17] Wilhelm Schmidt. Stehende Schwingungen in der Grenzschicht zweier Flussigkeiten. *SB Akad. Wiss. Wien, Ia*, 117:91–102, 1908.

[18] Robert Hays Spigel and Jörg Imberger. The classification of mixed-layer dynamics of lakes of small to medium size. *Journal of physical oceanography*, 10(7):1104–1121, 1980.

[19] Jörg Imberger and John C Patterson. Physical limnology. In *Advances in applied mechanics*, volume 27, pages 303–475. Elsevier, 1989.

[20] Leon Boegman, G N Ivey, and J Imberger. The degeneration of internal waves in lakes with sloping topography. *Limnology and oceanography*, 50(5):1620–1637, 2005.

[21] Rafael de Carvalho Bueno, Tobias Bleninger, Huaxia Yao, and James A Rusak. An empirical parametrization of internal seiche amplitude including secondary effects. *Environmental Fluid Mechanics*, 2020.

[22] Daniel Bourgault, Peter Galbraith, and Cédric Chavanne. Generation of Kelvin-Helmholtz Billows and Internal Solitons at Geophysical Fronts. In *EGU General Assembly Conference Abstracts*, volume 18, page 7099, 2016.

[23] Bruce R Sutherland. *Internal gravity waves*. Cambridge University Press, 2010.

[24] D A Horn, J Imberger, and G N Ivey. The degeneration of basin-scale internal waves in lakes. In *Thirteenth Australasian Fluid Mechanics Conference*, pages 863–866, Monash University, 1998.

[25] D A Horn, Jorg Imberger, and G N Ivey. The degeneration of large-scale interfacial gravity waves in lakes. *Journal of Fluid Mechanics*, 434:181–207, 2001.